UDRI
UNIVERSITY of DAYTON RESEARCH INSTITUTE

UDR-TR-2000-00131

# Report

## Diesel Cold Start Improvement Using Thermal Management Techniques

Scott D. Stouffer
Arthur B. Lewis
Thomas J. Whitney
Michael L. Drake



**Prepared For:**

**U.S. Army Research Office**
**PO Box 12211**
**Research Triangle Park**

**FINAL REPORT**

# REPORT DOCUMENTATION PAGE

Form Approved
OMB NO. 0704-0188



| 1. AGENCY USE ONLY ( Leave Blank) | 2. REPORT DATE<br>October, 00 | 3. REPORT TYPE AND DATES COVERED<br>Final Report 9 Feb 98 - 01 Jul 00 |
|---|---|---|

4. TITLE AND SUBTITLE

Diesel Engine Cold Start Improvement Using Thermal Management Techniques

5. FUNDING NUMBERS

DAAG 55- 98-1-0035

6. AUTHOR(S)
Scott D. Stouffer
Arthur B. Lewis
Thomas J. Whitney
Michael L. Drake

7. PERFORMING ORGANIZATION NAME(S) AND ADDRESS(ES)

University of Dayton Research Institute
300 College Park
Dayton, OH 45469-0110

8. PERFORMING ORGANIZATION REPORT NUMBER

9. SPONSORING / MONITORING AGENCY NAME(S) AND ADDRESS(ES)

U. S. Army Research Office
P.O. Box 12211
Research Triangle Park, NC 27709-2211

10. SPONSORING / MONITORING AGENCY REPORT NUMBER

ARO 38352.1-EG-CCE

11. SUPPLEMENTARY NOTES

The views, opinions and/or findings contained in this report are those of the author(s) and should not be construed as an official Department of the Army position, policy or decision, unless so designated by other documentation.

12 a. DISTRIBUTION / AVAILABILITY STATEMENT

Approved for public release; distribution unlimited.

12 b. DISTRIBUTION CODE

13. ABSTRACT (Maximum 200 words)

The objective of the research program was to investigate, develop, and demonstrate thermal energy storage systems for the improvement of the starting characteristics of Army Diesel engines exposed to cold temperatures overnight. Because of the effect of the oil temperatures on starting work, a passive thermal protection system that used Phase Change Materials (PCM) and insulation was designed for the oil pan and filter. Waste heat was stored in the PCM during engine operation, and was released back into the oil system after engine shutdown. Experimental tests were conducted with the PCM applied to the oil pan and filter of an M925 5-ton truck. After engine shut-off the oil temperature at the bottom of the pan was maintained at +50°F during a 12 hr exposure to average air temperature of 13°F. During cold start tests conducted after overnight cold exposure, the engine with the PCM applied to the oil system started faster and required much less cranking energy from the batteries than the baseline engine under similar conditions. A secondary benefit of the warmer oil is the improved engine lubrication at startup, which can reduce engine wear. A passive thermal protection system was also built and tested for the battery box.

14. SUBJECT TERMS

Diesel Engine, Cold Starting, Lubrication, Phase Change Materials, Vacuum Insullation

15. NUMBER OF PAGES
126

16. PRICE CODE

| 17. SECURITY CLASSIFICATION OR REPORT | 18. SECURITY CLASSIFICATION ON THIS PAGE | 19. SECURITY CLASSIFICATION OF ABSTRACT | 20. LIMITATION OF ABSTRACT |
|---|---|---|---|
| UNCLASSIFIED | UNCLASSIFIED | UNCLASSIFIED | UL |

# Cold Climate Energy Program

## Final Progress Report

Scott D. Stouffer
Arthur B. Lewis
Thomas J. Whitney
Michael L. Drake

University of Dayton

Oct 30, 2000

# Foreword

This report summarizes the research and development study conducted for the US Army Research Office Cold Climate Research Program under Grant Number DAA55-9801-0035 between February 9, 1998 and June 30, 2000. Dr. David Mann of the Army Research Office served as the grant officer representative for ARO. The program was conducted in the Aerospace Mechanics Division of the University of Dayton Research Institute. Mr. Blaine West is the UDRI Aerospace Mechanics Division leader. Dr. Scott Stouffer of UDRI was the principal investigator and Mr. Arthur Lewis served as the program manager.

A detailed technical summary of the research and development efforts conducted under this grant is presented in the report entitled "Diesel Engine Cold Start Improvement Using Thermal Management Techniques", UDR-TR-2000-00131.

## Statement of the Problem Considered

Diesel engines rely on autoignition of the compressed fuel/air charge in the cylinder. It is well known that for a given Diesel Engine any ambient air temperature, there is a minimum cranking speed for starting and this minimum cranking speed for starting increases as the ambient air temperature decreases.

Achieving sufficient cranking speed to start a Diesel engine is a problem in cold weather. The cranking speed of an engine depends on the battery strength and the frictional resistance of the engine. The frictional resistance of the engine increases as the temperature decreases primarily because of the large increase in the viscosity of the oil that occurs as the temperature drops. The increase in the viscosity is shown in Figure 1.3 for typical 15W-40 oil. Note that for most heavy vehicles in the "lower 49" United States 15W-40 oil is the preferred viscosity grade. The high viscosity oil not only increases the friction in moving engine parts but also causes an increased load on the oil pump.

The frictional load on the engine during cranking must be overcome by the starting system. Typically lead-acid batteries and an electric starter motor are used to crank the engine. However, some Diesel engines use an air turbine for starting. The strength of lead-acid batteries is known to drop as the temperature decreases. To make matters worse, a cold lead-acid battery does not recharge as well as a warm battery, resulting in a progressive decrease in battery strength during extended cold weather. As a battery discharges its specific gravity decreases and its freezing point increases. Freezing results in bent battery plates, ruptured battery cases, and resultant catastrophic failure of the battery.

The objective of the research program was to investigate, develop, and demonstrate the use of thermal energy storage systems to improve the starting characteristics of Army Diesel engines exposed to cold temperatures overnight. The approach investigated was to use stored waste heat to maintain the temperatures of critical components and systems at levels high enough to allow starting. Because of the high impact of the battery and oil temperatures on starting work, thermal management systems were designed for the oil pan, oil filter and battery box.

The battery box thermal management system consisted of state-of-the-art-vacuum insulation and resistance heating. A passive thermal protection system that used Phase

Change Materials (PCM) contained in Energy Storage Devices (ESD) for thermal storage was designed for the oil system. The PCM-ESD system was designed to fit on the outside of the oil pan and oil filter. During operation of the engine, waste heat from the engine was conducted through the outside of the oil pan and oil filter and was stored in the PCM as it melts. After engine shutdown, the thermal energy stored in the PCM-ESD was released back to the oil system as the PCM freezes. Insulation was applied to the outside of the PCM to decrease the energy lost to the surroundings.

While the primary interest in the PCM-ESD system is improved starting, a secondary benefit of the PCM-ESD system is the improved oil flow for lubrication of engine parts at startup, which may reduce engine wear.

## Summary of Results

The purpose of this study was to examine means of storing the waste heat generated during Diesel engine operation to improve the starting performance of Diesel engines after overnight exposure to cold weather. The goal of the program was to develop a system to improve the starting characteristics of the Diesel engine so that it would reliably re-start after exposure to cold weather for a period of at least 12 hours. Thermal management of two critical temperature-sensitive systems, the battery and the oil system, was pursued to accomplish this goal. The battery and oil temperatures are important because of their relation to the cranking speed, which is a critical consideration in the starting of a Diesel Engine. Cold batteries provide less power and cold oil leads to higher resistance during cranking. Therefore, if the oil and batteries are maintained at a higher temperature level the engine will start much easier.

Concept-demonstration thermal management systems were designed for the oil pan, oil filter, and battery box of a US Army five-ton tactical truck. Phase change materials (PCM) and advanced insulation were used in the design of the thermal management systems. The PCM was used in passive energy storage devices (PCM-ESD), which were attached to the oil pan and oil filter. The PCM-ESD stored thermal energy during engine operation and released the energy back to the oil system as the vehicle cooled-down to prevent the temperature of the oil from dropping too low overnight. The insulation prevents the loss of the energy stored in the PCM-ESD to the environment. It was found that the battery produced little waste heat during its charging cycle, therefore the thermal management system for the battery was based on active heating of the

batteries by electric resistance heaters and the prevention of heat loss by state of the art vacuum insulation.

All three of the thermal management systems were studied in cooling tests conducted in a 0°F cold chamber. The performance of the thermal management systems was compared to the baseline component cool-down rate. It was found that the thermal management systems reduced the cooling rate for all three of the systems.

The time required to cool at the top of the oil pan from room temperature to 32°F was increased by almost a factor of two with the PCM-ESD system. An even greater effect was seen on the oil at the bottom of the pan; the time required to reach 32°F was extended by a factor of 12. The oil filter PCM-ESD system was also shown to be effective. The presence of the PCM-ESD system on the oil filter increased the time to drop from room temperature to 32°F by a factor of 4. The tests of the insulated battery box showed that the temperature decreased by less than 25°F over a 16 hr period, which was a factor of over 2.9 times the required time for the baseline configuration.

The PCM-ESD thermal management systems for the oil pan and oil filter were tested on the engine during operation, cool-down and restart tests conducted while the truck was exposed to the winter environment in Dayton, OH. The temperatures of the oil system, block, and other components were measured during engine operation and cool-down tests with and without the PCM-ESD system applied to the engine. Cranking performance was determined by measuring the cranking voltage, current and engine speed at startup, for both the baseline engine and the PCM-ESD equipped engine.

The tests showed that that the thermal management system maintained the oil temperature at the bottom of the pan above 50°F for longer than 12 hrs when exposed to average ambient temperatures as low as 13°F. The PCM-ESD system was able to maintain the oil temperature at the bottom of the pan more than 25°F above the ambient air temperature for up to 14-hrs exposure to the cold. The application of PCM-ESD to the oil filter was also shown to be effective in maintaining the oil temperature over 20°F above ambient conditions overnight. The result of the higher oil temperatures in the oil pan and oil filter was that the engine started faster, requiring a factor of 2-6 times less cranking energy from the batteries.

This study resulted in a successful concept demonstration of thermal management systems for the battery and oil system of a US Army 5-ton tactical truck, which are capable of maintaining the temperatures of the oil and battery at elevated temperature during exposure to cold weather overnight. The successful concept demonstration shows that a Diesel engine equipped with passive energy storage devices applied to the oil system can be shut off for longer periods in cold weather and reliably start. The application of a PCM-ESD system to Diesel engines could reduce or eliminate fuel use and engine wear due to overnight idling in cold weather.

The tests of the concept-demonstration thermal management system for the oil conclusively showed that it is possible to use a totally passive thermal protection based on PCM and insulation to maintain the oil in both the oil pan and oil filter at elevated levels for extended time periods after shutdown. Another benefit of the higher oil temperatures in the pan was that the block temperature was also maintained at higher temperature levels. As a result of the higher oil temperatures, the engine was shown to re-start in much less time, using less cranking energy from the battery. The reduction in the cranking work reduces the charge that must be delivered back to the battery during inefficient battery charging at low temperatures. Another benefit of the higher oil temperatures at startup provided by the PCM-ESD system is the improved flow of the lubricant and the lubrication of engine components. The use of a passive PCM-ESD on the oil filter ensures that the oil filter is not bypassed because of excessive pressure drop.

The cold chamber tests of the battery box showed that it is possible to build a practical actively heated insulated battery box that could maintain batteries at elevated temperatures overnight.

## Publications

There has been one comprehensive report summarizing the research program.

UDI-TR 2000-00131 Diesel Cold Start Improvement Using Thermal Management Techniques

UDRI hopes to present excerpts from the work at upcoming scientific SAE, and ASME meetings.

## Participating Scientific Personnel

### Professional Personnel

Dr. Scott Stouffer
Mr. Arthur Lewis
Mr. Thomas Whitney
Mr. Michael Drake
Dr. Deems Emmer
Dr. Kelly Kissock

### Participating Students who have received degrees while participating on the project

| | |
|---|---|
| David J. Weinert | BS Mechanical Engineering 1998 |
| Kyaw Wynne | MS Mechanical Engineering 1999 |
| John M. Hanning | MS Mechanical Engineering 1998 |
| Timothy Tkacz | BS Mechanical Engineering (will obtain in Summer 2001) |

## Report of Inventions

There have been two invention disclosures resulting from the research:

1. "Thermal Management of Hydraulic Systems using Passive PCM/Insulation "

2. " Internal combustion Engine Cold Climate Thermal Protection By the use of Phase Change/Insulation Systems"

UDRI is pursuing technology transfer opportunities for these technologies.

# Diesel Cold Start Improvement Using Thermal Management Techniques

**Research conducted under Army Research Office**
**Grant Number DAA55-9801-0035**

**Scott D. Stouffer**
**Arthur B. Lewis**
**Thomas J. Whitney**
**Michael L. Drake**

**University of Dayton Research Institute**
**Dayton OH**

## *Abstract*

The objective of the research program was to investigate, develop, and demonstrate the use of thermal energy storage systems to improve the starting characteristics of Army Diesel engines exposed to cold temperatures overnight. The approach investigated was to use stored waste heat to maintain the temperatures of critical components and systems at levels high enough to allow starting. Because of the high impact of the battery and oil temperatures on starting work, thermal management systems were designed for the oil pan, oil filter and battery box.

The battery box thermal management system consisted of state-of-the-art-vacuum insulation and resistance heating, and was shown to maintain the battery temperature above 46°F overnight. A passive thermal protection system that used Phase Change Materials (PCM) contained in Energy Storage Devices (ESD) for thermal storage was designed for the oil system. The PCM-ESD system was designed to fit on the outside of the oil pan and oil filter. During operation of the engine, waste heat from the engine was conducted through the outside of the oil pan and oil filter and was stored in the PCM as it melts. After engine shutdown, the thermal energy stored in the PCM-ESD was released back to the oil system as the PCM freezes. Insulation was applied to the outside of the PCM to decrease the energy lost to the surroundings.

Experimental tests were conducted with the PCM-ESD systems applied to the oil pan and oil filter of a US Army M925 (5-ton) truck. At the lowest average air temperature that the truck was exposed to overnight, 13°F, the oil temperature measured near the bottom of the pan was +50°F after 12 hours exposure to the cold. During all of the tests conducted, the thermal protection systems maintained the temperature of the oil in both the oil filter and oil pan more than 21°F above ambient air temperatures for periods over 14 hrs. During cold start tests conducted after overnight exposure to the cold, the engine with the PCM-ESD applied to the oil system started faster and required much less time and cranking energy from the batteries to start than the baseline engine exposed to similar conditions.

While the primary interest in the PCM-ESD system is improved starting, a secondary benefit of the PCM-ESD system is the improved oil flow for lubrication of engine parts at startup, which may reduce engine wear.

## *Table of Contents*


Abstract ..... i
List of Figures ..... iv
List of Tables ..... viii
Foreword ..... ix
Acknowledgements ..... x
Section 1 Introduction ..... 1
1.1 Problems with starting Diesel Engines in Cold Weather ..... 1
1.2 Cold Start Improvement Methods (State of the Art) ..... 5
1.3 The UDRI Approach to Cold Start Improvement - Engine Thermal Management ..... 11
1.4 Overview of the Report ..... 15
Section 2 Design of Thermal Management System ..... 16
2.1 Test Vehicle ..... 16
2.2 Design and Test Conditions ..... 18
2.3 Thermodynamic Design Considerations ..... 18
2.3.1 Oil Pan Thermal Storage ..... 18
2.3.2 Oil Filter Thermal Storage ..... 21
2.3.3 Battery Thermal Storage ..... 24
2.4 Design Method and Analysis for PCM-ESD Applied to the Oil Pan ..... 26
2.4.1 Volumetric Thermal Storage Capacity for PCM Forms ..... 26
2.4.2 Conduction Heat Transfer Considerations ..... 28
2.4.3 Conduction Enhancement of the PCM ESD ..... 33
2.4.4 Performance Estimates of PCM-ESD Incorporating Flexcore Honeycomb on Oil Pan ..... 35
2.4.4.1 PCM Materials ..... 35
2.4.4.2 Performance Estimates For Oil Pan PCM ESD ..... 37
2.5 Final Design Configuration of the Thermal Protection System ..... 44
2.5.1 Oil Pan PCM-ESD Design ..... 44
2.5.2 Oil Filter PCM-ESD Design ..... 52
2.5.3 Insulated Battery Box Design ..... 54
Section 3 Instrumentation ..... 58
3.1 Temperature Measurements ..... 58
3.2 Wind Speed ..... 58
3.3 Heat Flux Gages ..... 58
3.4 Startup Transient Instrumentation ..... 59
3.5 Data Acquisition System ..... 60
Section 4 Results of Experimental Tests ..... 62
4.1 Cold Chamber Tests of Thermal Protection Systems ..... 62
4.1.1 Oil System Thermal Protection System Test Apparatus and Procedure ..... 62
4.1.2 Oil Pan PCM-ESD Cold Chamber Test Results ..... 64
4.1.3 Oil Filter PCM-ESD Cold Chamber Test Results ..... 67
4.1.4 Insulated Battery Box Cold Chamber Tests ..... 70

4.2 Baseline Engine Test Program ..... 77
4.2.1 Engine Temperatures during Driving of the Baseline Vehicle ..... 77
4.2.2 Baseline Engine Cool Down Tests ..... 78
4.2.3 Effect of Insulation on Oil pan and oil filter ..... 85
4.2.4 Baseline Starting and Cranking Performance Tests ..... 88
4.3 Experimental Tests with the PCM-ESD System Applied to the Engine ..... 96
4.3.1 Engine Test Program with PCM-ESD Installed on the Engine Oil System ..... 96
4.3.2 Results for Oil Pan PCM-ESD during Operation and Cool-Down Tests ..... 98
4.3.2.1 The Effect of Insulation Type on the Performance of the Oil Pan-PCM System ..... 110
4.3.3 Oil filter PCM-ESD Tests ..... 112
4.3.4 Engine Cranking and Starting Results ..... 115
Section 5 Summary and Conclusions ..... 121
5.1 Summary ..... 121
5.2 Conclusions ..... 122
Section 6 Suggested Areas for Further Investigation ..... 124
6.1 Further Studies of the Existing PCM-ESD System ..... 124
6.1.1 Test at Lower Ambient Air Temperatures ..... 124
6.1.2 Determination of the Effect of the Oil-Filter ESD on Engine Cranking ..... 124
6.2 Improvements to the Present System ..... 124
6.3 Extension of the System to Operate at Much Lower Operating Temperatures ..... 125
6.4 Application of PCM-ESD to Other Temperature Sensitive Engine Systems ..... 125
Section 7 References ..... 126

## *List of Figures*


Figure 1.1 Ideal Compression Temperatures for Air Temperature as a Function of Compression Ratio ..... 3
Figure 1.2 Dependence of the Final Compression Temperature on Ambient Temperature and Cranking Speed ..... 4
Figure 1.3 Temperature-Viscosity Relationship for a Typical 14W-40 Oil ..... 4
Figure 1.4 Swing-fire Heater Installed on the Hood of a US-Army M939 Series Truck ..... 8
Figure 1.5 Battery Pads for US Army M-939 Series (5-ton) Truck Equipped with Arctic Kit ..... 8
Figure 1.6 Sander's Engine Heating Device ..... 10
Figure 1.7 Sander's Engine Heating Device Mounted on Diesel Exhaust ..... 10
Figure 2.1 US Army 5-Ton Cargo Truck ..... 17
Figure 2.2 Cummins C6TA8.3 Diesel Engine Installed in the Test Vehicle ..... 17
Figure 2.3 Oil Pan for Cummins C6TA (8.3 liter) Diesel ..... 19
Figure 2.4 Oil Pan Installed on M925 Truck ..... 20
Figure 2.5 Comparison of the Temperature Change of the Oil and Pan to Equal the Thermal Storage in PCM Mass ..... 21
Figure 2.6 Oil Filter Mounted on Cummins C6TA 8.3 liter Engine ..... 23
Figure 2.7 Comparison of the Temperature Change of the Oil and Filter to Equal the Thermal Storage in PCM Mass ..... 23
Figure 2.8 Photograph of the Battery Box in the Test Vehicle ..... 25
Figure 2.9 Comparison of Thermal Storage in the Batteries vs. Thermal Storage in the Latent Heat of the PCM ..... 25
Figure 2.10 Energy Storage Potential of PCM-ESD Applied to the Oil Pan ..... 28
Figure 2.11 One-Dimensional PCM-ESD Layer for Heat Conduction Study ..... 29
Figure 2.12 Thermal Model of the Phase Change Enthalpy ..... 30
Figure 2.13 Temperature Distribution and Energy Storage for Case 2 (PCM Gel, 2"-Thick) ..... 31
Figure 2.14 Temperature Distribution and Energy Storage for Case 4 (PCM Powder, 2"-Thick) ..... 32
Figure 2.15 Energy Stored in PCM Covers for Oil Pan ..... 33
Figure 2.16 The Use of High Conductivity Fins to Provide a Shorter Thermal Path Through the Lower Conductivity PCM ..... 34
Figure 2.17 Hexcell Flexcore Honeycomb (A) End-View of Flexcore, (B) Flexcore Wrapped Around the Surface of Oil Pan ..... 35
Figure 2.18 Thermal Storage (Relative to a Baseline at -4°F) and Specific Heat of the Hexadecane-PCM Gel ..... 36
Figure 2.19 Heat Paths Considered in Performance Estimate Calculations ..... 38
Figure 2.20 Finite Element Grid Used for Modeling the PCM-ESD ..... 39
Figure 2.21 Simulation of Oil Temperature and PCM-ESD Temperatures for Case Without Flexcore ..... 41
Figure 2.22 Simulation of Oil Temperature and PCM-ESD Temperatures for Case With Flexcore Thickness ..... 42
Figure 2.23 Effect of Hexcell Flexcore on Oil Temperature During

Engine Cool-Down ..... 42
Figure 2.24 Simulation of Effect of PCM Mass on Performance of Oil Pan PCM-ESD ..... 43
Figure 2.25 Simulation Effect of Insulation on the Oil Pan PCM ESD Performance ..... 44
Figure 2.26 Sketch of the PCM-ESD Installed on the Oil Pan ..... 46
Figure 2.27 Photograph of PCM-ESD #3 Showing Curvature to mate with the Bottom of Oil Pan ..... 47
Figure 2.28 Proof-of-Concept PCM-ESD Installed on the Oil Pan ..... 48
Figure 2.29 ESD #1 Shown from the Side Facing the Oil Pan ..... 49
Figure 2.30 Polyisocyanurate Oil Pan and PCM-ESD Insulation for the Oil Pan ..... 50
Figure 2.31 Oil Pan PCM-ESD during Test Installation ..... 51
Figure 2.32 Vacuum Insulation Installed on the Oil Pan PCM-ESD ..... 51
Figure 2.33 Drawing of Oil Filter PCM-ESD ..... 53
Figure 2.34 Top View Photograph of Oil Filter ESD during Construction ..... 53
Figure 2.35 Oil Filter PCM-ESD Installed on Engine ..... 54
Figure 2.36 Simplified Assembly Drawing of the Insulated Battery Box ..... 56
Figure 2.37 Photograph of the Insulated Battery Box ..... 57
Figure 3.1 Heat Flux Gage ..... 59
Figure 3.2 Tachometer Used for the Determination of Engine Speed ..... 60
Figure 3.3 Schematic of the Data System ..... 61
Figure 4.1 The Oil Pan Thermal Test Stand Used for the Cold Chamber Tests ..... 63
Figure 4.2 The Oil Filter and Oil Filter PCM-ESD Mounted in the Test Stand for the Cold Chamber Tests before Application of the Insulation ..... 64
Figure 4.3 Cold Chamber Test of the Baseline Oil Pan ..... 66
Figure 4.4 Comparison of the Oil Temperatures With and Without the PCM-ESD System during the Cold Chamber Cool-Down Tests ..... 66
Figure 4.5 Temperatures Inside of ESD #3 During the Cold Chamber Tests of the Oil Pan ..... 67
Figure 4.6 Baseline Tests of the Oil Filter in the Cold Chamber ..... 68
Figure 4.7 Comparison of the Oil Temperatures Measured at the Center of the Oil Filter during Cold Chamber Tests ..... 69
Figure 4.8 Cold Chamber Test of the Oil Filter Equipped with PCM-ESD ..... 69
Figure 4.9 Battery Cell and Surface Temperatures Measured during the Baseline Cool-Down Test ..... 70
Figure 4.10 Comparison of First-Order Thermal Models for a Single Battery and Four Batteries ..... 72
Figure 4.11 The Battery Cell Temperatures Measured During the Cold Chamber Test of the Insulated Battery Box ..... 73
Figure 4.12 The Battery Cell Temperatures and the Cold Junction Temperature of the Data System during the Cold Chamber Test of the Insulated Battery Box ..... 74
Figure 4.13 Comparison of the Insulated Battery Box and the Baseline Thermal Model for Four Batteries ..... 75

Figure 4.14 Comparison of the Average Battery Cell Temperature for the Insulated Battery Box Case and the Pretest Prediction of the Battery Cell Performance ..... 76
Figure 4.15 Engine Block and Oil Pan Temperature Measured During Driving of the Test Vehicle on January 25, 1999 ..... 78
Figure 4.16 Block Temperatures Measured During Cool-Down Test on February 14, 1999 ..... 80
Figure 4.17 Oil System Temperatures Measured During Cool-Down Test on February 14, 1999 ..... 80
Figure 4.18 Exhaust Pipe Temperatures Measured During Cool-Down Test on February 14, 1999 ..... 81
Figure 4.19 Fuel Filter Temperatures during Typical Baseline Test ..... 82
Figure 4.20 Average Battery Cell, Truck Cab and Ambient Air Temperatures during Battery Recharging Experiment ..... 83
Figure 4.21 The Oil and Block Temperatures Measured during Baseline Cool-Down Tests ..... 84
Figure 4.22 The Effect of Insulating the Oil Pan on the Oil Temperature Measured at the Dipstick During Operation ..... 85
Figure 4.23 Oil Filter Insulation Installed on the Engine ..... 86
Figure 4.24 Effect of Oil Filter Insulation on the Oil Filter Temperature during Cool Down ..... 87
Figure 4.25 Cranking Performance during Start on December 10, 1999 ..... 89
Figure 4.26 Cranking Performance of Engine During Start on December 24, 1999 ..... 90
Figure 4.27 Relationship Between the Cranking Work and Cranking Time Measured during the Baseline Tests ..... 92
Figure 4.28 Cranking Work vs. Oil Temperature at the Dipstick for the Baseline Cranking Tests ..... 93
Figure 4.29 Cranking Work vs. Oil Filter Temperature for the Baseline Cranking Tests ..... 93
Figure 4.30 Cranking Work vs. the Average Block Temperature for the Baseline Cranking Tests ..... 94
Figure 4.31 Cranking Work vs. the Ambient Air Temperature for the Baseline Cranking Tests ..... 95
Figure 4.32 Engine Speed during Engine Operation Period of a Typical Test with PCM-ESD Applied to the Engine ..... 98
Figure 4.33 Oil Temperatures Measured During the First Test with the PCM-ESD System Applied to the Oil Pan (Jan 28 2000) ..... 99
Figure 4.34 Oil Temperatures at the Top (Dipstick) and Bottom (oil plug) of the Oil Pan during Engine Cool-Down Tests With and Without the PCM-ESD ..... 101
Figure 4.35 The Oil Temperatures and the Temperatures Measured at the Center of the Backside of the Four Oil Pan ESD's During the First Cool-Down Test (January 28 2000) ..... 101
Figure 4.36 Oil Temperatures and Backside ESD Temperatures During Charging of Cold ESD's During Test on February 20 2000 ..... 103

Figure 4.37 Temperature Measured on the Backside of ESD #1 vs. the Average Air Temperature after Engine Shut-off ..... 103
Figure 4.38 Temperature Measured on the Backside of ESD #2 vs. the Average Air Temperature after Engine Shut-off ..... 104
Figure 4.39 Temperature Measured on the Backside of ESD #3 vs. the Average Air Temperature after Engine Shut-off ..... 104
Figure 4.40 Temperature Measured on the Backside of ESD #4 vs. the Average Air Temperature after Engine Shut-off ..... 105
Figure 4.41 The Oil Temperature Measured at the Dipstick at Various Times after Engine Shut-Off vs. the Average Air Temperature ..... 106
Figure 4.42 Oil Temperature Measured at the Bottom of the Oil Pan at Various Times after Engine Shut-Off vs. the Average Air Temperature ..... 106
Figure 4.43 The Difference Between the Oil Temperature at the Bottom of the Oil Pan and the Air Temperature (Cases with PCM-ESD) ..... 107
Figure 4.44 Difference Between the Oil Temperature at the Bottom and Top of the Oil Pan for PCM-ESD Cases ..... 108
Figure 4.45 The Difference Between the Oil Temperature Measured at the Dipstick and the Block Temperature at Engine Restart ..... 109
Figure 4.46 Difference Between the Block and Air Temperature ..... 109
Figure 4.47 Heat Transfer Measured on the Outside Surface of the Oil Pan-ESD Insulation covering ESD #4 During Tests on February 16, 2000 (Polyisocyanurate Insulation) and March 17, 2000 (Vacuum Insulation) ..... 110
Figure 4.48 The Effect of the Type of Insulation on the Temperature Measured at the Bottom of the Oil Pan Test on March 17 with Vacuum Insulation, Test on February 16 with Polyisocyanurate Insulation ..... 111
Figure 4.49 Oil Filter and Oil Filter ESD Temperatures During a Typical Operation and Cool-Down Period ..... 113
Figure 4.50 Comparison of Oil Filter Surface Temperatures During Engine Cool-Down Tests Showing the Effect of the PCM-ESD ..... 113
Figure 4.51 Oil filter Temperature Before Engine Restart as a Function of the Time after Engine Shutdown and Air Temperature ..... 114
Figure 4.52 Starting Performance of the Baseline Engine Configuration on January 14, 2000 ..... 116
Figure 4.53 Starting Performance of the Engine Configuration with PCM-ESD on January 29, 2000 ..... 117
Figure 4.54 Cranking Time and Average Air Temperature vs. Cool-Down Time ..... 117
Figure 4.55 Cranking Work vs. Cool-Down Time ..... 118
Figure 4.56 The Cranking Work vs. the Oil Temperature at the Dipstick ..... 119
Figure 4.57 Cranking Work vs. Oil Filter Temperature (on Backside of Filter) for Cases with PCM-ESD Applied to the Oil Pan ..... 120

## *List of Tables*


Table 1.1 Technical Contacts During First Phase of the Research ..... 12
Table 2.1 Oil Pan Characteristics ..... 19
Table 2.2 Oil Filter Thermal Characteristics ..... 22
Table 2.3 Batteries Used in the Test Vehicle ..... 24
Table 2.4 Characteristics of PCM Used for Initial Design Calculations of Oil System PCM-ESD ..... 27
Table 2.5 Hexadecane Gel Properties ..... 36
Table 2.6 PCM-ESD Dimensions for the Proof of Concept Thermal Protection System ..... 46
Table 2.7 Specifications for the Oil Filter ESD ..... 52
Table 4.1 Engine Operation Schedule for the Baseline Tests ..... 79
Table 4.2 The Conditions during Baseline and Insulated Oil System Engine Cool-Down Tests ..... 84
Table 4.3 Summary of Baseline Cranking Test Data ..... 91
Table 4.4 Summary of Tests with the PCM-ESD Applied to Oil System ..... 97

## *Foreword*

This report summarizes the research and development study conducted for the US Army Research Office Cold Climate Research Program under Grant Number DAA55-9801-0035 between February 9, 1998 and June 30, 2000. Dr. David Mann of the Army Research Office served as the grant officer representative for ARO. The program was conducted in the Aerospace Mechanics Division of the University of Dayton Research Institute. The UDRI Aerospace Mechanics Division is headed by Mr. Blaine West. Dr. Scott Stouffer of UDRI was the principal investigator and Mr. Arthur Lewis served as the program manager.

## *Acknowledgements*

The authors would like to thank the Army Research Office for providing support for this study through Grant Number DAA55-9801-0035. Dr. David Mann of the Army Research Office served as the program manager for the grant.

The authors would like to recognize the assistance of the following University of Dayton personnel, students, and faculty: Mr. Donald R. Askins, Mr. Tim Tkacz, Mr. David Hopkins, Ms. Mary Galaska, Dr. Deems Emmer, Dr. Lloyd Huff, Mr. Mike Hannig, Mr. D.J Weinert, Ms. Amy Mielke, Mr. Kyaw Wynne, and Dr. Kelly Kissock.

The authors would also like to thank their industrial partners and military contacts for their support in conducting this research project. In particular, the technical expertise in the application of Phase Change Materials supplied by Mr. Hans Koellner of Phase Change Laboratories, and Mr. Alan Field of the Shumann-Sasol Corporation, and their consultant, Mr. Ival Salyer, was greatly appreciated. The matching funds supplied by PCL were also greatly appreciated.

VacuPanel Incorporated of Xenia, OH supplied the Vacuum insulation. The support and technical assistance of their president, Mr. Chris Meyer and Engineer Nick Wynne are appreciated. A special thank you goes out to Mr. George Roth of VacuPanel who supervised the manufacturing of the PCM Gel that was used for the final concept demonstration.

The authors appreciate the helpful advice about Diesel operations in cold climates from Dr. Peter Schihl, and Dr. Ernest Swartz of TARDEC, Col. Dennis Gassert of the University of Dayton Army ROTC unit, Mr. Jim Storey of the US Army Test Command, and Mr. Ed Walkup of Waste Management Incorporated.

The authors wish to thank the Ohio Army National Guard, and Major Jess Simpson for loaning the test vehicle to UDRI for the concept demonstration project, as well as allowing access to National Guard maintenance personnel for technical consultations.

A special thank you goes to CW1 Andrew Bollinger of the Ohio National Guard and his staff at OMS #20 of Piqua, OH for all of their support and advice. Mr. Bollinger, in particular, spent many hours of his own time to ensure that we obtained access to a test vehicle for the experimental program.

# *Section 1*
# *Introduction*

## 1.1 Problems with Starting Diesel Engines in Cold Weather

Diesel engines power everything from small generators to ships. Diesel engines are favored for trucks because of their high torque output. Both 2-stroke and 4-stroke diesel engines are currently in use by the US Army and industry. Diesel engines may be further classified as either opened chamber or divided chamber engines. In the divided-chamber Diesel engine, there is a pre-combustion chamber located in the head. Often a glow plug is used in this type of engine to enhance the ignition during a cold start. A glow plug is a hot resistance element that is heated by electric current that is supplied by the battery. Divided chambers are often used in the design of small Diesels. In contrast, the open-chamber engine, which is usually found on large truck engines is simpler in design and has no pre-combustion chamber and usually no glow plugs.

The two requirements that must be met for the starting and operation of an internal combustion engine are:

1. The delivery of fuel and air to cylinders.
2. Ignition of the air fuel mixture.

A Diesel engine differs from a spark ignition engine in that the ignition temperature is reached by compression of the gas rather than by a spark. In a diesel engine high-pressure diesel fuel is injected into the cylinder near the end of the compression stroke. If the temperature of the fuel-air charge in the cylinder is above the autoignition limit (725°F, 385°C) the fuel-air mixture will begin to burn. If the charge temperature is not above the autoignition limit it will not burn.

Diemand[1-4] gives an overview of operational problems of Diesel and other engines in cold climates. The problems can be grouped in two broad categories: fuel supply and achieving sufficient fuel-air temperatures in the cylinder.

Fuel supply problems occur because the formation of wax crystals at low temperatures prevents the flow of fuel to the fuel injection pump or from the injection pump to the cylinders. A secondary problem resulting from cold fuel is the formation of large fuel droplets, which have poor vaporization. Fuel additives are often used to suppress the pour

and cloud points of Diesel fuels. Fuel is often blended for specific geographic regions. Diesel fuel intended for use in Florida is typically different than that intended for use in Alaska.

For a Diesel engine the temperature of the fuel-air mixture in the cylinder near the end of the compression stroke depends on several factors, namely,

1. The compression ratio
2. The ambient air temperature
3. The fuel temperature
4. The temperature of the cylinder walls, cylinder head and Pistons
5. The cranking speed

Diesel engines are characterized by large compression ratios. The compression ratio is defined as the maximum volume in cylinder divided by the minimum volume in the cylinder. While typical compression ratios for spark ignition engines run from 7 to 11, typical diesel engine compression ratios range from 14 to 18. The upper limit on the temperature at the end of the compression stroke may be calculated from the isentropic relationship:

$$T_2 = T_1\left(\frac{V_1}{V_2}\right)^{\gamma-1} = T_1(r)^{\gamma-1}, \qquad (1.1)$$

where: r is the compression ratio, and $\gamma$ is the specific heat ratio.

Figure 1.1 shows the temperature, $T_2$, for an isentropic compression of air at the end of the compression stroke. Also shown in Figure 1.1 is the ignition limit for typical diesel fuel. The compressed-air temperature increases with the compression ratio and the ambient air temperature. At first glance it would appear that it would be no problem to achieve ignition of the diesel fuel except at very low ambient air temperatures. However, in an actual Diesel engine there are several factors that tend to lower the actual temperature of the fuel-air mixture below the theoretical temperature that is calculated by the isentropic assumption. The first factor is the addition of cold fuel, which lowers the final temperature because of the thermal mass and latent heat of vaporization of the fuel. The next factor is the heat loss to the cold cylinder walls. There is also "blow-by", which is the flow of air and fuel past the piston rings. Blow-by results in less fuel/air in the cylinder leading to lower pressures and

temperatures in the cylinder. Another way of thinking about blow-by is that it effectively lowers the compression ratio. The effect of both the blow-by and the heat transfer to the walls becomes more severe as the cranking speed is lowered.

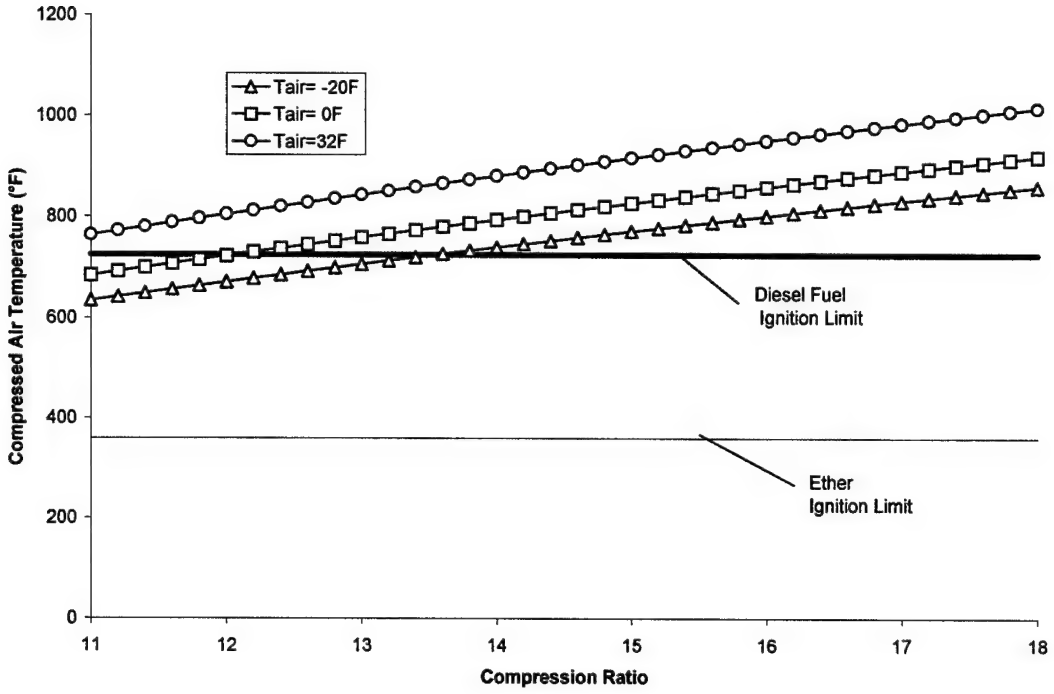


**Figure 1.1**
**Ideal Compression Temperatures for Air as a Function of Compression Ratio**

Figure 1.2 shows the calculated maximum air temperature in the cylinder as a function of ambient temperature and cranking speed. The results shown in Figure 1.2 were calculated for a particular engine. The curves for other engines will be different depending on the compression ratio and other factors such as engine wear, oil, and clearances, but it is representative of the trends that one could expect to see for another engine. Figure 1.2 points out two important factors to consider in the cold starting of a Diesel engine. First, for any ambient air temperature, there is a minimum cranking speed for starting. Secondly, this minimum cranking speed for starting increases as the ambient air temperature decreases.

Achieving sufficient cranking speed to start a Diesel engine is a problem in cold weather. The cranking speed of an engine depends on the battery strength and the frictional resistance of the engine. The frictional resistance of the engine increases as the temperature decreases primarily because of the large increase in the viscosity of the oil that occurs as the

temperature drops. The increase in the viscosity is shown in Figure 1.3 for typical 15W-40 oil. Note that for most heavy vehicles in the "lower 49" United States 15W-40 oil is the preferred viscosity grade. The high viscosity oil not only increases the friction in moving engine parts but also causes an increased load on the oil pump.

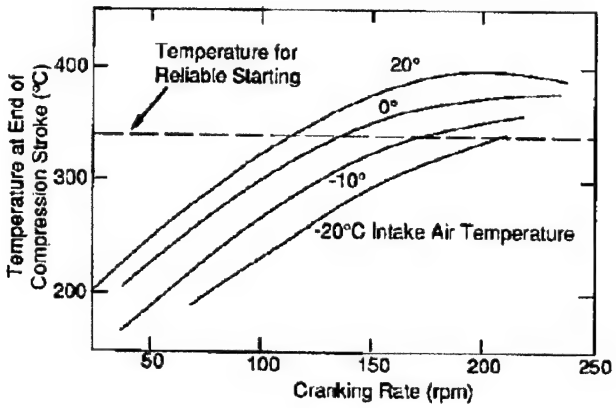


**Figure 1.2**
**Dependence of the Final Compression Temperature on Ambient Temperature and Cranking Speed (From Reference 1)**

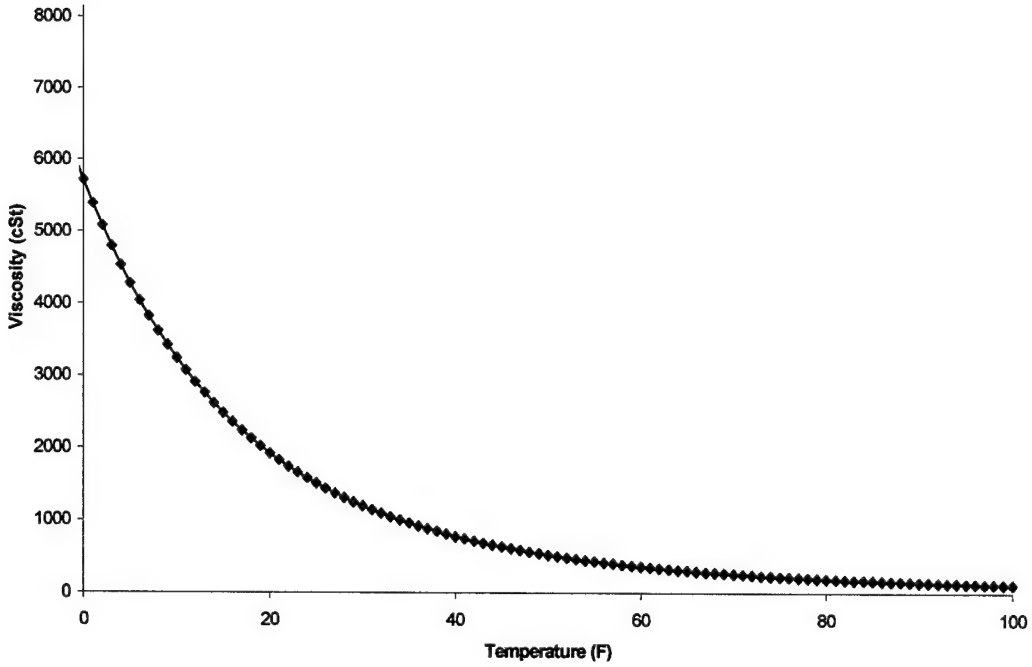


**Figure 1.3**
**Temperature-Viscosity Relationship for a Typical 15W-40 Oil**

The frictional load on the engine during cranking must be overcome by the starting system. Typically lead-acid batteries and an electric starter motor are used to crank the engine. However, some Diesel engines use an air turbine for starting. The strength of lead-acid batteries is known to drop as the temperature decreases. To make matters worse, a cold lead-acid battery does not recharge as well as a warm battery, resulting in a progressive decrease in battery strength during extended cold weather. As a battery discharges its specific gravity decreases and its freezing point increases. Freezing results in bent battery plates, ruptured battery cases, and resultant catastrophic failure of the battery.

## 1.2 Cold Start Improvement Methods (State of the Art)

The simplest method for dealing with cold starting is to totally avoid the problem by shutting the engine off for short time periods or by not shutting the engine off at all when the ambient temperature drops below a certain level. There are several problems with this technique. The most obvious problem is the huge amount of fuel that is wasted. For commercial operators this practice causes increased operating costs in addition to the air pollution. In addition there is the wear and tear on the engine which results in increased maintenance costs. When an engine is idled at low ambient temperatures, condensation of moisture can build-up within the crankcase, which will cause increased wear. For the Army there are also possible concerns of increased noise and infrared signatures for the idling trucks along with the extension of the logistical tail of a combat unit imposed by the additional fuel that is required.

Other techniques that are used to improve starting of Diesels in cold weather are discussed below.

**Excess Fuel Injection-** At startup extra fuel is injected into the cylinder. The extra fuel performs several functions that aid the engine-starting process. First, the oil takes up more cylinder volume at top dead center, which will decrease the volume available for air and thus increase the effective compression ratio. The excess fuel also tends to accumulate in the gaps between the cylinder rings and piston and cylinder walls, which promotes better compression. Both of these effects tend to increase the maximum temperature in the cylinder and the probability of autoignition. An environmental disadvantage of this method is the

potential for the generation of high levels of carbon monoxide, hydrocarbons, and soot due to excessively rich fuel-air mixtures.

**Air Heating Techniques** – There are several techniques for heating the air stream before it flows into the intake manifold. In some engines a "pre-burner" that operates on a lean mixture of fuel-air heats the air. This approach adds to the complexity of the intake and overall engine system. Other engines use an electric resistance heater (powered by the battery) in the intake manifold. A variation on this technique is to heat a glow plug for several minutes before starting to create a hot spot in the cylinder and to increase the temperature of the cylinder head. Note that power and battery capacity used for the electric resistance heaters and/or glow plugs is not available for driving the engine starter.

**Ether Injection-** Diethyl-ether or "ether" as it is more commonly known, is effective as a starting fluid because it autoignites at much lower temperatures (360°F (182°C)) than Diesel fuel (725°F, 385°C). The indiscriminant use of too much ether at startup can cause severe engine damage. For this reason, modern trucks, including many of the US army's tactical trucks use an Ether injection system that injects a metered quantity of ether into the intake manifold for startup. Ether systems are very compact and lightweight and are favored as a starting aid for tactical trucks. However, it should be noted that because of safety concerns ether is not used in US Army combat vehicles[5].

The use of Ether is restricted to low temperatures air (20 F) due to concerns about igniting the ether in the intake system causing an explosion. Therefore, Ether systems and air heating systems are usually incompatible as starting aids.

**Auxiliary Electric Resistance Heaters-** For applications where electricity is readily available, electric resistance heaters are often used to maintain temperature of the engine block, the oil and the batteries at elevated levels for extended periods of time. While this method often provides some help for starting, the cost of electricity can be substantial over long periods of time. In addition, this method is worthless when there is no source of electricity available for heating. Certainly the Army in the field cannot rely on electric block heaters. Other operators who routinely rely on electric block heaters can have problems if electricity is not available. One example would be the case of an electric power outage.

**Pony Engines-** some vehicles incorporate a device known as a pony engine in parallel with the vehicle cooling system. A pony engine is a small engine that is operated while the main

engine is shut off and is often used to produce electrical power for truckers while the engine is shut-off. A byproduct of the pony engine is the waste heat that is rejected to the coolant system and is used to maintain the temperature of the main diesel engine above the ambient temperature. The principal advantages of the pony engine are that it uses less fuel than that used by the larger Diesel engine at idle, and that it runs under a higher load than the larger Diesel engine, so that condensation is less of a problem. However, it should be noted that the pony engine increases the cost and complexity of the overall engine system and still uses fuel.

**Fuel Fired Heaters** – Fuel fired heaters may also be used for extreme arctic conditions. Figure1.4 shows a pulse-jet heater (known as a Swing-fire, which the Army issues to units that routinely operate in Arctic). The heater and the associated pump and coolant lines are used to circulate heated coolant through an engine for the purpose of heating the block before starting. In some vehicles, such as the M-900 series Diesel trucks, the heater is also used to circulate coolant through battery heater pads shown in Figure 1.5, which are placed under the batteries. A disadvantage of the fuel-fired heater is that it usually requires an extended time period (an hour or more) to warm the engine to a level high enough to allow it to start. On the other hand, the Swing-fire heater can be activated to warm up a vehicle that has been exposed to the cold for several weeks without operating.

**Alternative Working Fluids** – For vehicles that operate year round in extreme Arctic environments, different oils, diesel fuels, and battery acid are often used. Examples of practices in northern and central Alaska include the following[11]:

1. The use of a special arctic grade oil, which has a much lower viscosity at low temperatures than 15W-40.
2. The use of lower cloud and pour point Diesel Fuel #1 and DFA (Diesel Fuel Arctic), instead of Diesel Fuel #2.
3. The use of higher specific gravity battery Acid, which lowers the freezing point of the electrolyte.

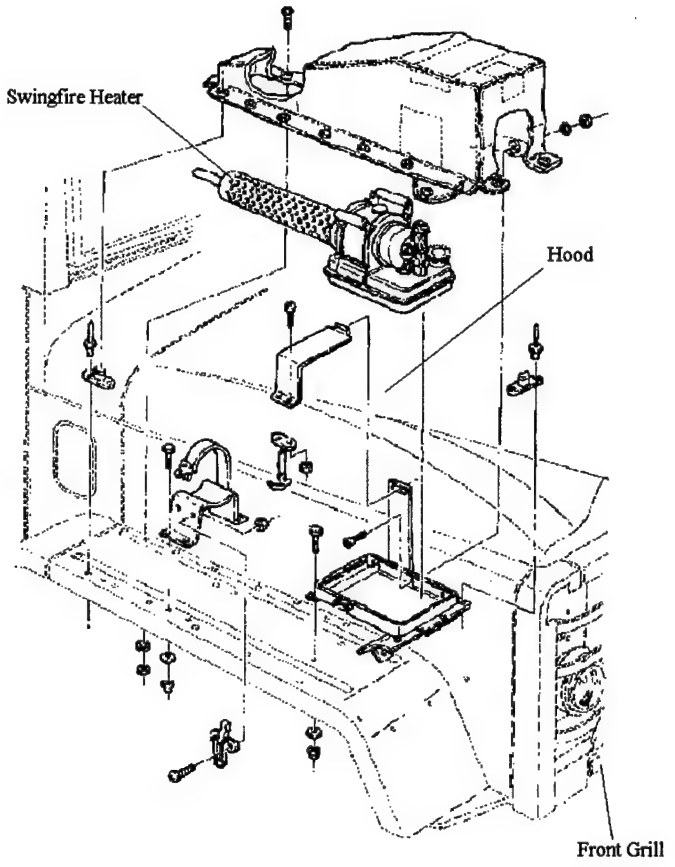


**Figure 1.4**
**Swing-fire Heater Installed on the Hood of a US-Army M 939 Series Truck (Reference 6)**

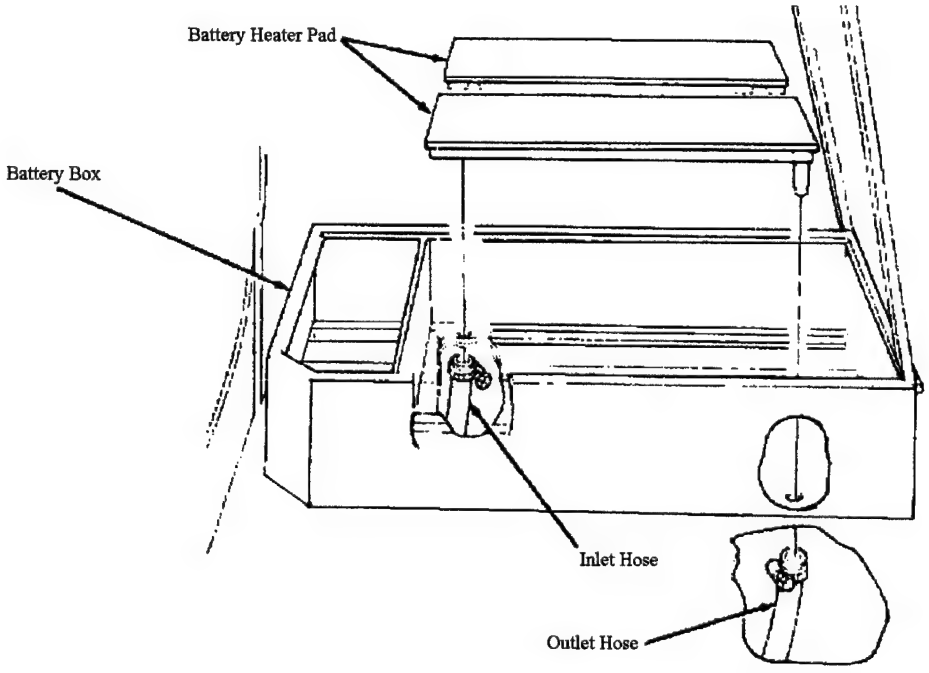


**Figure 1.5**
**Battery Pads for US Army M-939 Series (5-ton) Truck Equipped With Arctic Kit (Reference 6)**

**Latent Heat Storage Heaters** –There are two known R&D efforts by other investigators that have used phase change materials (PCM) for thermal storage. The stored thermal energy was used to pre-heat the diesel engine before starting. PCM are useful as a thermal storage medium because of the potential to store huge amounts of energy in a small volume. PCM store the energy by going through a solid to liquid phase transition (latent heat of fusion) and release it when they refreeze.

Sanders[7] developed an engine-heating device in which the energy stored in the PCM was used to heat the engine coolant that was used to pre-heat the engine before starting. The coolant was circulated through the engine heating device and the rest of the engine by an auxiliary pump before starting. A sketch of the engine-heating device used by Sanders is shown in Figure 1.6. The exhaust stream heated the PCM in this device. The PCM used for this application was Lithium Nitrate ($LiNO_3$) which is a salt that melts around 490°F and stores around 150 BTU/lbm as latent heat. The high temperature of the PCM allows rapid heating of the coolant that was passed through it. In addition because of the high temperature change of the PCM, the device stores a significant amount of sensible energy. The device used 15 lbm of the PCM and was charged by the exhaust of the engine in less than two hours.

In qualitative field tests the device allowed starting of a diesel engine after being shut down for 12 hrs in an average ambient air temperature of 18°F. Figure 1.7 shows a drawing of the Engine heating device installed on the exhaust system. Because of the excessive back pressure caused by the device, the additional complication of a by-pass valve had to be installed on the exhaust system to allow the unit to be by-passed when necessary.

Schatz[8] used a different approach to create a device that he termed a "heat battery". The engine coolant during engine operation heated the heat battery. The coolant was passed over fins that contained the PCM material. The particular PCM used for this application was a hydrated barium salt ($Ba(OH)_2*8H_20$) which melts between 120 and 172°F. The PCM fins were contained within a vacuum insulation enclosure. The device was sized for a small diesel-powered car and weighed around 22 lbm.

After sitting in the cold for an extended time period, an auxiliary electric water pump is used to pump the cool coolant through the heat battery. The warm coolant can then be used to either warm the passenger compartment, clear frost off of the windshield, or pre-heat the engine before starting. Schatz[8] noted that the starting limit of a Diesel-powered car was improved from 3°F to –18°F (-16°C to –28°C).

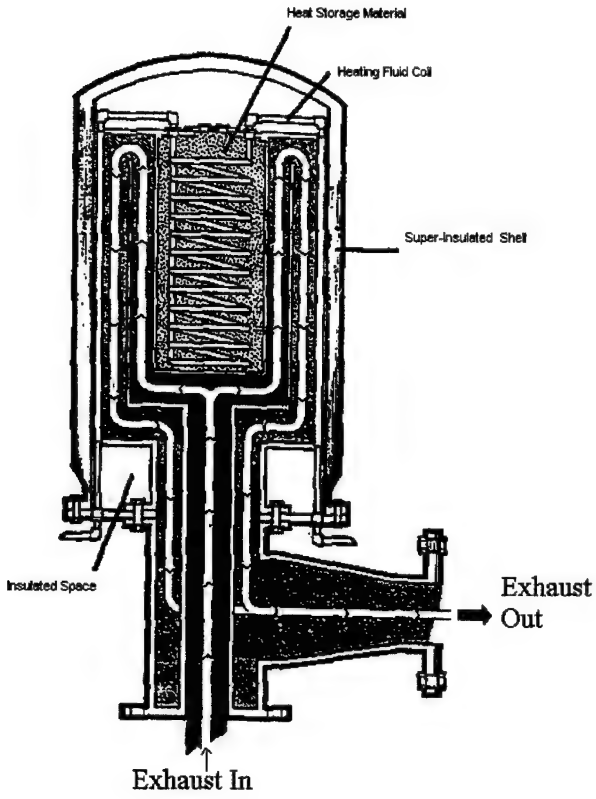


**Figure 1.6**
**Sander's Engine Heating Device (from Reference 7)**

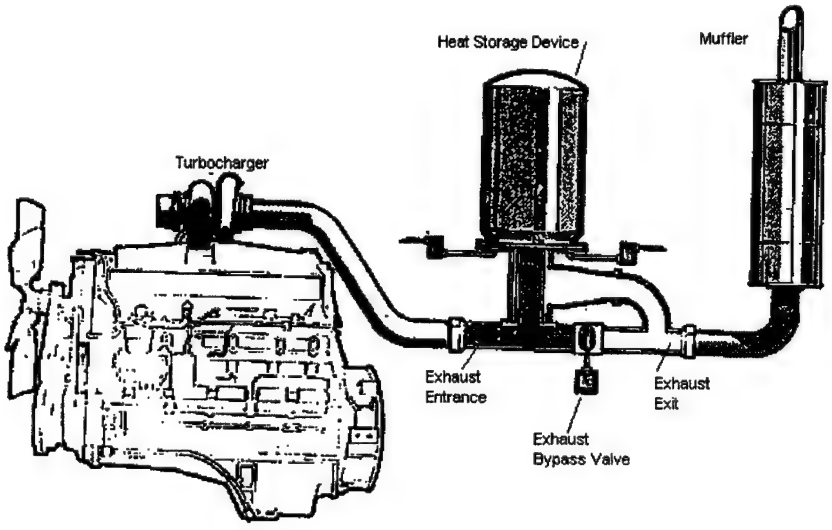


**Figure 1.7**
**Sander's Engine Heating Device Mounted on Diesel Exhaust (From Reference 7)**

## 1.3 The UDRI Approach to Cold Start Improvement- Engine Thermal Management

The personnel of the University of Dayton Research Institute have considerable experience working with Phase Change Materials. This experience extends from the development of the phase change materials, to the thermal and mechanical design of the PCM application, through test and evaluation of the completed design. Previous PCM application development studies conducted at UDRI have included medical applications, food service, heat reduction for housing, and transient laser-diode cooling. UDRI engineers also have experience in working with a local manufacturer of state of the art vacuum insulation material. Because of this experience, UDRI proposed a program to develop a cold start system based on passive thermal protection of the engine or subsystems of the engine from the cold using a combination of phase change materials and advanced insulation.

The following goals for the system were established early in the program:

1. The system will allow the engine to re-start after sitting in the cold for over 12 hours.
2. The system should be relatively low cost.
3. The system should be simple with few moving parts or controls. If possible, the system should be completely passive.
4. Any PCM would be non-corrosive and environmentally-safe at the end of its useful life
5. The system should be low maintenance.
6. The system lifetime should exceed expected lifetime of the vehicle.
7. The system should have the potential to work in combination with other Diesel Cold Start enhancements.

The first phase of the research was conducted to obtain information on Diesel operation and cold starting. UDRI conducted a literature search and discussed the problems of cold starting Diesels with Army and civilian fleet operators. A list of the technical contacts is shown in Table 1.1

**Table 1.1**
**Technical Contacts During First Phase of the Research.**

| Contact | Location |
|---|---|
| Industrial Waste Disposal | Dayton, OH |
| Army National Guard | Columbus, Piqua, and Kettering, OH |
| US Army Tank-Automotive Research Development and Engineering Center (TARDEC) | Warren, MI |
| US Army Test Command | Fort Greeley Alaska |
| US Army Cold Regions Research and Engineering Laboratory (CRREL) | Hanover, NH |
| Interstate Batteries | Texas |
| Fairborn City Schools | Fairborn, OH |

At the start of the research it was not known which systems would give the highest payoff when maintained at elevated temperatures. It soon became clear that the objective of this work should not be to simply keep the entire truck system hot (or even warm) overnight by a "Brute Force Approach," but rather to maintain the temperature of key engine systems high enough to allow starting. The following six parts of the engine system were examined to determine the benefits and drawbacks of thermal management with phase change materials and advanced insulation:

1. Intake Air

   Effect – Increasing the ambient air intake temperature increases the compressed air temperature.

   Drawbacks-There are several potential drawbacks to using PCM to heat the inlet air. First, although the total amount of amount of energy required to heat the inlet air would be small the heat transfer rates need to be high which implies high temperature and/or high-pressure loss through any heat exchanger. Second, the PCM probably could not be passively-coupled to a waste heat source, which means that some active means of heating the PCM would be necessary. Third, air heating is incompatible with the use of Ether injection, which is offered as an option on some engines.

2. Heat the Fuel

   Effect: A common cold weather problem is the formation of wax in the fuel system particularly in the fuel filter, which can result in clogging of the fuel system. If the fuel is blocked there is no fuel injected and the engine will not run. Three approaches are currently used to prevent fuel system blockage:

   A. Warm fuel is recycled from the injection pump back to the fuel tank.

B. Additives are mixed with the fuel to depress the pour point of the fuel.
C. In extremely severe environments electrical heaters may be used to heat to fuel filter.

Drawbacks: The fuel-air mixture ratio for Diesel engines is roughly 15 to 1. Considering the differences between the specific heat of air and diesel fuel, the amount of sensible energy carried into the cylinder by increasing the fuel temperature is only one-tenth that of increasing the air temperature $(mC_p)_{air} \approx 10(mC_p)_{fuel}$. Therefore, increasing the fuel temperature has minimal impact on the temperature in the cylinder near the end of the compression stroke.

After taking baseline measurements on the test vehicle used for the experimental study, it was determined that the both the fuel tank and the fuel filter were directly exposed to little waste heat during engine operation. A PCM-based fuel heater would also need to be actively heated in the test vehicle, adding further complexity to a device that would be expected to have marginal impact.

3. Block and Coolant Temperature

Effect: Increased block temperature will cause lower heat transfer losses to the cylinder walls and lower friction during cranking. Evidence of the effectiveness of maintaining the block at elevated temperatures is shown by the prominent use of block heaters. Coolant temperature alone does little to enhance starting. The use of heated coolants to increase the temperature of the block will enhance starting and it should be noted that the two latent heat engine heaters discussed in the section above circulate heated coolant through the block to warm it up before starting.

Disadvantages: For application of PCM to the engine block in a passive application there are problems with interference from the components (cooling lines, dipstick, accessory equipment, the fan etc.) which attach to the block. These objects will provide short conduction paths to the cold ambient air. It is thought that an effective passive application of PCM to the block will require large amounts of PCM, which will add to the cost and to physical interference problems in engine maintenance. For this reasons it is probable that a passive application of PCM to engine blocks would only be cost effective on large Diesel engines with large clearance space around the block.

Applications which circulate coolant through heated PCM are possible but will require the additional complication and costs associated with pumps, coolant lines and valves that will be required to circulate the fluid.

4. Battery Temperature

Effect: A warmer battery means more power to the starter and thus more cranking speed, which, in turn translates into higher charge temperatures in the cylinder and better cold starting. Batteries in the United States are rated in terms of the current that can be drawn at 0°F (the cold cranking amps, or CCA, specification).

If the battery temperature drops below 0°F the battery resistance rises dramatically. As the temperature is increased to (32°F, 0°C) the available current increases by 25%. If the battery temperature increases to 80°F the available current increases by 40 % over the CCA. Above 80 °F there is no performance advantage associated with further increases in battery temperature. Also, extended exposure to temperatures above 130°F can lead to shortening of battery life. An insulated battery enclosure, which may also contain PCM in contact with the batteries, would have the potential to lower the heat transfer losses from the batteries.

Disadvantages: In early tests it was determined that the batteries did not self-heat enough during discharge and recharging to elevate the battery temperature significantly. Thus the batteries would require some form of active heating probably from engine coolant or even electric power from the alternator. Application of an actively heated battery will require that the battery not be overheated.

4. Oil Temperature

Effect: Warmer oil has less viscosity, thus the engine obtains a higher cranking speed. Electric oil heating elements have been used in arctic conditions. The protection of the oil is amenable to passive protection with PCM. The engine oil is heated after passing through the engine.

Disadvantages: In early considerations of this technique one concern was that the presence of a covering of either PCM and/or insulation to the oil pan would overheat the oil because of the lower heat transfer from the oil pan. However it should be

noted that many newer engines have plastic or fiberglass covers for the oil pan that contain damping foam for acoustic considerations, and the oil for most engines is actively cooled in an oil cooler.

After examining the benefits and problems associated with the various engine systems listed above, it was decided that the approach to be followed in the present study would be to maintain the oil temperature and the battery temperature at elevated levels with the intent of increasing the cranking speed. It was thought thermal management of these two areas would be the most productive in terms of the performance, costs, and simplicity of the thermal protection system. In addition, thermal management of these two systems is compatible with other cold start aids currently in place on engines, such as ether injection and block heaters. It should also be noted that maintaining the lubricant temperature at elevated levels could reduce wear during starting and the early phases of engine warm-up by improving the lubricant flow. Under extreme conditions the engine could be damaged because it is operated without adequate lubricant flow to all of the moving parts when using starting aids such as Ether.

### 1.4 Overview of the Report

Chapter Two of this report discusses the development of the thermal protection systems for the oil system and the battery. The instrumentation used during the experiments is discussed in Chapter Three and the Results of the experimental tests are presented in Chapter Four. The Summary and Conclusions are presented in Chapter Five and suggestions for extensions of the results are discussed in Chapter Six.

## *Section 2*
## *Design of Thermal Management System*

### 2.1 Test Vehicle

Early in the research program, a representative from the Ohio Army National Guard (OHANG) agreed to supply the University of Dayton Research Institute with a truck for use in the proposed tests. Several candidate Army vehicles were examined early in the program, including the HMMWV, HEMTT and the 5-Ton (M925) Cargo truck. The main criteria for the selection of the test vehicle were:

1. History of cold start problems with the vehicle as identified by the OH-ANG personnel.
2. Susceptibility of the vehicle to cold start problems in a reasonably short time period (overnight).
3. Room within the engine and battery compartment for application of thermal protection system.
4. Ability to store and operate the truck within a limited space available at the University of Dayton.
5. Availability for long term loan to the University of Dayton for design, application, and test of thermal protection system.

After consideration of the five factors listed above, a single test vehicle was selected for thermal protection system development in cooperation with the Ohio ANG. The test vehicle was a US ARMY 5-ton cargo truck (M925A2 WW), which is shown in Figure 2.1. The engine for the test vehicle is a Cummins 6CTA8.3. The engine shown in Figure 2.2, is an inline six cylinder, four-stroke, Turbo-Diesel with a bore of 4.49 in, and stroke of 5.31 in, and a displacement of 505 $in^3$ (8.3liters). The engine is equipped with an ether injection system, which was not used during the study. The dry weight of the engine is 1220 lbm.

**Figure 2.1**
**US ARMY 5-Ton Cargo Truck (M925A2 WW)**

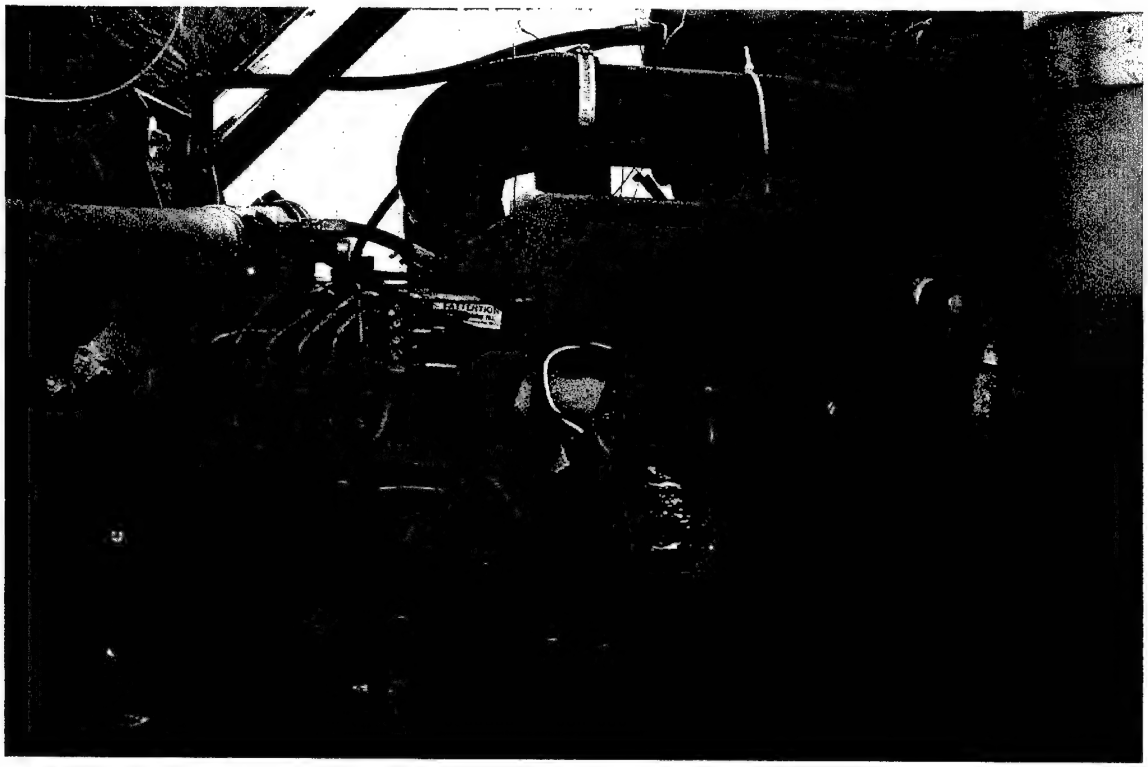

**Figure 2.2**
**Cummins C6TA8.3 Diesel Engine Installed in the Test Vehicle**

## 2.2 Design and Test Conditions

The thermal management system was design assuming an ambient temperature of 0°F for the following reasons:

1. The Ambient air temperature of 0°F is the lowest test condition that could be expected during a typical winter in Dayton, OH which is where the test program was conducted. The ASHRAE[9] standard temperatures for Dayton in the winter are -1°F (99 percentile), and +4°F (97% percentile), which means that during 99 percent of a typical winter the temperature is above –1°F, and 97% of the winter the temperature is above 4°F.
2. Vehicles that are continuously exposed to more severe environments already employ many active thermal control devices and special lubricants to aid starting. However, it was thought that the thermal management technology could be adapted to work at lower ambient temperatures after demonstration at higher ambient temperature levels.

Tests were conducted in both a cold chamber (components only) and outside (components installed on the truck). The cold chamber tests were all conducted at an ambient air temperature of 0°F. Outdoor tests on the truck were conducted in parking lots in Piqua, and Dayton Ohio, where the temperature was not controlled and ranged from 0°-35°F over most of the tests.

## 2.3 Thermodynamic Design Considerations

The first step in the design of the thermal protection system was to determine the potential thermal storage of reasonable quantities of PCM relative to the component or system being protected. The potential of the PCM thermal storage for the oil system and the battery is discussed in this section.

### 2.3.1 Oil Pan Thermal Storage

The oil is pumped through the engine by a positive displacement gear pump, which is driven off of the camshaft. At the rated speed of 2100 rpm, the pump will deliver 16 gallons/min. The temperature of the oil ranges from 210°-260°F at rated speed, therefore,

there is the potential to recover waste heat from the heated oil during operation. During cranking and/or operation of the Cummins 6CTA engine, the oil in is drawn from the oil sump near the bottom of the pan into the pump. The oil is then pumped through the oil cooler, the oil filter, the turbocharger bearings, and then to the rest of the moving engine parts through a network of parallel passages, before returning to the oil pan as heated oil.

The oil pan for the test vehicle is shown in Figures 2.3 and 2.4 and the oil pan details are given in Table 2.1. It should be noted that because of the axle components that are in close proximity to the oil pan, the shape of the oil pan has an irregular curvature on the bottom side (See Figure 2.4). The specific irregular shape of the oil pan is unique to engines used for the 5-ton truck and is not used on the commercial version of the Cummins 6CTA.

**Table 2.1**
**Oil Pan Characteristics**

| | |
|---|---|
| Material | Steel (0.07 inch nominal thickness) |
| Weight | 17 lbm |
| Nominal Oil Capacity | 20 quart (37 lbm of 15W-40 oil) |
| Surface Area | 750 $in^2$ |
| Thermal mass of Pan ($mC_p$) | 1.6 BTU/°F |
| Thermal mass of oil ($mC_p$) | 16.7 BTU/°F |
| Combined (oil + pan) thermal mass | 18.3 BTU/°F |

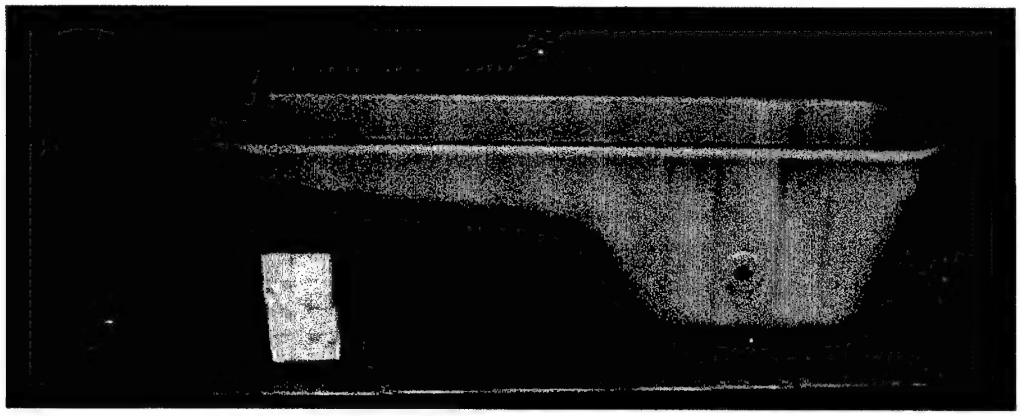

**Figure 2.3**
**Oil Pan for Cummins C6TA (8.3 liter) Diesel**

The possible effect of a passive cover for the oil pan using a PCM-ESD attached to the pan and covered with insulation on the outside was considered by comparing the latent heat storage in the PCM to the thermal storage in the oil pan and the oil. The oil

and the oil pan can store thermal energy by increasing in temperature (known as the "sensible" energy storage). The energy stored is calculated by:

$$\Delta E = mC_p\Delta T \tag{2.1}$$

where, m is the mass, $C_p$ is the specific heat, $\Delta E$ is the energy change, and $\Delta T$ is the temperature change. The required temperature rise, $\Delta T$, in the oil pan and oil to equal the energy stored in the latent heat of the PCM can be calculated as follows:

$$\Delta T_{Oil+Pan} = \frac{(m\Delta H)_{PCM}}{(mC_p)_{Oil+Pan}} \tag{2.2}$$

where $\Delta H_{PCM}$ is the latent heat of fusion for the PCM, and m is the mass of the PCM.

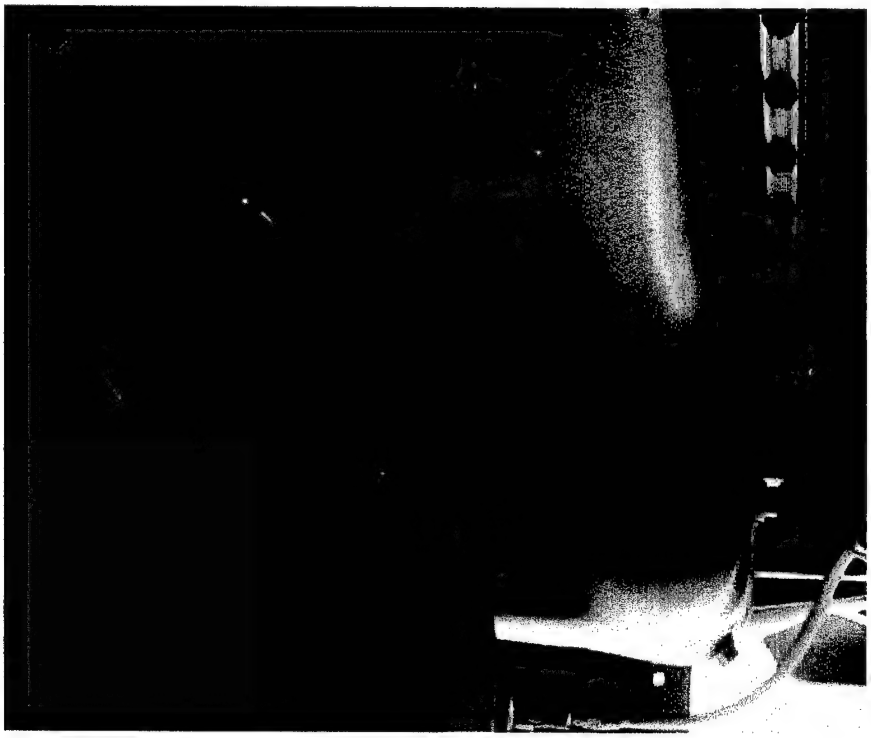

**Figure 2.4**
**Oil Pan Installed on M925 Truck**

Figure 2.5 shows required temperature rise in the oil and pan to equal the energy stored in the PCM. The two lines plotted in Figure 2.5 correspond to the approximate range of the latent heat of the candidate PCM (50-75 BTU/lbm) that were considered for the

application. It can be seen that the addition of small (relative to the total mass of the oil and pan) amounts of PCM can add significant thermal storage to the oil pan. For example, the energy stored in the latent heat of 18 lbm of PCM is equivalent to the energy that would be lost when the oil and pan decreases by 50-75 °F (depending on which PCM is used). Therefore, it was concluded that the application of PCM to the outside of the oil pan could store enough energy to be a promising means of maintaining the oil temperature at an elevated level.

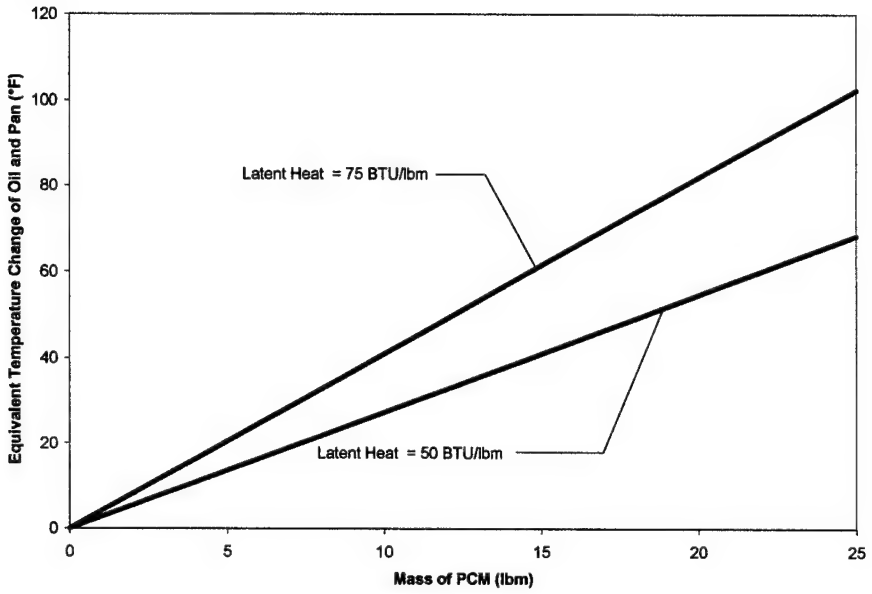


**Figure 2.5**
**Comparison of the Temperature Change of the Oil and Pan to Equal the Thermal Storage in PCM Mass**

### 2.3.2 Oil Filter Thermal Storage

The oil filter is also of interest in the consideration of cold starting and initial operation for several reasons. First, having a source of warm oil at the oil filter location places warm oil closer to the moving parts of the engine to be lubricated, and ensures that oil drawn from the pan flows through a warm filter rather than through a cold one. Secondly, a warm oil filter also reduces the load on the oil pump at startup. Note that because the oil filter is a location of potential large pressure loss in the oil system when the oil is cold, many engines use an oil filter by-pass valve that operates at a given

differential pressure. For the Cummins 6CTA engine the differential bypass pressure is 20 psi. When the oil filter is bypassed, any impurities, which would normally be captured by the filter, are passed through to the rest of the engine where they can cause increased wear.

Figure 2.6 shows the oil filter and oil cooler for the Cummins 6CTA engine. The dimensions and weight of this filter are listed in Table 2.2.

**Table 2.2**
**Oil Filter Thermal Characteristics**

| | |
|---|---|
| Oil filter type | NAPA 1649 |
| Weight | 2.5 lbm |
| Nominal Oil Capacity | 1.9 quart (3.6lbm of 15W-40 oil) |
| Dimensions | 4.5 inch Diameter x 8 inches long |
| Thermal mass of filter ($mC_p$) | 0.28BTU/°F |
| Thermal mass of oil ($mC_p$) | 1.62BTU/°F |
| Combined (oil + filter) thermal mass | 1.9 BTU/°F |

The potential energy storage in a passive PCM-ESD for the oil filter was examined by comparing the temperature rise of the oil and filter that is required to equal the energy stored in the latent heat of the PCM. Figure 2.7 shows the result of the comparison. Two lines are plotted, which correspond to the expected range of the latent heat of the candidate PCM (50-75 BTU/lbm). It can be seen that three lbm of the PCM can store the same amount of energy (as latent heat) as the sensible heat stored in increasing the oil and oil filter temperature by 80-120°F. Because the PCM can store large quantities of energy relative to the sensible energy storage in the oil and oil filter, it was concluded that a passive PCM-ESD could be useful for thermal management of the oil filter.

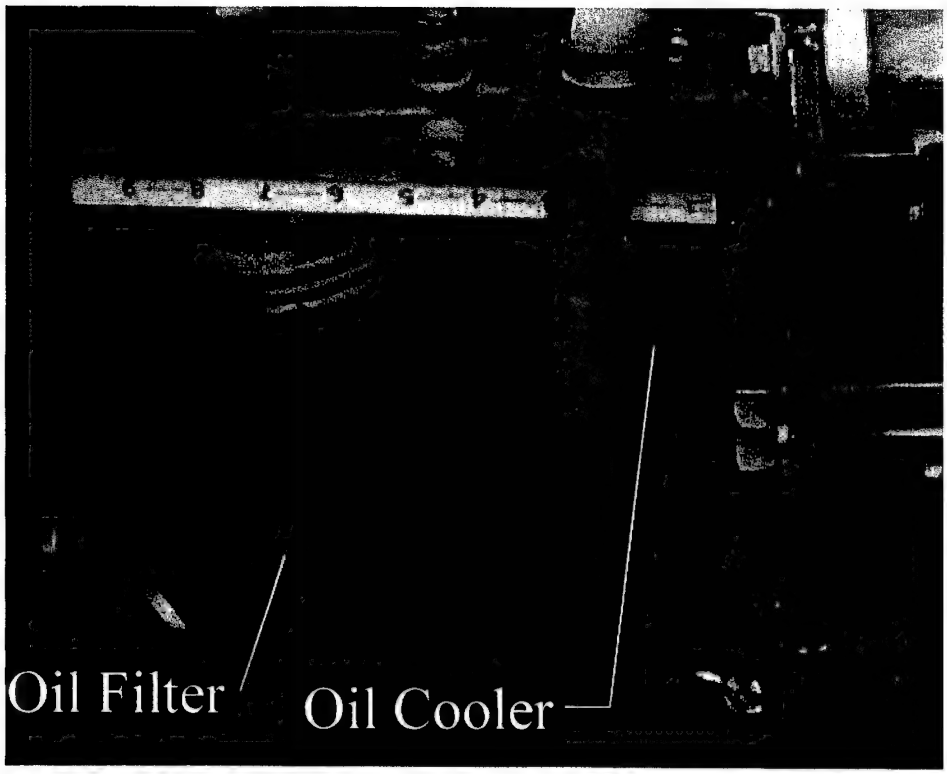


**Figure 2.6**
**Oil Filter Mounted on Cummins C6TA 8.3 liter Engine**

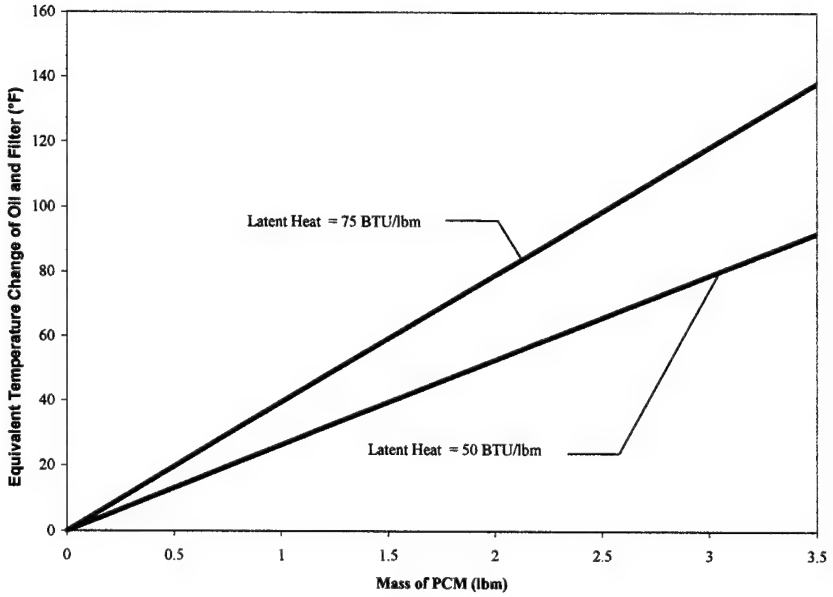


**Figure 2.7**
**Comparison of the Temperature Change of the Oil and Filter to Equal the Thermal Storage in PCM Mass**

### 2.3.3 Battery Thermal Storage

An additional restriction is imposed on the design of the thermal management of the battery that is not present in the design of thermal protection of oil systems: the avoidance of large thermal gradients between the cells of each battery. The concern is that high thermal gradients correspond to high thermal mismatch between the cells which, in turn, leads to large differences in the electrical resistance. A high resistance (cold) cell in series with a low resistance (warm cell) can cause a loss in available cranking current.

The test vehicle uses four 12-volt batteries in a series-parallel configuration for starting the truck and operation of auxiliary devices. The details and dimensions of the batteries and battery box are given in Table 2.3. A photograph of the battery box is shown in Figure 2.8. Note that there is limited space around the batteries for the addition of PCM. The battery box sits on the floor of the cab and forms the base of the passenger seat. The thermal storage of the sensible heat of batteries is compared to the PCM latent heat and the results are shown in Figure 2.9. At the conservative limit of 17 lbm of PCM, which allows space in the battery box for insulation, the PCM adds minimal thermal capacity to the thermal storage already present in the batteries. The latent heat storage of the 17 lbm of PCM adds less thermal storage than simply increasing the temperature of the batteries by 6°F. For this reason, PCM thermal storage was not explored further as part of the thermal management system for the batteries. Instead, the approach selected was to explore thermal management of the batteries using vacuum insulation to reduce the heat lost from the batteries and use an active means (electric resistance) to heat the batteries during operation of the vehicle.

**Table 2.3**
**Batteries Used in the Test Vehicle**

| | |
|---|---|
| Battery Type | Exide 6-TN, 12Volt |
| Number and Arrangement | Four in a series/parallel configuration |
| Location of Battery Box | Under Passenger seat |
| Battery Weight | 4x78 lbm = 312 lbm |
| Battery thermal Mass ($mC_p$) | 243 BTU/°F |

**Figure 2.8**
**Photograph of the Battery Box in the Test Vehicle**

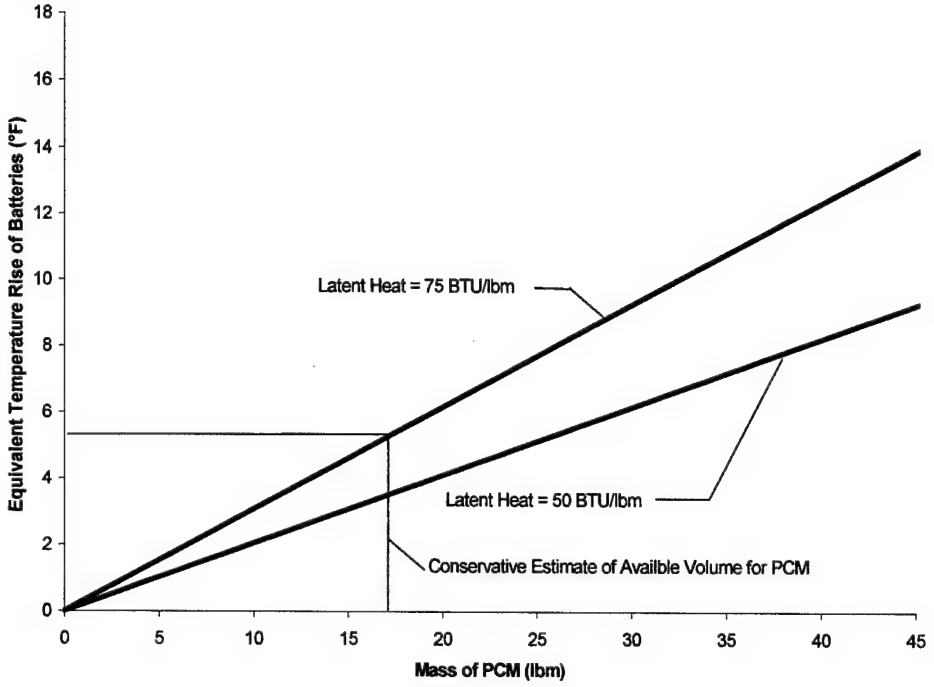


**Figure 2.9**
**Comparison of Thermal Storage in the Batteries vs. Thermal Storage in the Latent Heat of the PCM**

## 2.4 Design Method and Analysis for PCM-ESD Applied to the Oil Pan

### 2.4.1 Volumetric Thermal Storage Capacity for PCM Forms

The relative merits of various PCM-ESD treatments for the oil pan of the test vehicle were examined on the basis of potential energy storage relative to a reference temperature of 32 °F. The selection of 32°F as the reference point was motivated by the desire to maintain the oil above a temperature of 32°F.

It was assumed that the oil pan, with an approximate surface area of 700 $in^2$, was covered by PCM-ESD over 70% of the surface (500 $in^2$) and the rest of the oil pan surface would be covered by insulation alone. The reason for this assumption was that in practice it would be difficult to completely cover the oil pan with a significant thickness of PCM considering problems with interference on assembly of the retrofitted PCM-ESD to the vehicle. It should be noted that if the PCM-ESD system were designed along with the engine before the vehicle is designed, the fractional surface area coverage of the oil pan with the PCM-ESD could easily be increased.

Two forms of PCM, which melt and freeze around 45°F, were considered in the analysis. The gel and powdered forms were selected for the study because it was thought that the two forms represented the best combination of thermal expansion characteristics, energy storage per volume, and cost. The properties of the PCM used for the analysis are shown in Table 2.4. The properties were based on the best available information at the time of the analysis and are representative of the properties of Gels and powders formed from silica and a commercially available hydrocarbon-based PCM. As shown in Table 2.4 the gel has a higher fraction of PCM and higher density corresponding to higher energy storage per volume.

**Table 2.4**

**Characteristics of PCM Used for Initial Design Calculations of Oil System PCM-ESD**

| | Gel | Powder |
|---|---|---|
| Constituents | 77% PCM/ 23% Silica | 65% PCM/ 35% silica |
| Latent Heat (BTU/lbm) | 59 BTU/lbm | 50 BTU |
| Specific Heat (BTU/lbm °F) | 0.53 | 0.49 |
| Density (lbm/ft$^3$) | 56 | 34.5 |
| Thermal Conductivity (BTU/ft-hr-°F) | 0.11 | 0.03 |
| Approximate Melt Temperature (°F) | 45 | 45 |

The energy storage capacity and thermal conduction characteristics were considered for four cases, corresponding to the 2 forms of PCM and PCM-ESD thickness of either 1 or 2 inches:

Case 1: 1 inch thick PCM gel layer (16lbm PCM)
Case 2: 2 inch thick PCM gel layer (32lbm PCM)
Case 3: 1 inch thick PCM powder layer (10 lbm of PCM)
Case 4: 2 inch thick PCM powder layer (20 lbm PCM)

The results shown in Figure 2.10 demonstrate that with the PCM there is a significant increase in energy storage relative to the energy stored in the oil and pan alone. The relative energy storage of the PCM cover relative to the oil and pan improves as the temperature drops. For example, at 50°F the energy stored in two inches of gel is 7 times the energy storage (relative to a reference of 32°F) of the oil and pan. This result emphasizes a major advantage of PCM for thermal management. Not only does the PCM store large amounts of energy, but also it stores it at a temperature that is close to the target temperature. It is usually possible (within practical limits) to increase the thermal energy stored in a component by increasing its temperature. However, heat is quickly lost from hot components, while energy stored at a lower temperature is lost at a lower rate.

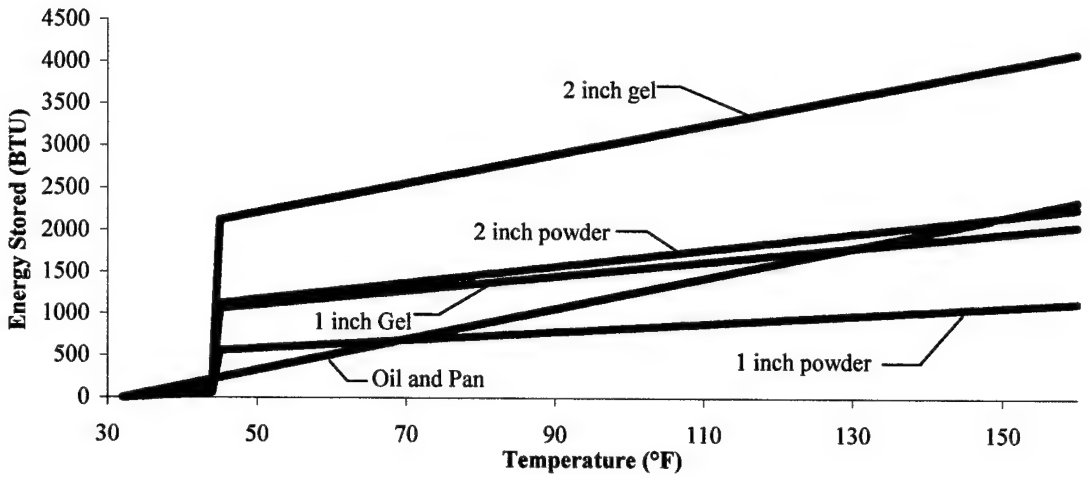


**Figure 2.10**
**Energy Storage potential of PCM-ESD applied to the Oil Pan**

### 2.4.2 Conduction Heat Transfer Considerations

On the basis of potential energy storage of both forms of the PCM are attractive. However, conduction heat transfer through the PCM limits the amount of energy stored during engine operation. The limiting effects of heat conduction through the PCM were studied by considering heat conduction through a one-dimensional layer of PCM shown in Figure 2.11. The one-dimensional layer was an idealized representation of a PCM cover that that is placed in contact with the hot oil pan surface.

It was assumed that the PCM, initially at 32°F and insulated on the backside, is subjected to a surface temperature rise that is maintained for up to ten hours. The spatial distribution of the temperature in the PCM was calculated using the thermal analysis code TOPAZ[10]. TOPAZ is an implicit finite element code, which is used for the analysis of non-linear conduction problems.

In TOPAZ, the wall was divided into an evenly spaced grid of 100 elements per inch for the calculations. For simplicity it was assumed that there was no contact resistance between the oil pan surface and the top surface of the PCM –ESD layer shown in Figure 2.11. It was assumed that the oil pan surface (top surface of the PCM) was maintained at a constant temperature 160°F through out the calculation.

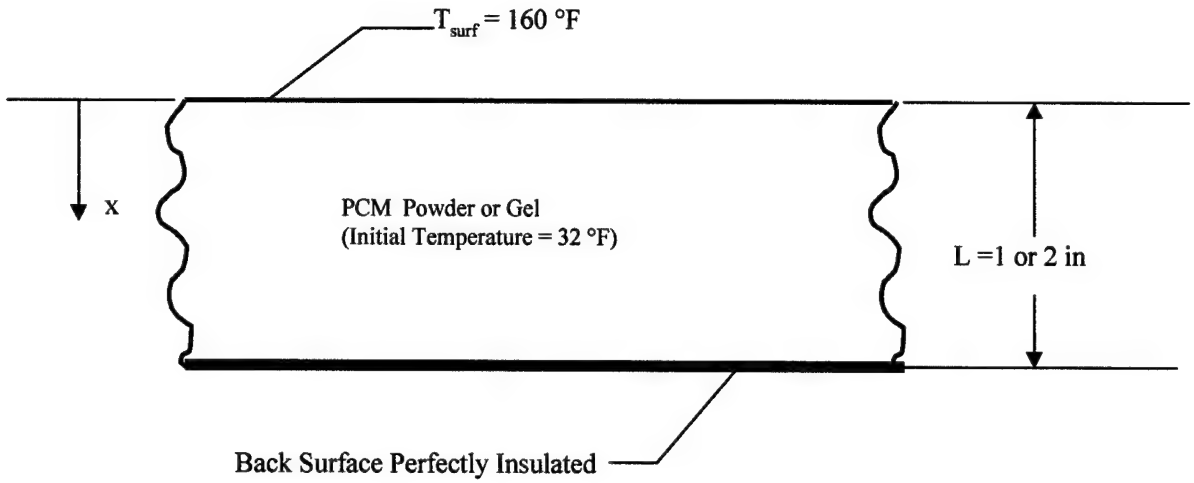


**Figure 2.11**
**One-Dimensional PCM-ESD Layer for Heat Conduction Study**

In heat conduction calculations involving PCM, non-linearity occurs because of the large changes in thermal properties associated with phase change. Algorithms have been specifically developed for phase change calculations that assume that the phase change occurs over an infinitesimal range of temperature. For the PCM considered in this study the phase change occurs over a finite temperature band. Experimental evidence of the finite width of the phase change is seen from Differential Scanning Calorimetry (DSC) measurements of the specific heat of the PCM. The effect of the phase change was approximated as shown in Figure 2.12. The specific heat was increased in a finite region around the phase change temperature so that the latent heat of the PCM, $\Delta h$ was calculated by:

$$\Delta h = \Delta T \, C_{P,} \qquad (2.3)$$

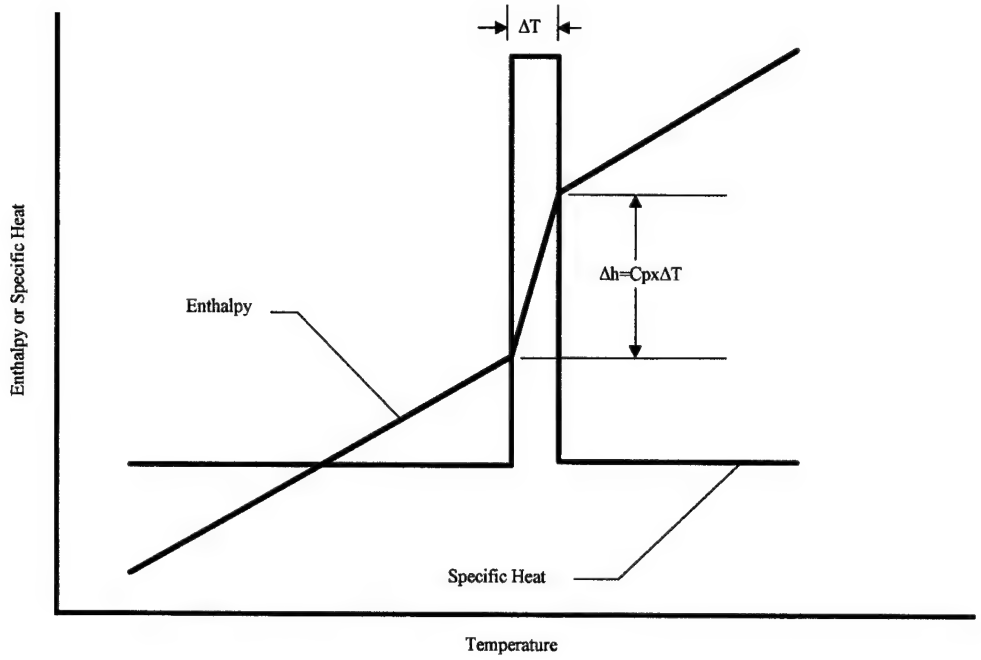


**Figure 2.12**
**Thermal Model of the Phase Change Enthalpy**

Figure 2.13 shows the temperature history for progressive depths through the PCM-ESD, as a function of time for case 2 (2" of PCM gel). All of the gel PCM changes phase within the first 5 hrs. After ten hours the minimum temperature (on the back face of the PCM) is 141°F. The energy storage of the PCM-ESD (relative to a 32°F reference) is also shown in Figure 2.13. Because of the high temperature increase of the PCM above the melting point, roughly 50% of the energy stored in the PCM-ESD stored as latent heat of phase change and the rest is from the sensible energy of the PCM. At the end of ten hours the PCM-ESD has absorbed 94 % of the ideal capacity of 4114 BTU, which would be realized if all of the PCM had reached the top surface temperature.

The results for case 4 (2" thick PCM powder) are shown in Figure 2.14. Because of the lower thermal conductivity of the powder, the temperature rise at depths away from the hot surface is less for the powder than for the gel form. The temperature distribution in Figure 2.14 shows that over nine hours are required for all of the PCM to change phase. After ten hours the powder temperature ranges from 160°F at the surface to 68°F on the back face. The energy storage for this case is also shown in Figure 2.14. The total energy storage stored for this case is only 73% of the ideal storage of 2248 BTU.

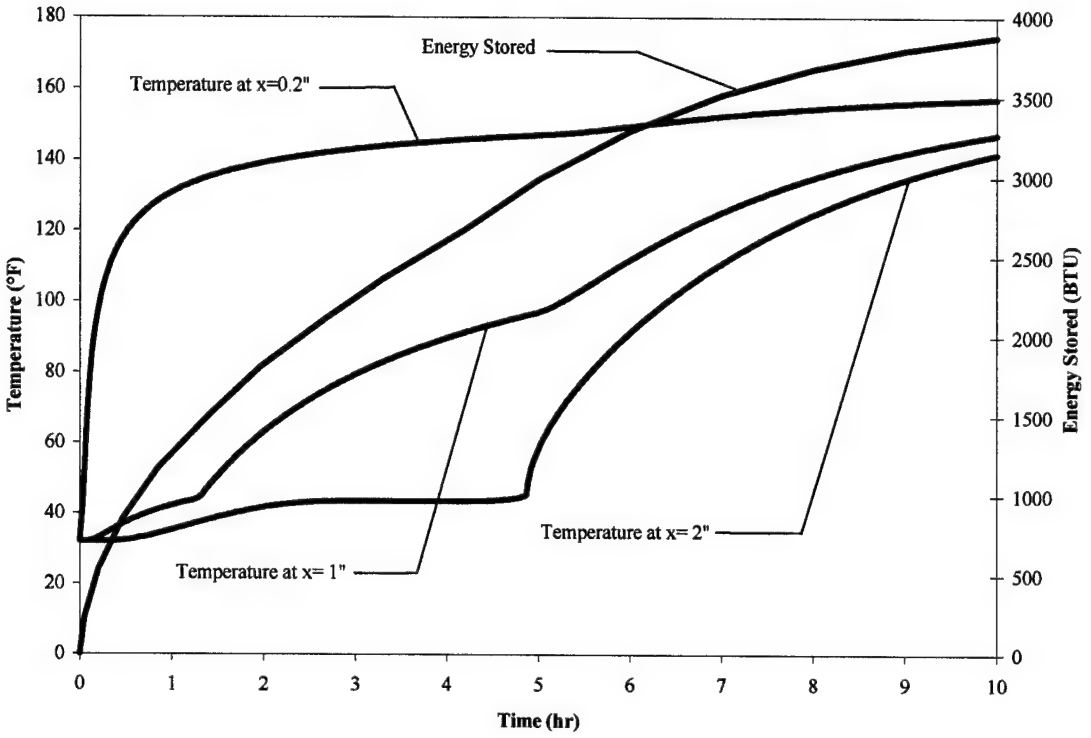


**Figure 2.13**
**Temperature Distribution and Energy Storage for Case 2 (PCM Gel, 2"-Thick)**

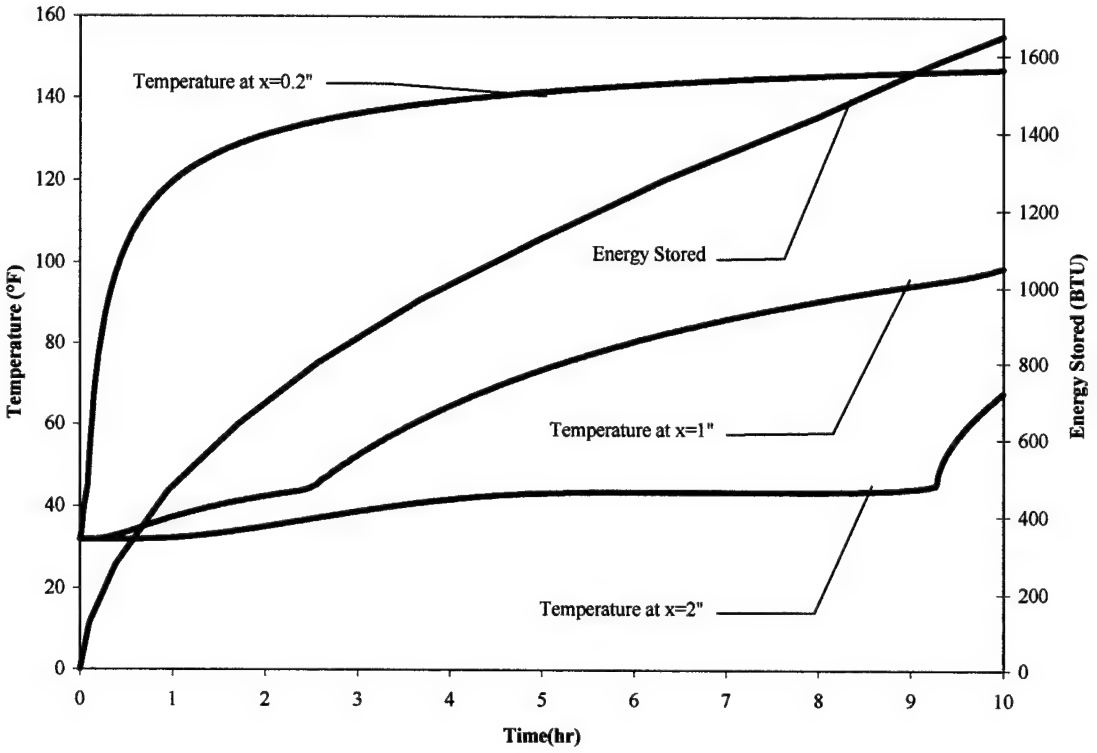


**Figure 2.14**
**Temperature Distribution and Energy Storage for Case 4 (PCM Powder, 2" thick)**

A summary of the energy stored for the four cases is shown Figure 2.15. Both of the 1-inch thick layers of PCM become almost "fully charged" by the end of ten hours. The two PCM-gel cases store more energy in two hours of exposure to the hot top surface than the two PCM-powder cases can store in ten hours. Although the ideal energy storage of the 2" thick layer of PCM-powder is more than that of the 1" PCM-gel layer the greater storage capacity of the thicker PCM-powder is not realized because of the low thermal conductivity of the powder. On the basis of energy storage density and ease of heat transfer it was determined that the gel is the preferred form of the PCM.

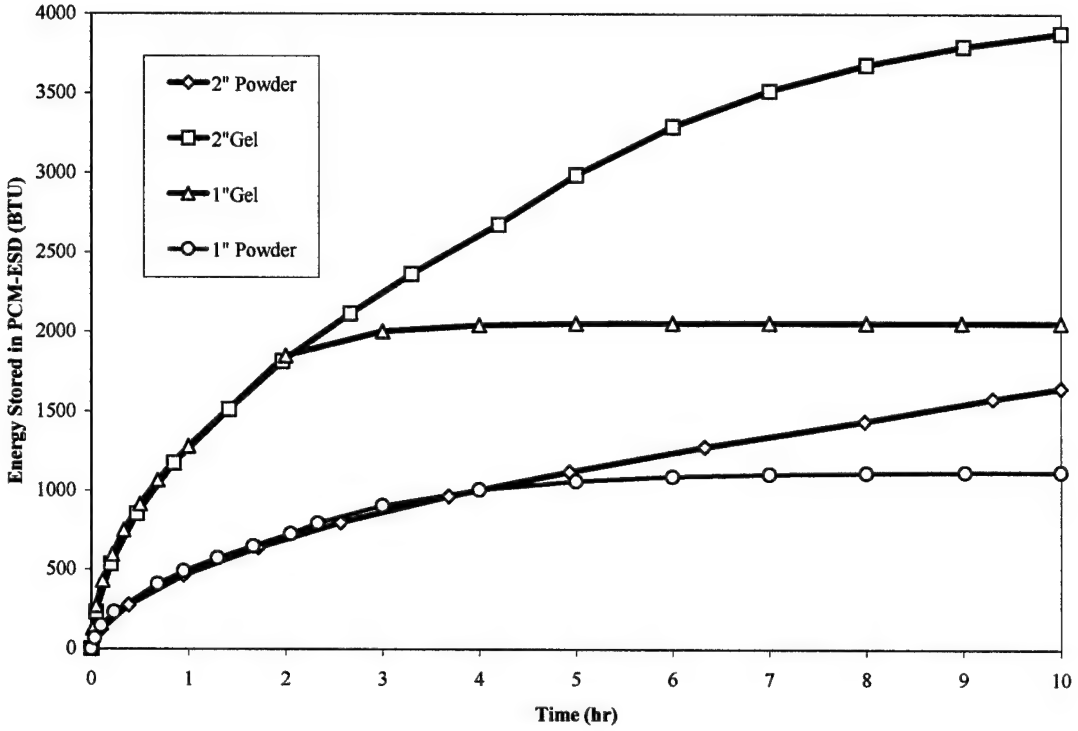


**Figure 2.15**
**Energy Stored in PCM Covers for Oil Pan**

### 2.4.3 Conduction Enhancement of the PCM-ESD

The results of the one-dimensional layer study considered above clearly emphasize the importance of "short thermal path," which can be realized by a short physical path length or a high thermal conductivity, or both. Because thin layers of material correspond to low amounts of thermal energy storage, other means were examined to enhance conduction through the PCM.

Fins made of a high thermal conductivity material are a common method of enhancing heat conduction through a lower conductivity. As shown in Figure 2.16, a narrow fin can provide a shorter thermal path through a lower thermal conductivity medium. High thermal conductivity materials, particularly aluminum and copper, were considered for incorporation into the ESD's as fins. After considering the relative merits of conductivity, material costs, and manufacturing costs, a commercially available aluminum honeycomb was chosen to enhance conduction through the PCM.

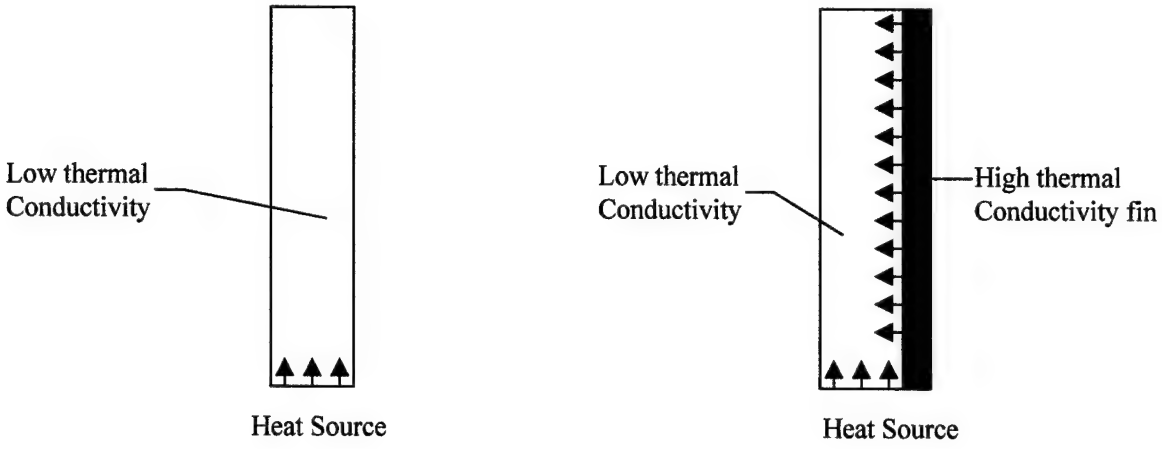


**Figure 2.16**
**The Use of High Conductivity Fins to Provide a Shorter Thermal Path Through the Lower Conductivity PCM**

The Aluminum honeycomb chosen for the concept development ESD design was Flexcore flexible aluminum honeycomb, manufactured by Hexcell Corporation (see Figure 2.17). The honeycomb is made from 0.0019-inch thick walls of 5052 Aluminum. As shown in Figure 2.17 (B), the Flexcore will bend or compress along one axis. When the Flexcore is fully expanded it has a density of only 3.1 lbm/ft$^3$ and has a nominal cell spacing of 40 cells per ft. The aluminum Flexcore displaces less than 2% of the total volume of the PCM-ESD, but provides a much shorter thermal path as a result of its higher thermal conductivity (over 1200 times that of the PCM).

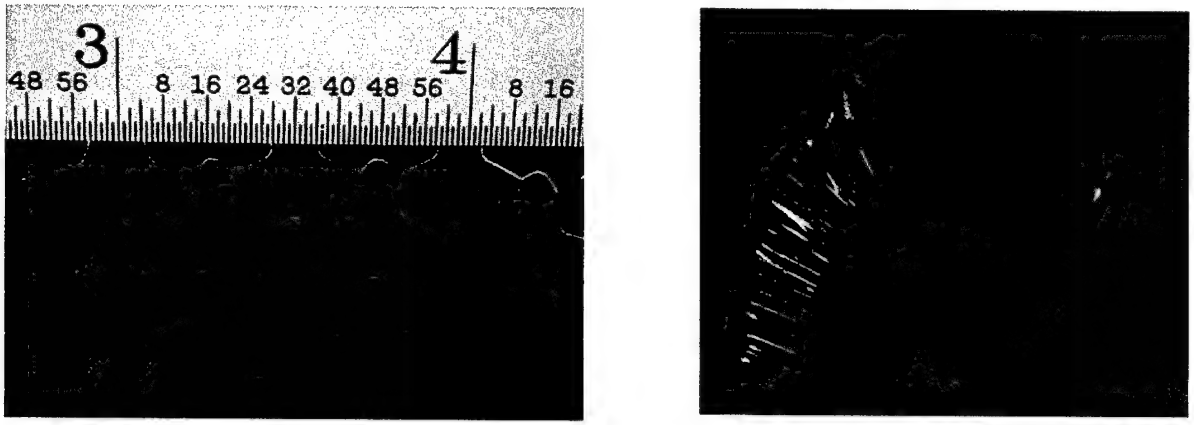


(A) (B)

**Figure 2.17**
**Hexcell Flexcore Honeycomb (A) End-View of Flexcore, (B) Flexcore Wrapped Around the Surface of Oil Pan**

### 2.4.4 Performance Estimates of PCM-ESD Incorporating Flexcore Honeycomb on Oil Pan

#### 2.4.4.1 PCM Material

The PCM selected for the proof of concept design was a gel composed of 75% hexadecane ($C_{16}H_{18}$) and 25% Silica. Hexadecane is a linear alkyl hydrocarbon and was chosen because of its high latent heat of fusion and the location of its freezing point (≈66°F) relative to the design goal of 32°F for the oil temperature. The high melting point for the PCM was chosen to provide a significant temperature difference between the PCM and the oil to enhance heat conduction from the PCM to the oil as the PCM freezes. The drawback of increasing the PCM phase change temperature is that the temperature potential to the outside cold environment increases, which increases the rate of heat lost to the outside environment. The hexadecane is the PCM and the silica serves as a stabilizing matrix. The PCM was contained in the gel form because of its low thermal expansion relative to the neat form. The Hexadecane was 99% pure and the remaining 1% consists of various other hydrocarbons. The silica used to form the gel was Cabot BXS-303, which a hydrophobic form of silica.

The specific heat and the total thermal energy content of the gel were determined by Differential Scanning Calorimetry (DSC). DSC is a well-developed technique for determining the apparent specific heat over a range of temperatures. A plot of the specific heat and thermal energy content of the hexadecane-gel is shown in Figure 2.18. A large peak can be observed in the specific heat between 55 and 71 °F as the PCM changes phase. Note

that as the PCM gel freezes it hardens but does not undergo significant expansion or contraction. Other properties of hexadecane are listed in Table 2.5.

**Table 2.5**
**Hexadecane Gel Properties**

| Property | Value |
|---|---|
| Specific Gravity | 0.85 |
| Melt Peak | 66 °F |
| Specific Heat (frozen) | 0.41 BTU/lbm °F |
| Specific Heat (thawed) | 0.55 BTU/lbm °F |
| Latent Heat | 76 BTU/lbm (between 55°F and 71°F) |
| Vapor Pressure of Neat Hexadecane 75 °F | $4 \times 10^{-4}$ PSI |
| Vapor Pressure of Neat Hexadecane 350 °F | 1.2 PSI |
| Boiling Point of Neat Hexadecane | 549 °F |

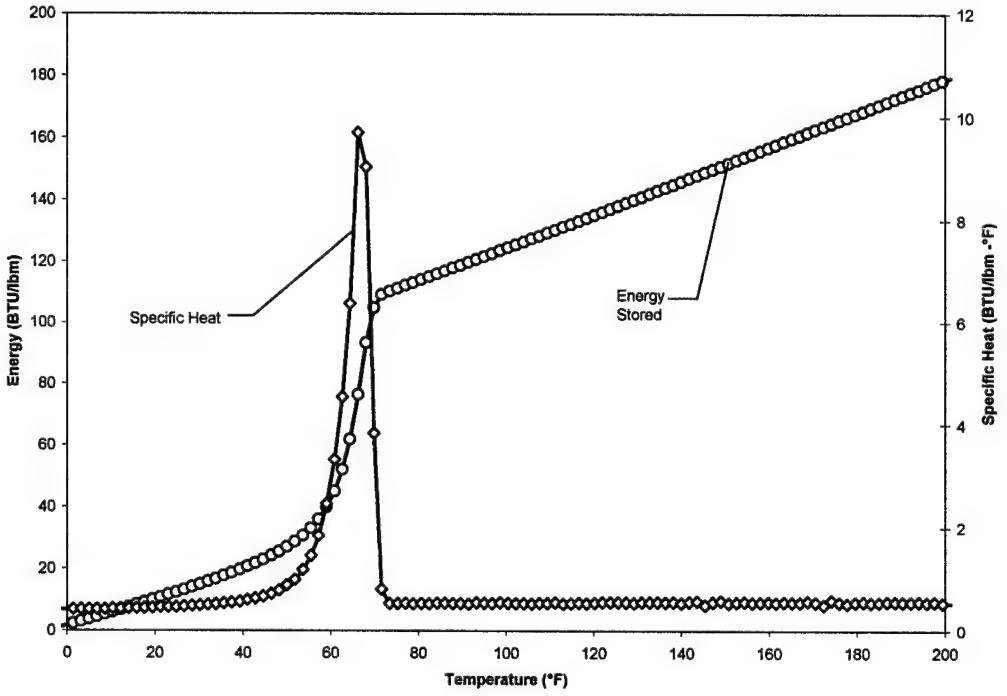


**Figure 2.18**
**Thermal Storage (Relative to a Baseline at –4°F) and Specific Heat of the Hexadecane-PCM Gel (75% Hexadecane-25% Silica)**

### 2.4.4.2 Performance Estimates For Oil Pan PCM-ESD

After selecting the hexadecane PCM performance estimates were conducted using finite element analysis. The heat transfer through representative PCM-ESD layers, with and without the Hexcell Flexcore honeycomb, and with various masses of PCM and insulation thickness, was characterized.

A conceptual sketch of the thermal model used for the calculations is shown in Figure 2.19. The oil was considered as a lumped thermal mass, which means that at any given time all of the oil is at a single temperature throughout. The lumped thermal mass assumption greatly simplifies the analysis by removing the considerations of natural convection of the oil. While it is recognized that in practice the oil will contain thermal gradients, natural convection resulting from the presence of the PCM-ESD heat sources on the sides and bottom of the pan will tend to encourage oil mixing and uniformity. This mixing of the oil is in contrast to the baseline oil pan where natural convection without a heat source on the pan bottom and sides will lead to thermal stratification of the oil.

In the model there are three heat loss paths from the oil in the pan to its surroundings. Heat Loss Path 1 is the combination of the conduction through the oil pan to the engine block and the convection from the top surface of the oil to the block. The convection heat transfer from the top surface of the oil to the inside of the engine block was modeled using a cavity convection model. The conduction from the oil pan to the block was modeled assuming that the only thermal resistance was that in the pan between the top surface of the oil and block. The conservative assumption of zero contact resistance (due to the bolts and gasket) was assumed for the connection between the oil pan and the block. The block temperature for the model was calculated by extrapolating the block temperature measured during baseline cool-down tests conducted at 20°F to 0°F. Conduction through the oil suction tube was not modeled because of insufficient knowledge of the geometry when the calculations were performed; however, it was thought that the omission of the suction tube would be offset by the conservative nature of the assumptions for conduction through the oil pan.

Path 2 is conduction from the surface of the oil pan through the insulation placed around the pan to the outside environment. The thermal resistance of the insulation in Path 2 was a parameter in the analysis. Path 3 is between the oil and the PCM/ESD. It was assumed that the oil and inner layer of the PCM-ESD were in perfect contact (no contact resistances or thermal resistance of the oil pan). The final heat loss path considered in the model, Path 4, is

the conduction through the insulation on the backside of the PCM-ESD to the environment. The insulation on the outside of the pan was also a parameter in the analysis. The area of the oil pan assumed to be covered by the PCM-ESD was 325 $in^2$ and the rest of the oil pan was assumed to be covered by insulation alone.

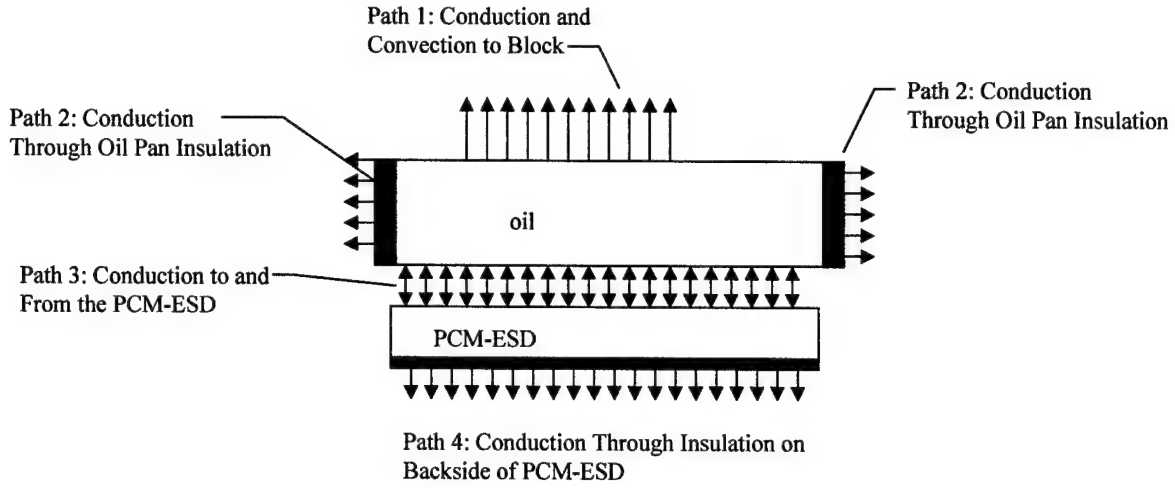


**Figure 2.19**
**Heat Paths Considered in Performance Estimate Calculations**

Heat conduction through the PCM-ESD was modeled using the finite element code TOPAZ. A two-dimensional axi-symmetric grid was used to represent a single cell of the Aluminum Flexcore and the PCM. The cell of the Flexcore and PCM was modeled assuming cylindrical geometry for the cell with an equivalent radius (0.16 inch-diameter) rather modeling the more complicated cross section (See Figure 2.17A) that would have required a three-dimensional calculation. The grid used to model the PCM-ESD is shown in Figure 2.20. A total of 2625 elements (21 radial x 125 deep) were used to model the PCM-ESD and insulation layers. The large number of elements was required to accurately model conduction through the thin aluminum (high conductivity) Flexcore material. The model used for all of the calculations assumed that the PCM-ESD layer was 2" thick and that the layer of insulation on the backside of the PCM was 0.5" thick. Various levels of insulation on the backside of the PCM-ESD (denoted as $R_{pcm}$) and on the rest of the pan ($R_{pan}$) were considered during the analysis. The mass of the PCM was changed from case to case by varying the density of the PCM.

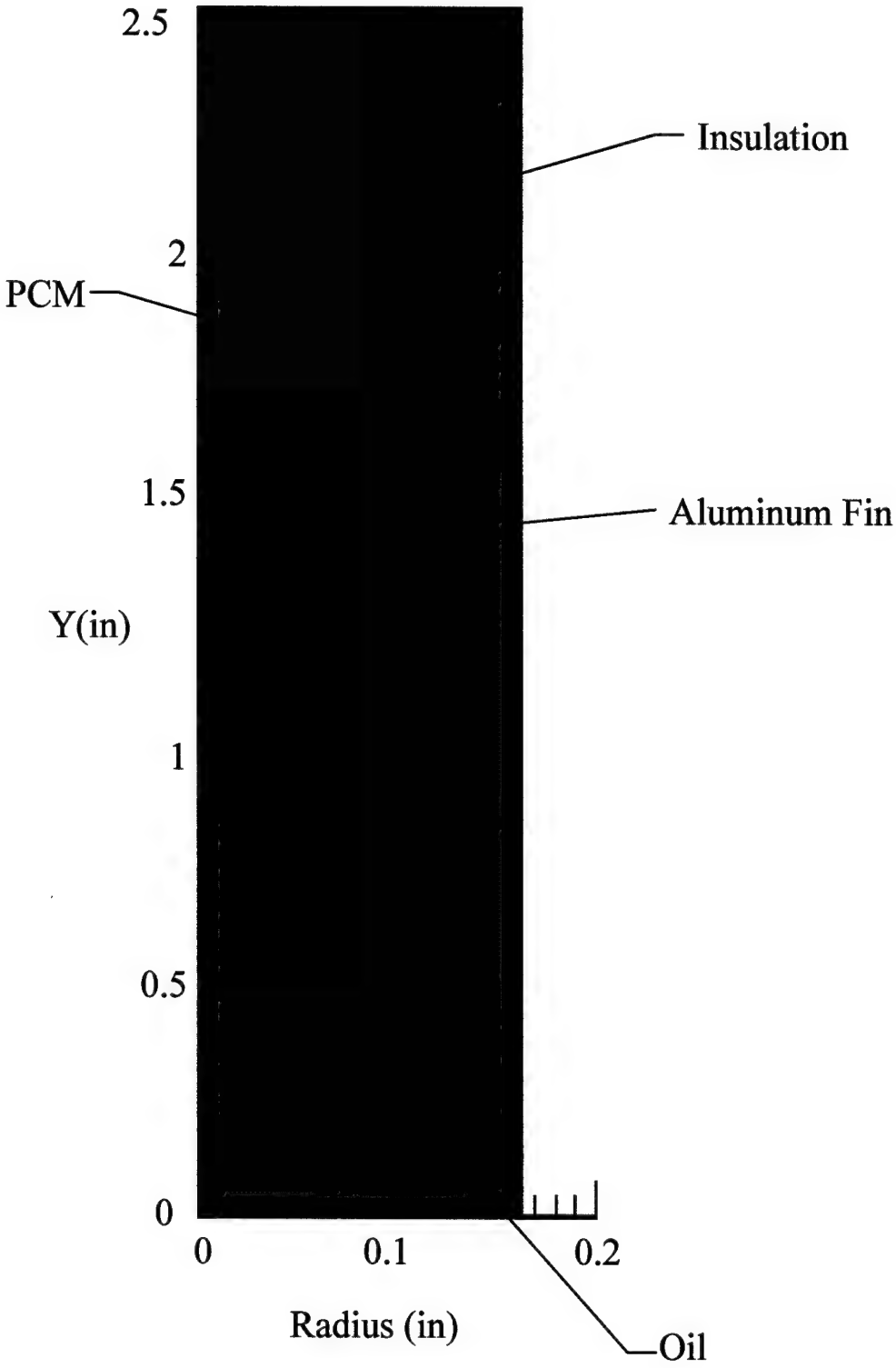


**Figure 2.20**

**Finite Element Grid Used for Modeling the PCM-ESD (Grid Aspect Ratio Not to Scale)**

The thermal loads from paths 1 and 2 were applied to the top surface of the oil, which was considered to be in perfect thermal contact with the inner surface of the PCM-ESD. All of the analysis assumed that the outside air temperature was a constant 0°F and that the engine operated for 6 hrs and then shut off. The maximum oil temperature (203°F) during operation was based on the oil temperatures measured during baseline tests of the vehicle, which are discussed in Section 3 of this report.

The results from the first two cases, shown in Figures 2.21 and 2.22, show the effect of the Flexcore (aluminum honeycomb) on the performance of the PCM-ESD. The first case (Figure 2.21) assumed no addition of Flexcore and the second case (Figure 2.22) assumed that Flexcore was incorporated through the 2" PCM thickness. The PCM mass (20lbm) and the insulation thickness on both the outside of the ESD and the rest of the oil pan were the same for both cases. The insulation on the outside of the PCM-ESD corresponds to a single layer of ½" polyisocyanurate insulation ($R_{PCM}$=3.5 hr-ft-°F/BTU). The insulation on the outside of the rest of the pan ($R_{pan}$=10.5 hr-ft-°F/BTU) corresponds to a 1.5-inch thick layer of polyisocyanurate.

The case without the Flexcore (Figure 2.21) shows large temperature gradients across the entire PCM-ESD during both engine operation and engine cool-down as a result of the low thermal conductivity of the PCM. All of the PCM-ESD does not pass through phase change during the six-hour engine operation period. In fact, the maximum temperatures on the backside of the PCM-ESD occur over 2.75 hrs after engine shut down. At the end of the time period there is excess energy stored in the ESD but the low conductivity prevents sufficient flow of energy to maintain the oil at an acceptable temperature.

The addition of a layer of Flexcore aluminum causes a dramatic effect in the heat conduction in and out of the PCM-ESD. The results shown in Figure 2.22 show that the temperature gradients across the PCM-ESD are lowered as a result of the higher conductivity across the PCM. The addition of the aluminum Flexcore allows the ESD to be charged in less than 2 hours in contrast to over six hours without the Flexcore. In addition, the PCM temperatures at the end of engine operation were much higher than those calculated for the case without the Flexcore. A comparison of the oil temperatures (Figure 2.23) shows that the PCM-ESD is most effective if the conductivity is enhanced by the high conductivity Flexcore. Because of the low thermal conductivity of the PCM, the case without the Flexcore material stores less energy during engine operation and the heat transfer back to the oil is

lower than that for the case with the Flexcore. Note that if the operation time of the engine were shorter the difference between the two cases would be greater because of the poor conduction characteristics of the case without the Flexcore.

As a result of the marked difference shown by the presence of the Flexcore, it was decided that the Flexcore aluminum honeycomb would be incorporated in all subsequent calculations and in the final design of the PCM-ESD. The effect of the PCM mass on the oil temperature is shown in Figure 2.24. It is shown that the effect of the PCM mass is approximately linear. Decreasing the PCM mass from 20 lbm to 10 lbm decreases the time that the oil is above 32°F by approximately 3 hrs. Eliminating the PCM altogether would decrease the time that the oil is above 32°F by another 3 hrs. For PCM masses between 10 and 20 lbm, the time that the oil is above 32°F for the oil could be approximated by interpolation.

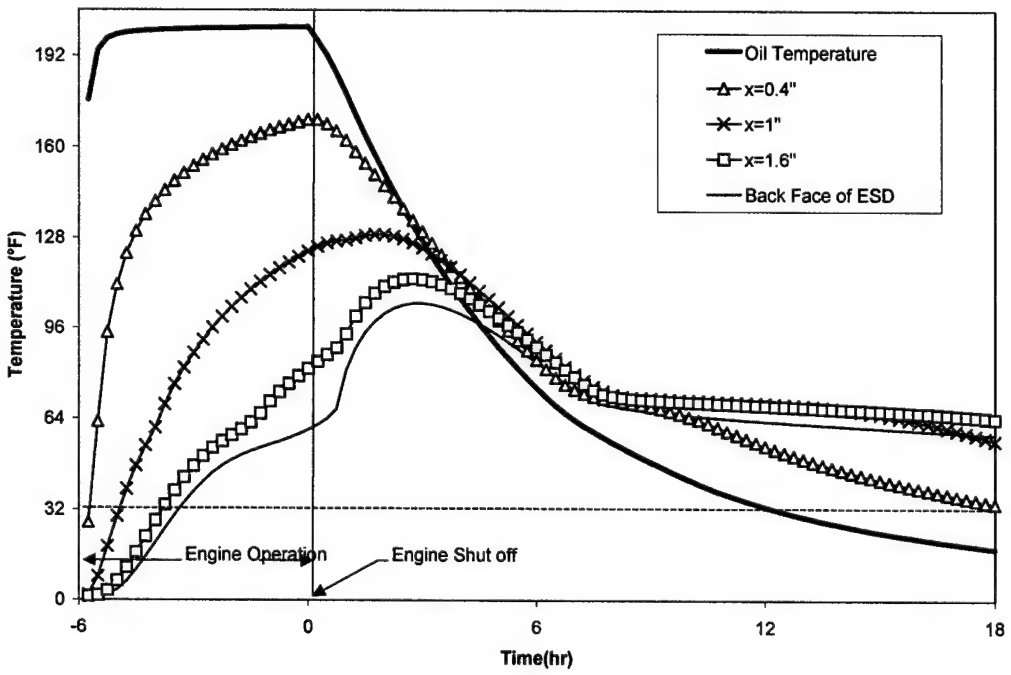


**Figure 2.21**
**Simulation of Oil Temperature and PCM-ESD Temperatures for Case Without Flexcore ($M_{pcm}$ = 20 lbm, $R_{pcm}$ =3.5, $R_{pan}$ =10.5)**

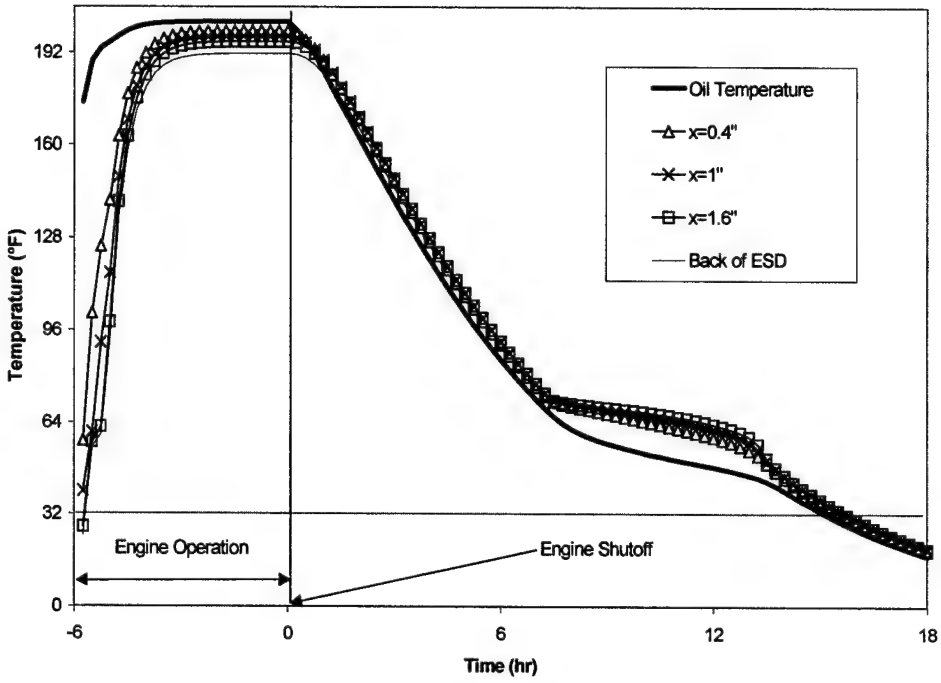


**Figure 2.22**
**Simulation of Oil Temperature and PCM-ESD Temperatures for Case With Flexcore Thickness = PCM Thickness ($M_{pcm}$ = 20 lbm, $R_{pcm}$ =3.5, $R_{pan}$ =10.5)**

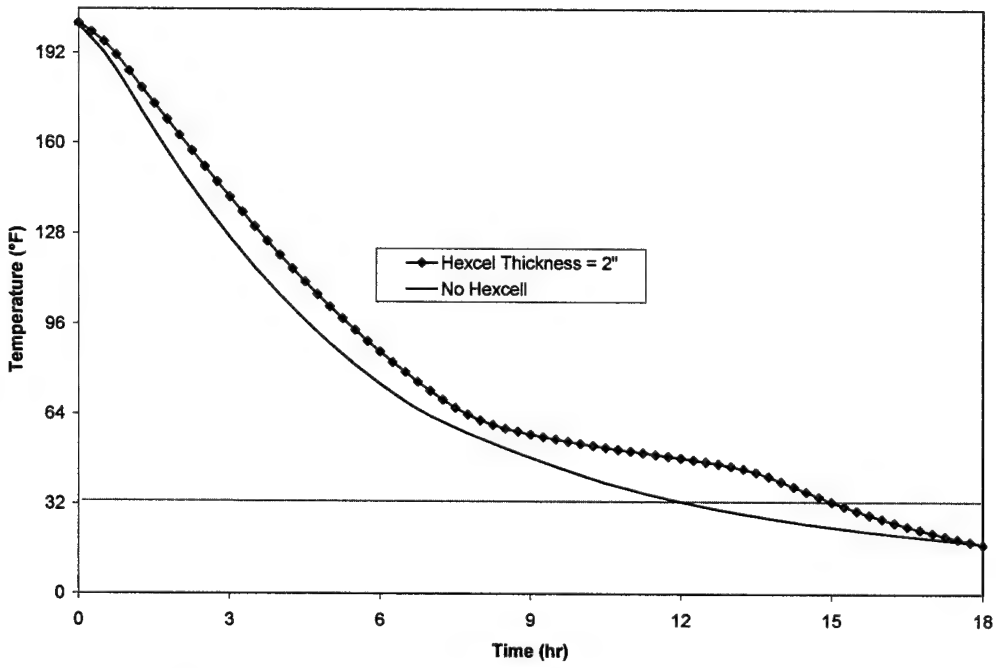


**Figure 2.23**
**Effect of Hexcell Flexcore on Oil Temperature During Engine Cool-Down ($M_{pcm}$ = 20 lbm, $R_{pcm}$ =3.5, $R_{pan}$ =10.5)**

The effect of insulation on the performance is shown in Figure 2.25. It is shown that a three-fold increase in the insulation surrounding both the oil pan and the ESD only increases the time that the oil is above 32°F by 45 minutes. The reason for the small incremental improvement is that that the predominant path for heat leakage is not through the insulation surrounding the oil pan ESD, but is through the engine block. Although the higher thermal resistance of the increased insulation decreases the energy lost from the oil pan, the energy is eventually lost by conduction through the block.

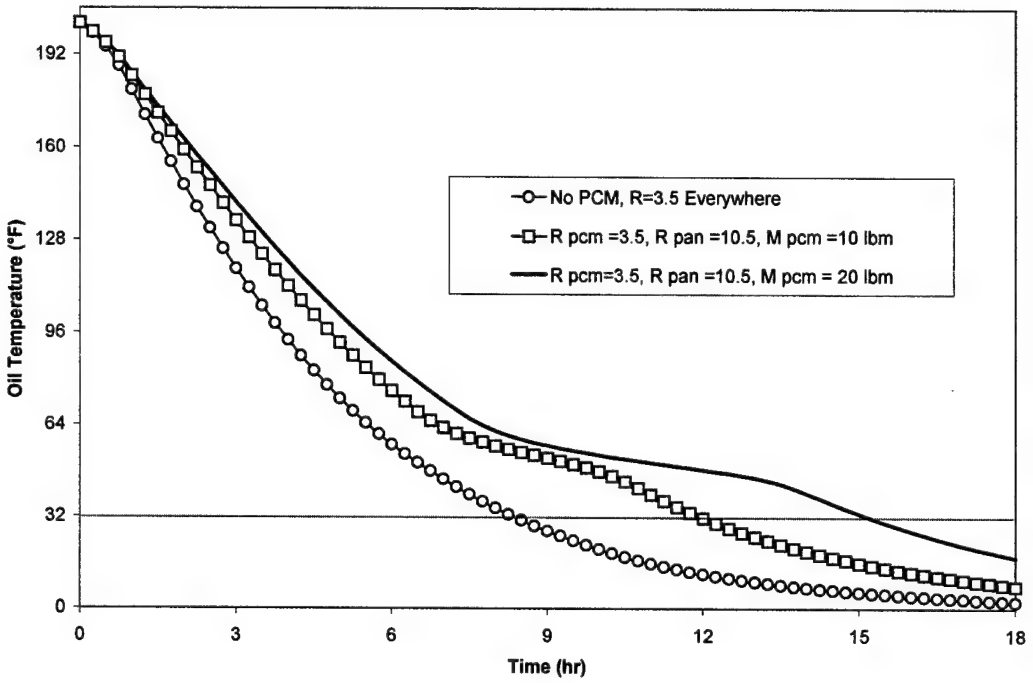


**Figure 2.24**
**Simulation of Effect of PCM Mass on Performance of Oil Pan PCM-ESD**

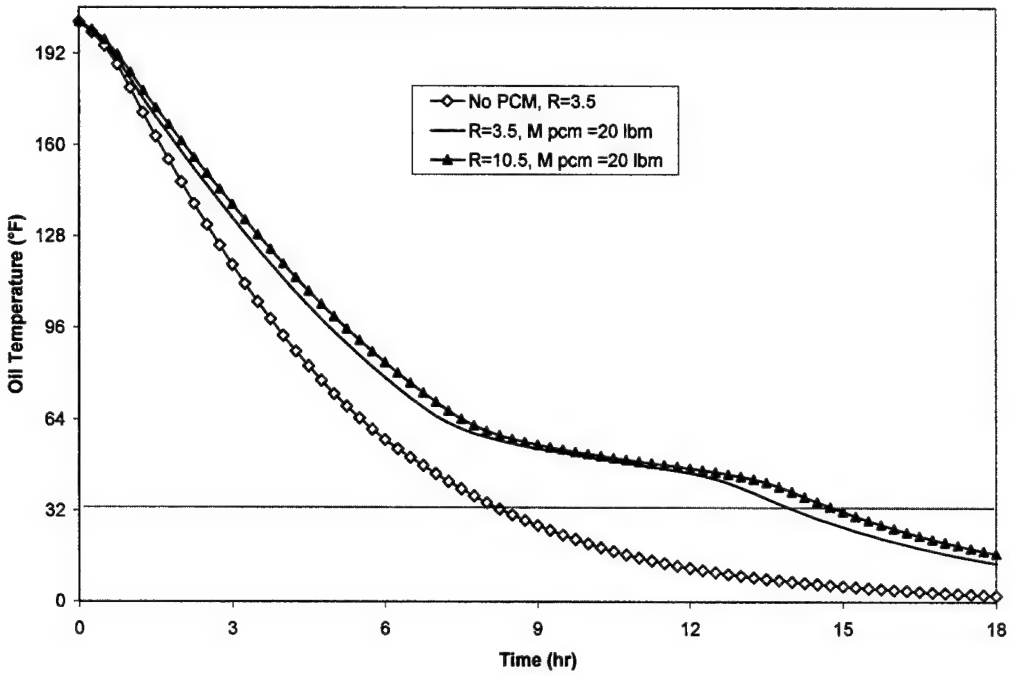


**Figure 2.25**

**Simulation Effect of Insulation on the Oil Pan PCM-ESD Performance**

## 2.5 Final Design Configuration of the Thermal Protection System

### 2.5.1 Oil Pan PCM-ESD Design

After conducting the analysis, which was discussed in the previous section, attention was turned to building a practical proof-of-concept PCM-ESD system for the test vehicle oil pan. Early in the design effort concepts which included a single outer shell were considered. However this method was not feasible because of concerns with installation. Note that the design of the oil pan PCM-ESD had to be retrofitted onto the vehicle in a parking lot in the middle of winter. Although there is plenty of space around the oil pan for a compact continuous shell, installation of a continuous shell was not possible because of interference from various chassis and suspension components. In fact, it was impossible to completely remove the oil pan from the truck without providing additional clearance between the bottom of the engine and the front drive train components. A vehicle jack could have alleviated some

of the clearance problems from the front axle and transfer case. However, one was not readily available and was not acquired because of safety and liability concerns.

The approach that was followed for the development of the PCM-ESD system was to design discrete units that could be readily installed on the outside of the oil pan without clearance problems. Four separate PCM-ESD units were designed to fit against the outer surface of the oil pan as shown in Figure 2.26. The dimensions for each of the PCM-ESD units are shown in Table 2.6. The units were box-shaped with the side that was placed against the pan contoured to fit the pan surface. An example of the complex surface curvature that was necessary to fit the contour of the oil pan is shown in Figure 2.27. To prevent leakage of the PCM (in the gel or vapor form), the ESD's were formed from welded carbon steel. Five of the sides were 14-gauge steel (0.070" nominal thickness) and the sixth side of the ESD was thicker (0.188 in) to provide sealable access holes for filling the device with PCM.

The total weight of the PCM installed in the four ESD units was 15.4 lbm. The energy storage potential in the latent heat of the PCM-ESD (51-71°F) is over 4 times the thermal energy storage of the oil and oil pan over the same temperature range. In the melted state (T>71°F) the sensible heat of the PCM contributes an additional 45% more thermal storage to the oil and oil pan.

Flexcore aluminum honeycomb was installed in the PCM-ESD before welding the back surface onto the PCM-ESD. The Flexcore was cut from one inch-thick stock and was layered for the thicker ESD's so that the honeycomb extended throughout the entire width and was tightly held between the front and back faces of the ESD.

The PCM was hexadecane gel (discussed above) and was added through the access ports. The PCM gel initially poured into the holes. However because of the high viscosity of the gel and the narrow clearances between the ESD walls and the honeycomb it became necessary to inject the PCM under pressure. Comparing the mass of the units before and after filling verified the mass of PCM injected. The mass of PCM injected was close to that expected on the basis of the available internal volume of the ESD.

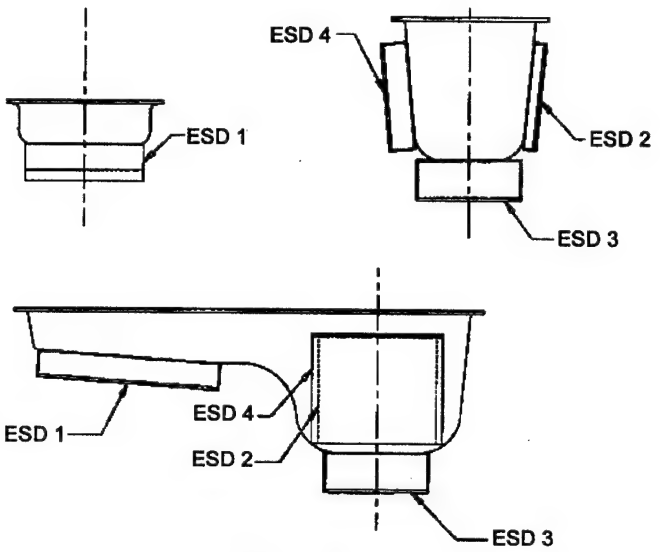


**Figure 2.26**
**Sketch of the PCM-ESD Installed on the Oil Pan**

**Table 2.6**
**PCM-ESD Dimensions for the Proof of Concept Thermal Protection System**

| ESD # | Location | PCM Mass (lbm) | Dimensions | Total Mass (lbm) |
|---|---|---|---|---|
| 1 | Back of Pan Bottom (shallow end) | 4.2 | 9" x 11" x 2" | 14 |
| 2 | Driver's Side (deep end) | 1.6 | 9"x 9" x 1" | 9 |
| 3 | Front of Pan Bottom (deep end) | 4.9 | 8"x 8 "x 3" | 12 |
| 4 | Passenger side (deep end) | 4.7 | 9" x 10" x 2" | 13 |

After the PCM-ESD's were filled, several of the welds leaked but were resealed by either laser welding or epoxy putty. It should be noted that after the test program was over the PCM-ESD units were again weighed and negligible mass was loss.

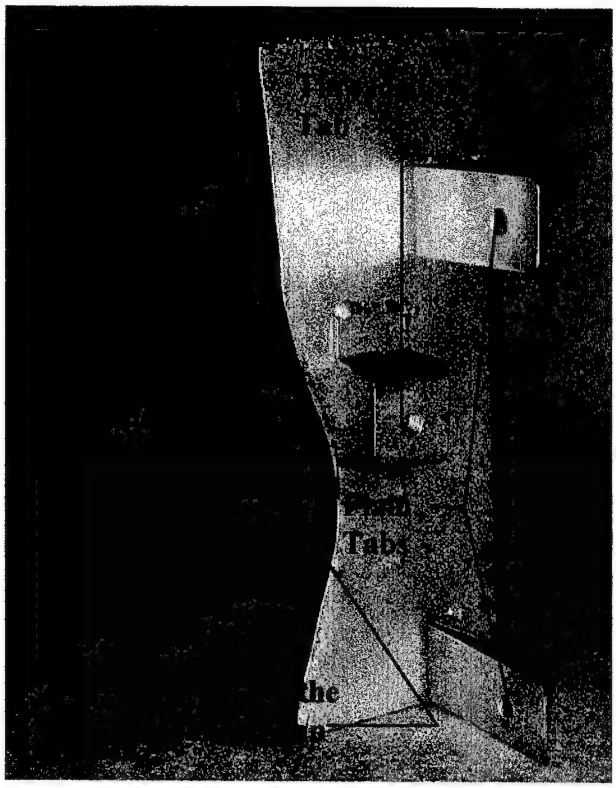

**Figure 2.27**

**Photograph of PCM-ESD # 3 Showing Curvature to mate with the Bottom of Oil Pan**

A photograph of the PCM-ESD's installed on the oil pan is shown in Figure 2.28. The attachment of the PCM-ESD system had to be reversible without any damage or permanent alteration of the vehicle. The PCM-ESD's were attached to the oil pan using a system of brackets and the existing oil pan bolts. ESD #1(Figure 2.29) was installed to the bottom of the shallow section of the oil pan using four steel straps, which were welded to the ESD and were designed to establish contact between the ESD and the oil pan. The two ESD's on the vertical sides of the oil pan (#2 and #4) were each held to the bottom of the engine block by two brackets, which were bolted to the block using the oil pan bolts. The final ESD (ESD #3) which mates with the bottom of the deep end of the oil pan, was attached to the ESD through four machine screws that passed through tabs that were welded to the ESD (See Figure 2.27). The two ESD's that were fitted on the vertical sides of the pan (ESD 's #2 and #4) were pulled toward the sides of the oil pan by two machine screws, which were threaded into tabs on ESD #3.

Although special steps were taken in the manufacture of the ESD's to insure the closest fit, and thus the best thermal contact between the ESD and the oil pan, thermal contact resistance was still a concern. To reduce the thermal contact resistance a thin coating

of high temperature grease, mixed with shredded steel (to enhance the thermal conductivity) was applied to the mating surfaces of the ESD and the oil pan during installation.

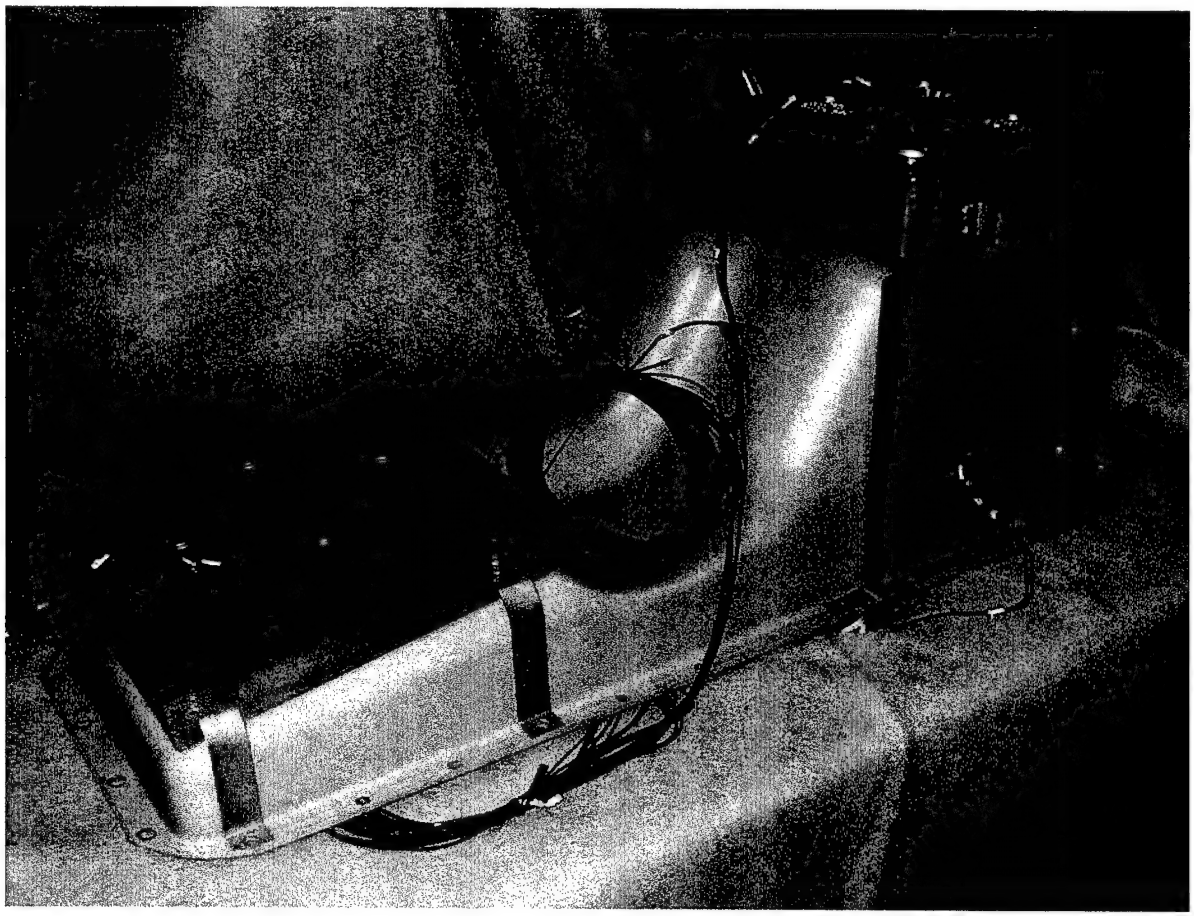

**Figure 2.28**
**Proof -of -Concept PCM-ESD Installed On the Oil Pan**

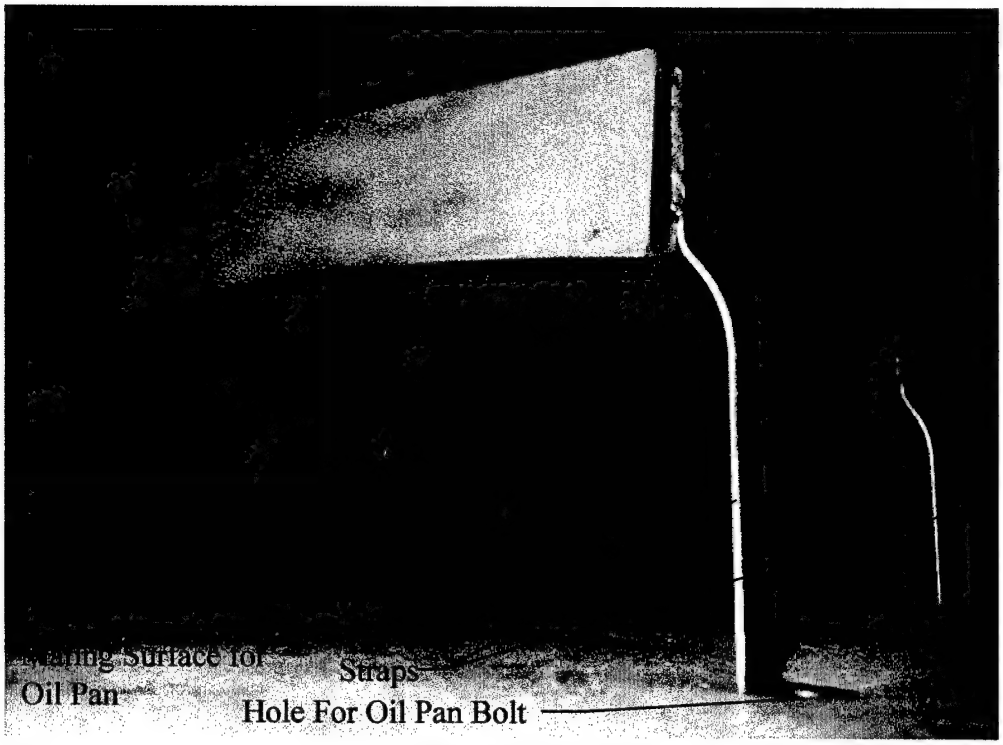


**Figure 2.29**
**ESD #1 Shown from the Side Facing the Oil Pan**

Two insulation shells were developed for the concept demonstration oil pan. The first shell, used for most of the tests, was formed from ordinary (commercially-available) 7/16-inch thick polyisocyanurate insulation, which has a nominal thermal resistance of R=3.5 hr-ft$^2$-°F/BTU, and a maximum useful working temperature of 250 °F. A photograph of the insulation shell fitted to the oil pan is shown in Figure 2.30. The insulation shell was installed in place on the truck oil pan using heat duct tape to form joints between the pieces.

The second insulated cover was formed from 19 pieces of ½" thick vacuum insulation which were specially made for the oil pan, by VacuPanel, Inc. of Xenia, OH. The vacuum insulation was of interest because of the potential lower thermal losses through the insulation (R-20 vs. R-3.5 for the polyisocyanurate). The vacuum insulation is formed by enclosing micro-porous silica forms with a thin film layer and then evacuating to the air to an absolute pressure level of less around 1 Torr. The combination of the low thermal conductivity through the panel and thin film thickness lead to effective thermal resistance of R-40/inch on large panels. For small panel dimensions, conduction through the film layer, around the edges of the panel reduces the effective thermal resistance of the panel. It was recognized that the use of many pieces of insulation with their resultant gaps is less efficient than a

single contoured insulation layer that has no gaps. However, the number of insulation pieces was dictated by the required clearances between the installation and the vehicle components surrounding the oil pan. Note that just one small puncture through the foil is enough to destroy the vacuum (and most of the thermal resistance), so the vacuum insulation had to be constructed so that it not only fitted, but also so that it did not get punctured on installation.

The vacuum insulation was not available until near the end of the program and was installed for the last two tests of the vehicle test program. As it was for the first insulation shell, the vacuum insulation was held together by heat-duct tape.

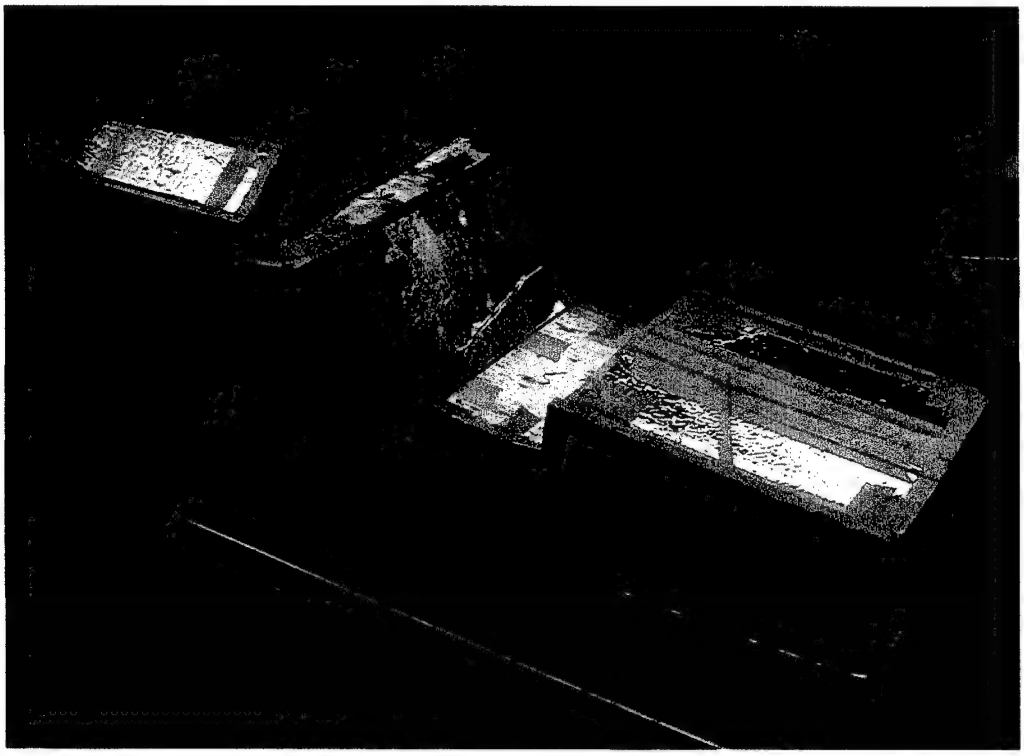

**Figure 2.30**
**Polyisocyanurate Oil Pan and PCM-ESD Insulation for the Oil Pan**

A photograph of the oil pan ESD's during installation is shown in Figure 2.31. The final installation of the oil pan ESD's and insulation was performed by two people working under adverse environmental conditions (temperature less than 20°F, windy and ice underneath the vehicle). Even with the adverse conditions the installation required less than two hours total, including the time required to attach the thermocouple leads to the oil pan

PCM-ESD's. Figure 2.32 shows a photograph of the oil pan ESD's covered with the VacuPanel insulation.

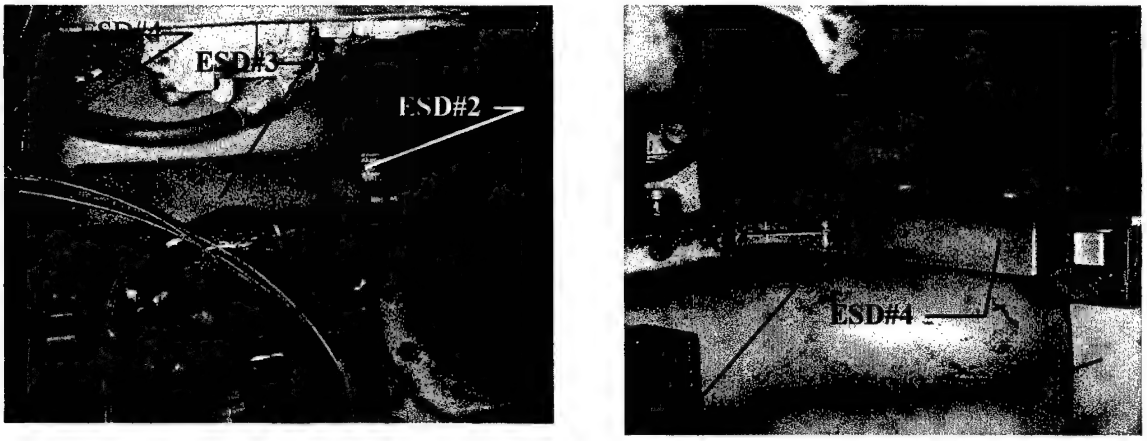


**Figure 2.31**
**Oil Pan PCM-ESD during Test Installation**

**Figure 2.32**
**Vacuum Insulation Installed on the Oil Pan PCM-ESD**

### 2.5.2 Oil Filter PCM-ESD Design

The construction for the oil filter PCM-ESD, like that for the oil pan ESD was 14 AWG welded steel, except for the top which was a heavier gage to allow a sealing cap to be fastened. The oil filter ESD was designed to use the available space up to three inches from the side surface of the oil filter. The specifications for the oil filter ESD are shown in Table 2.7. A drawing of the oil filter ESD is shown in Figure 2.33 and a photograph taken during construction of the ESD is shown in Figure 2.34. The ESD fits around half of the circumference of the oil filter and is held in place by steel straps wrapped around the perimeter of the oil filter and the ESD. Although the fit was tight between the oil filter and the ESD, a thin layer of high temperature grease mixed with shredded steel was placed on the interface of the ESD and oil filter to reduce contact resistance.

The outside of the oil filter ESD was insulated using conventional 7/16-inch thick polyisocyanurate insulation which has a nominal R-value of 3.5. For tests in the cold chamber the backside of the ESD was also insulated using the polyisocyanurate insulation. During installation on the truck there were unexpected clearance problems on the backside of the oil filter and thin flexible foam rubber insulation was used to insulate the backside of the oil filter. A photograph of the installed PCM-ESD is shown in Figure 2.35.

The total mass of the PCM in the ESD for the filter is 3.4 lbm, and the energy storage potential of the latent heat of the PCM-ESD (55-71°F) is over 8 times the sensible energy storage of the oil and oil filter over the same temperature range. In the melted state (T>71°F) the sensible heat of the PCM contributes an additional 45% more thermal storage to the oil and oil pan.

**Table 2.7**
**Specifications for the Oil Filter ESD**

| | |
|---|---|
| Nominal Dimensions | 6.75" x 5.5" x 5.0" |
| PCM Weight (lbm) | 3.4 |
| Total Weight (lbm) | 8.0 |
| Latent Energy Storage ( BTU) | 255 |

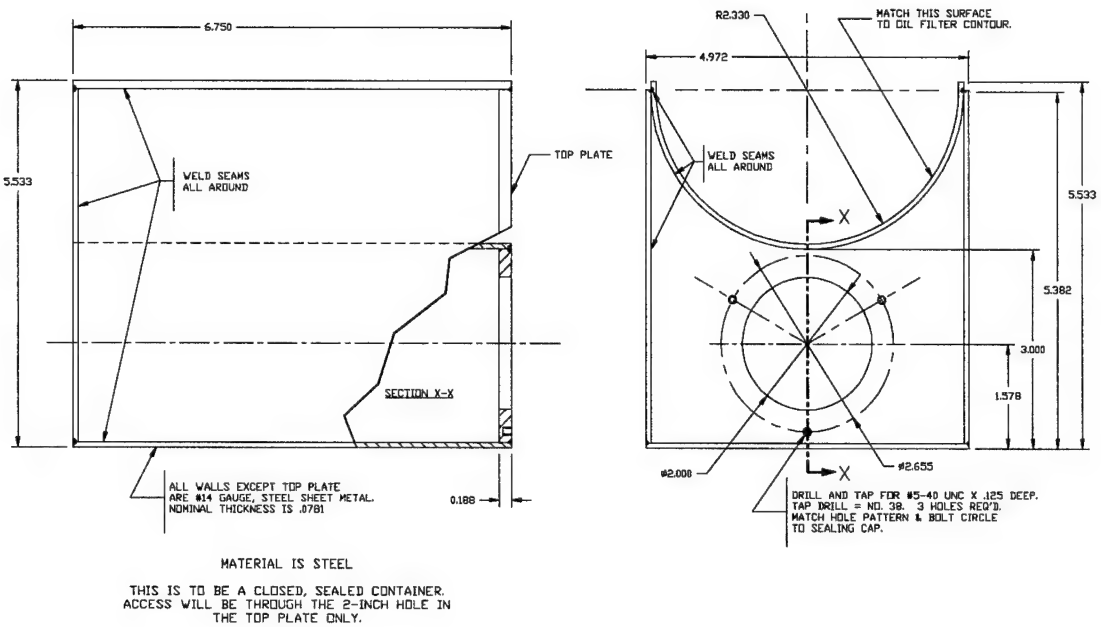


**Figure 2.33**
**Drawing of Oil Filter PCM-ESD**

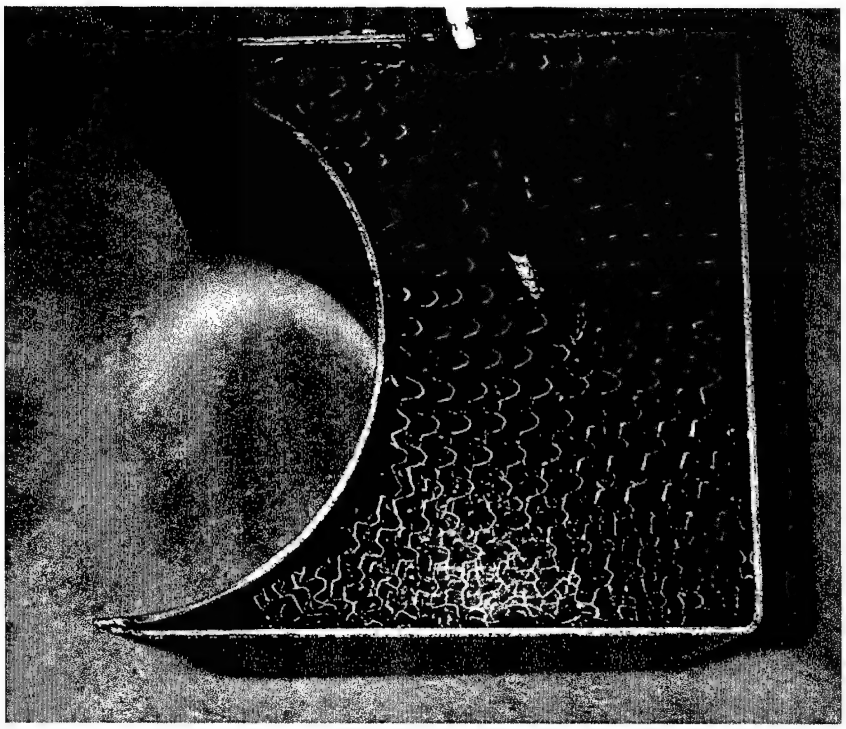

**Figure 2.34**
**Top View Photograph of Oil Filter ESD During Construction**

**Figure 2.35**
**Oil Filter PCM-ESD Installed on Engine**

### 2.5.3 Insulated Battery Box Design

As noted previously, the addition of PCM to the battery box only marginally increased the amount of energy that could be stored, relative to the potential energy storage of the batteries alone. Therefore an insulated battery box with no PCM was designed to replace the battery box of the test vehicle. The clearances between the walls of the stock battery box and the batteries were too low on four of the sides of the battery box to permit the installation of vacuum insulation into the box without puncturing the insulation. Therefore a new insulated battery box, which was slightly larger on two sides, was designed. The dimensions of the new battery box were 25.5" wide x 41" long x13.5 "tall, while the dimensions of the stock battery box were 23"wide x 41"long x 10.9" tall. The insulated battery box was designed to perform all of the practical functions of the original battery box, including restraint of the batteries (using the original hold-down clamps), battery cable passage for the starter and jumper cables, and the provision of a vent to allow the escape of hydrogen.

The stock battery box forms the base for the passenger seat in the 5-ton truck. Because the purpose of this effort was to conduct a practical concept demonstration of the

thermal management system for the truck rather than to manufacture a final production prototype, the insulated battery box was not designed to form the bottom of the passenger seat.

A simplified drawing of the insulated battery box is shown in Figure 2.36 and a photograph of the inside of the battery box is shown in Figure 2.37. The insulation used for battery box was formed from six custom-fit sheets of 1"-thick vacuum insulation, which were manufactured by VacuPanel Inc. of Xenia, OH. The vacuum insulation for the battery was formed by enclosing micro-porous open cell polymer foam with a thin film layer and then evacuating to the air to an absolute pressure level of less than 1 Torr. The combination of the low thermal conductivity through the panel and thin film thickness lead to effective thermal resistance of over R-30/inch on large panels (area of 1square ft). The one drawback of the insulation is that if the film is punctured most of the insulation value is lost.

Because of its fragility, consideration was given to the protection of the insulation from puncture and chemical attack from the sulfuric acid from the batteries. A 0.03" thick layer of polypropylene sheet was used to form a wall between the batteries and the vacuum insulation. The bottom layer of the vacuum insulation also had to be protected from puncture from the weight of the batteries. The first thought on the design of the bottom layer of insulation was to carefully place the batteries on top of the insulation. However, it was realized that the bottom layer of insulation would have to withstand both the weight of the batteries (312 lbm) in addition to the potentially greater vertical force supplied by the battery brackets to restrain the batteries. Therefore, the decision was made to support the batteries above the insulation layer without allowing contact with the insulation layer. The batteries were placed in metal trays that were supported by ten 1.3" thick x 1.25" diameter cylinders made of Ultem 1000, which is a low thermal conductivity polymer made by General Electric. With this configuration, the bottom vacuum-insulation panel sat underneath the batteries and was not placed in compression. The original battery box used ten threaded posts to restrain the batteries in place by the use of the brackets at the top of the batteries. This same pattern of posts and the original brackets were used in the insulated battery box and the threaded posts passed through the center of the ten cylinders that were used to support the weight of the batteries.

Since the design and construction of the battery box, there have been further advances made by VacuPanel, Inc. in coating vacuum panels which may allow the weight of the battery to be supported without damaging the vacuum insulation. If the newer

technology can be applied, the heat losses through the bottom of the battery box in the current design would be cut dramatically.

Extra allowances made on the tolerances of the insulation pieces (to ensure that the vacuum insulation panels would not interfere with each other on installation) resulted in the formation of gaps between panels. The gaps were sealed with foam weather stripping.

Thin silicon rubber-covered electric resistance heat pads were selected to supply the heat for the battery box. The resistance heaters were 8"x8"x1/16" thick pads and had a capacity of 600 watts each. The performance of the insulated battery box was tested during cool-down tests in a cold chamber. Because of the limited availability of the truck batteries at the end of the experimental program (when the vacuum insulation was complete) no tests were actually performed with the addition of heat to the batteries.

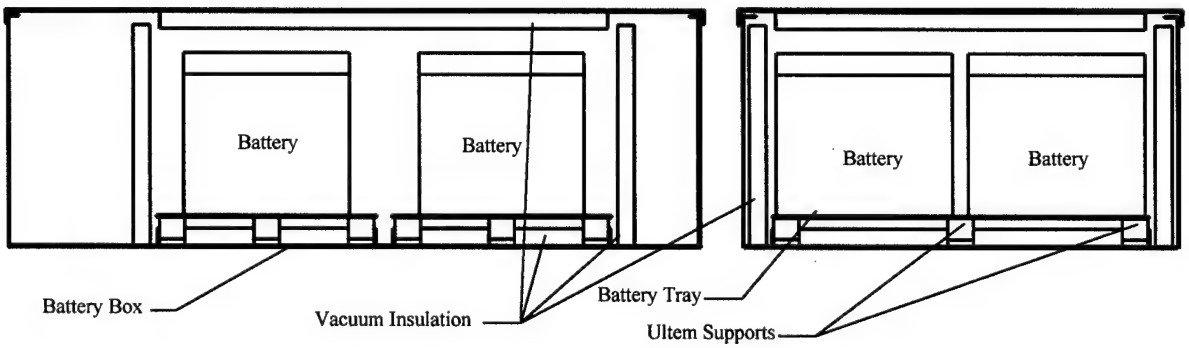


**Figure 2.36**
**Simplified Assembly Drawing of the Insulated Battery Box**

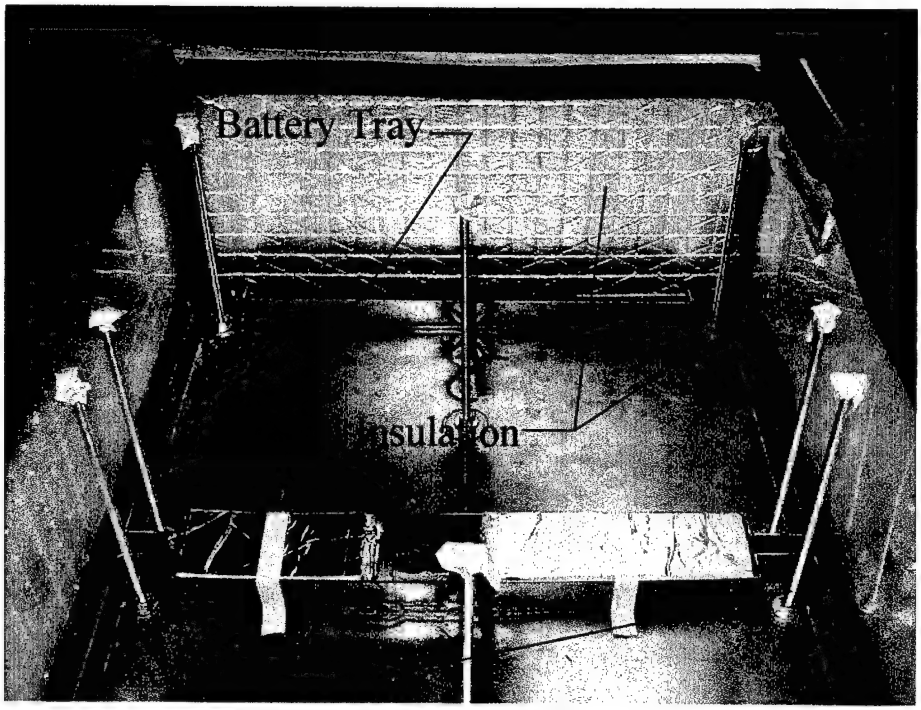


**Figure 2.37**
**Photograph of the Insulated Battery Box**

# *Section 3*
# *Instrumentation*

## 3.1 Temperature Measurements

Temperature measurements on components and fluid temperatures were measured using Type-T (copper-constantan) thermocouples. Most of the thermocouples were the exposed welded-bead type and were constructed using special error limit (+/- 1°F) wire. The thermocouple beads were taped to the surface of interest with metal foil tape. The remaining thermocouples were adhesive-backed thin-film construction (Omega model SA1-T) which attached directly to the surface using the pressure sensitive adhesive. Placing the thermocouple beads inside of a polypropylene sleeve filled with RTV electrically insulated the thermocouples used to determine the temperature of the battery acid inside the batteries.

## 3.2 Wind Speed

The wind speed was measured using a three-cup anemometer (Sirocco Model # 41) The output of the anemometer was a RMS voltage (0.01 Volt/mile per hour) which was proportional to the wind speed.

## 3.3 Heat Flux Gages

Heat flux gages were used to measure both the temperature and the heat flux on selected surfaces. The heat flux gages (RDF model 27070) were a layered thermopile design in which the temperature difference was measured over a thin layer of Kapton. The heat flux is inferred from the measured temperature difference over a known thermal resistance. The heat flux gages had a nominal sensitivity of 7 $\mu V/(BTU/ft^2\ hr)$. A photograph of the heat flux gages is shown in Figure 3.1. In addition to the thermopile the gages also had a small type-K thermocouple for the measurement of surface temperature.

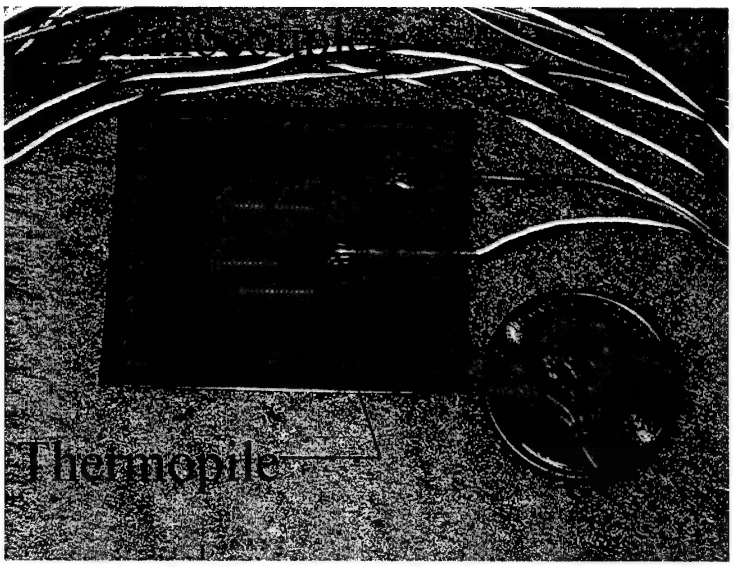


**Figure 3.1**
**Heat Flux Gage**

### 3.4 Startup Transient Instrumentation

During engine starting the starting current, battery voltage, and engine speed were all measured. The starting current was measured using a Hall-effect current transducer (LEM-LT 2000-S). The Hall-effect transducer produces a secondary current, which is nominally $1/5000^{th}$ of the primary (measured) current, which is passed through the opening in the Hall-Effect transducer. The current in the primary circuit was determined by measuring the voltage drop over a 1.5Ω resistor inserted in the secondary current loop. The Hall-effect transducer allowed the measurement of large currents up to 2000 amps while providing electrical isolation between the high current in the starting circuit and the data system. Because the secondary current signal was referenced to ground while all other signals were floating with respect to ground, the connection of the current signal leads to ground caused a small shift in the other signals. For this reason, a switch was placed in the signal lines for the current signal so that the current signal was shorted and isolated from ground at all other times except during the recording of the starting transient.

The battery voltage was measured by using a simple 102: 1 voltage divider to reduce the voltage signal before attaching the signal to the data acquisition system. The engine RPM was measured using a small tachogenerator (MicroMo model 1616 shown in Figure 3.2), which was coupled to the output of the Tachometer sending unit. The installed sensitivity of

the tachogenerator was 0.5V/1000 rpm and was found to be linear down to speeds as low as 20 rpm during calibration

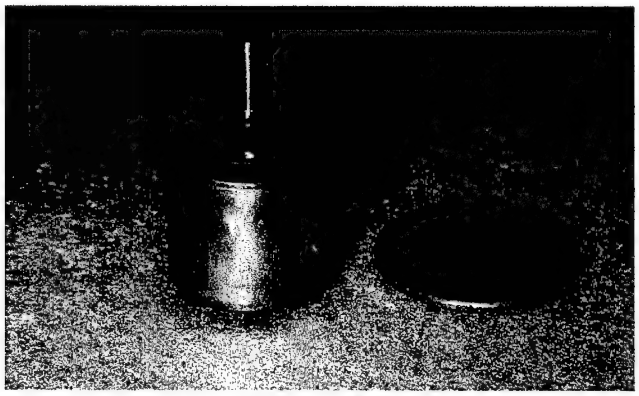

**Figure 3.2**
**Tachometer Used for the Determination of Engine Speed**

## 3.5 Data Acquisition System

Data for all of the tests conducted on the truck were collected using a portable notebook computer-based data acquisition system. A schematic diagram of the system is shown in Figure 3.3. The electrical leads were attached to the screw terminals for either of two multiplexer cards (National Instruments AMUX-64-T) that were "daisy chained" together. In addition to functioning as a multiplexer the AMUX 64-T card provided cold junction compensation for the thermocouples. The multiplexer card was attached to a 16-bit A/D card (National Instruments DAQCard-AI-16-XE-50) which resided in the PCMCIA slot of a Pentium 233-notebook computer.

The gain and the input voltage range of the A/D card were software-selectable for groups of channels. The voltage range, used for the thermocouples and the heat flux gages, was produced a voltage resolution error of +/- 3.05μV. The ideal temperature resolution for type-T thermocouples using this range was 0.15°F.

The data system was capable of measuring up to 62 separate differential signals and running on battery power for up to 3 hours. The software to drive the data system was written in LABVIEW™ (National Instruments). LABVIEW™ is an open ended graphical programming language.

All data were collected using a single program, which operated in either "fast" or "slow" data collection modes. The fast data collection mode captured the starting transients. In fast mode the data was collected at 200 Hz for a limited number of channels including the engine speed, battery current and voltage for a total time period of one minute. In slow data collection mode, which was used at all other times, the data were continuously recorded on all channels at a rate of once per minute. To improve the signal to noise ratio on low level signals, the data was recorded for 20 seconds at a rate of 50 Hz and then averaged to form a single reading for each channel which was recorded once per minute.

Because the data system was regularly exposed to temperatures below 32°F, a thermal protection system was designed. The entire data acquisition system was placed in a specially designed enclosure which was insulated and thermostatically-controlled to maintain the temperature of the data system at 65°F +/- 10°F when placed in a environment with an air temperature of 0°F.

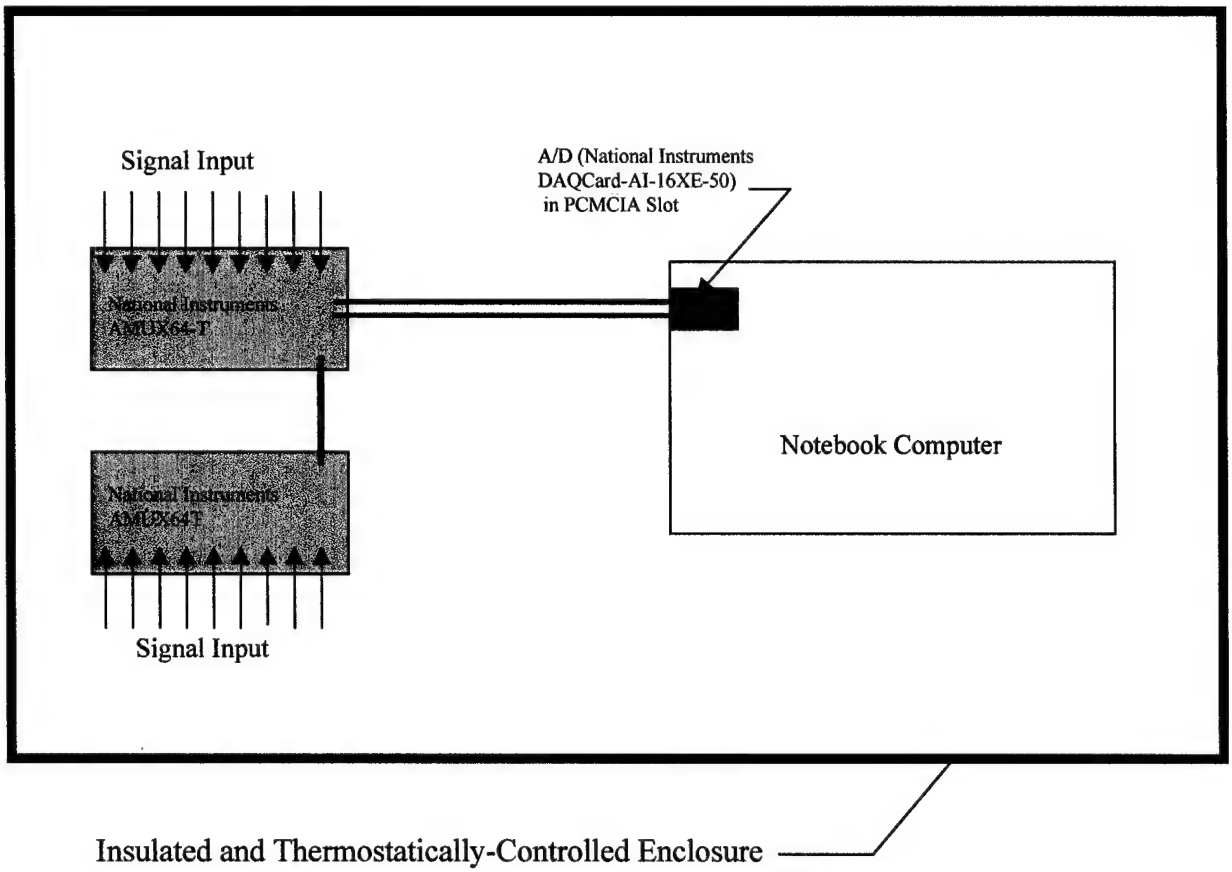


**Figure 3.3**
Schematic of the Data System

# *Section 4*
# *Results of Experimental Tests*

## 4.1 Cold Chamber Tests of Thermal Protection Systems

Cool-down tests were conducted in a 0°F cold chamber for the thermal protection systems for the oil pan, oil filter, and battery. The results of these tests are discussed in the sections below.

### 4.1.1 Oil System Thermal Protection System Test Apparatus and Procedure

Cold chamber tests were conducted with the PCM-ESD system applied to oil filter and oil pan. The purposes of the tests were:

1. To assess the performance of the PCM-ESD system applied to the component relative to the baseline performance (no PCM-ESD applied) in a conservative test with controlled conditions.
2. To identify any operational problems with the system before application to the vehicle.

The cold chamber tests were conducted by subjecting the filter or oil pan, which were filled with oil, to a step change in temperature from 75°F (room temperature) to 0°F, and measuring the temperatures of the components, oil, and air throughout the test. During operation of the vehicle, the surface of the PCM-ESD in contact with the protected component will be exposed to much higher temperatures, and thus to a higher effect of the sensible heat of the PCM-ESD. However, because the phase change of the Hexadecane-PCM occurs between 71°F and 55°F, the temperature range selected for the cold chamber tests contained the temperature range of maximum effect for the PCM-ESD.

Both the oil filter and oil pan ESD systems were tested in an environmental chamber that measured 28 in x 54 in x 23 in, and was capable of providing an ambient temperature of –40°F. The air inside the chamber was circulated through the chamber by a fan to avoid thermal stratification in the chamber. The uniformity of the air temperature within the chamber was verified by temperature measurements of the air at multiple locations.

Test stands were created to mount the oil pan and oil filter in the cold chamber. The tests in the cold chamber were conservative because the upper boundary of both test stands were exposed to the cold of the test chamber rather than duplicating the thermal mass and resistance of the engine block. The oil filter and oil pan cool at a slower rate when installed

on the vehicle because of (1) the greater thermal resistance of the conduction path through the engine block, and (2) the higher temperature boundary provided by the thermal mass of the engine block.

The thermal test stand used for the oil pan tests is shown in Figure 4.1. The stand was constructed of steel C-sections and had a thin steel cover for the top of the oil pan (not shown in the Figure) to decrease the convective heat loss from the oil pan. The oil pan was filled with 20 quarts of 15W-40 oil, which is the nominal capacity for the oil. Thermocouples were placed at the approximate dipstick location (at the top surface of the oil), into the oil at the bottom of the pan, through the drain plug of the oil pan, as well as on the surfaces of the pan, and the PCM-ESD units. The chamber air temperature was also measured throughout the tests.

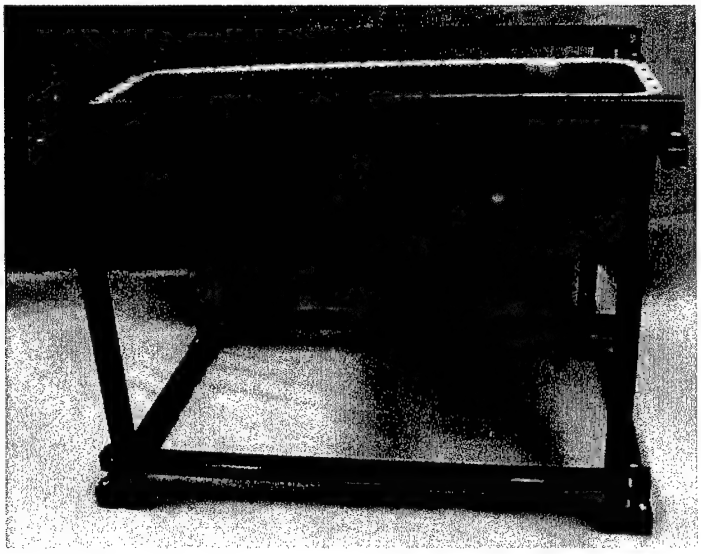

**Figure 4.1**
**The Oil Pan Thermal Test Stand Used for the Cold Chamber Tests**

The thermal test stand used for the oil filter tests is shown in Figure 4.2. A hollow threaded cap was used to tighten the oil filter against the bottom of the stand. The oil filter was filled with oil before mounting it to the stand. The temperature was measured on the outer surfaces of the oil filter, inside of the PCM-ESD, and inside of the center of the oil filter. The oil at the center of the oil filter was measured by a thermocouple inserted through a hole in the threaded cap that held the top of the oil filter against the test stand.

The insulation that was used for the surrounding shell for both oil pan and oil filter PCM-ESD during the cold chamber tests was 7/16" thick polyisocyanurate, which has an R-value of 3.5 BTU/ft$^2$-hr-°F.

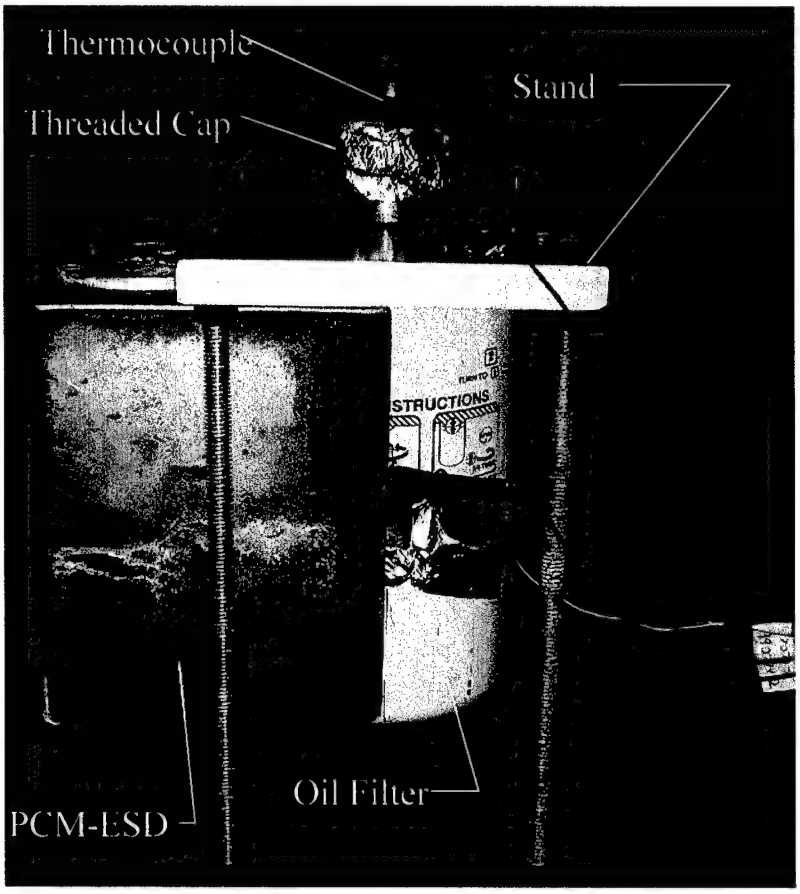


**Figure 4.2**
**The Oil Filter and Oil Filter PCM-ESD Mounted in the Test Stand for the Cold Chamber Tests before Application of the Insulation**

### 4.1.2 Oil Pan PCM-ESD Cold Chamber Test Results

Figure 4.3 shows the oil temperature measured at the approximate dipstick location (1" under the top surface of the oil), and near the bottom of the oil pan (measured through the oil plug), during the cool-down test of the baseline oil pan. The temperature at the bottom of oil dropped rapidly during the test, reaching 32°F in less than 37 minutes. The temperature at the top of the oil pan was observed to drop at the slower rate, which was expected because of the natural conduction of the warm oil to the top surface of the oil pan.

The oil temperatures measured during the cool-down test of the oil pan equipped with the PCM-ESD system are compared to the baseline case temperatures in Figure 4.4. Initially the temperature at the dipstick location dropped faster than during the baseline case. It was later found that the top cover of the oil pan was loose allowing more convection from the top surface of the oil near the dipstick location. However, even with increased heat loss from the top of the oil pan, the oil at the top of the pan required almost twice as much time to cool-down to the 32°F level as the baseline case.

The effect of the PCM-ESD system on the temperature at the bottom of the oil pan was much more pronounced. The oil at the bottom of the pan required more than 450 minutes to reach 32°F as compared to 37 minutes for the baseline case. In contrast to the baseline case, the oil temperature was higher at the bottom of the oil pan than it was at the dipstick location when the oil pan was equipped with the PCM-ESD. Note that the oil at the bottom of the pan was warmed by the PCM-ESD at the bottom of the oil pan (ESD #3, see Figure 2.26).

The temperatures on PCM-ESD #3 were measured at the center section of the ESD, at the inside surface (in contact with the bottom of the oil pan) and outside surfaces, and at a depth of 1" away from the inside surface, and are shown in Figure 4.5. After an initially steep temperature drop during the first hour of the test, the temperatures measured on and inside of the ESD leveled off at a temperature of about 62°F which is the apparent temperature of peak energy release of the phase change. The temperature of the outer surface of the ESD dropped faster than at the inside surface because of heat losses through the insulation to the ambient air, which caused the outside layers of the PCM to freeze first. The temperature measured at the inside surface of the ESD (which was in contact with the oil pan) was only slightly less than the temperature measured 1" deep into the PCM, which implies that the conduction loss throughout the PCM-ESD was low. Note that there was a large temperature difference between the oil at the bottom of the oil pan and the inside surface of the PCM-ESD, which is indicative of a high thermal resistance between the PCM-ESD surface and the thermocouple mounted at the bottom of the oil pan. It is thought that the major contributor to the high thermal resistance is the thermal contact resistance between the ESD surface and the oil pan surface. Although the oil pan ESD's were manufactured to have fit the complex contours of the oil pan there is an interfacial thermal contact resistance created by imperfect thermal contact. This thermal contact resistance was partially reduced, but not eliminated, by the use of thermal grease between the oil pan and the ESD.

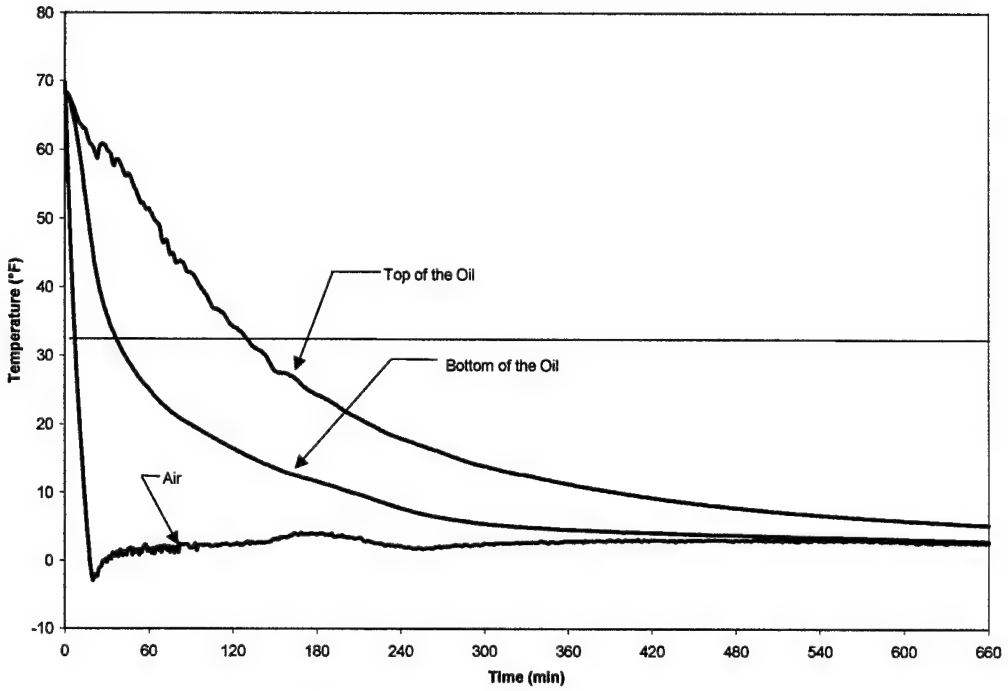


**Figure 4.3**
**Cold Chamber Test of the Baseline Oil Pan (Average Air Temperature = +2°F)**

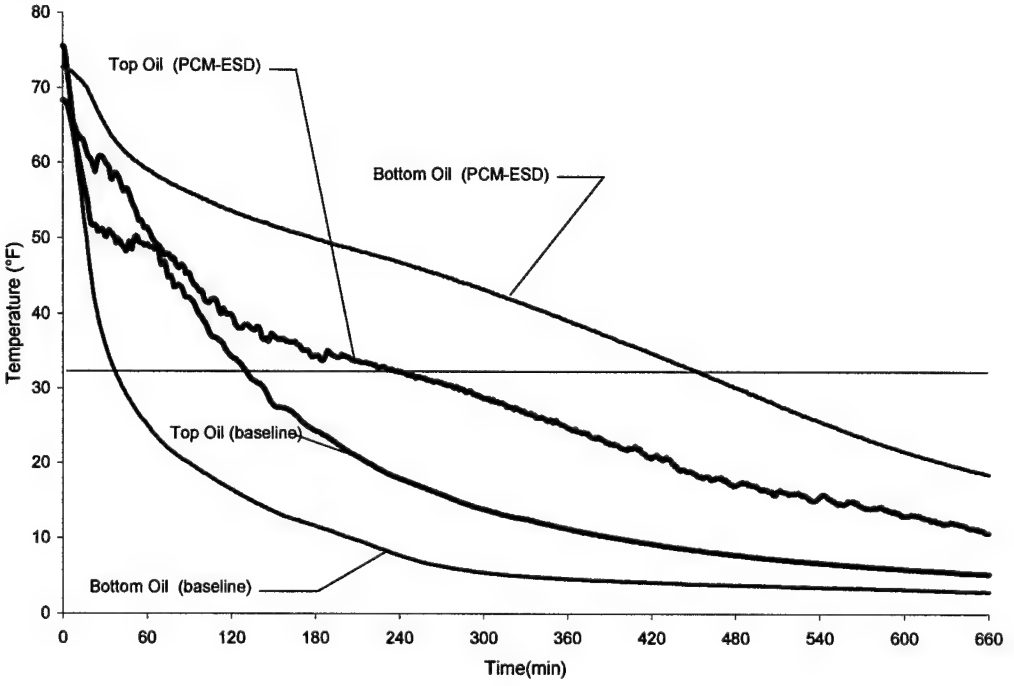


**Figure 4.4**
**Comparison of the Oil Temperatures With and Without the PCM-ESD System during the Cold Chamber Cool-Down Tests**

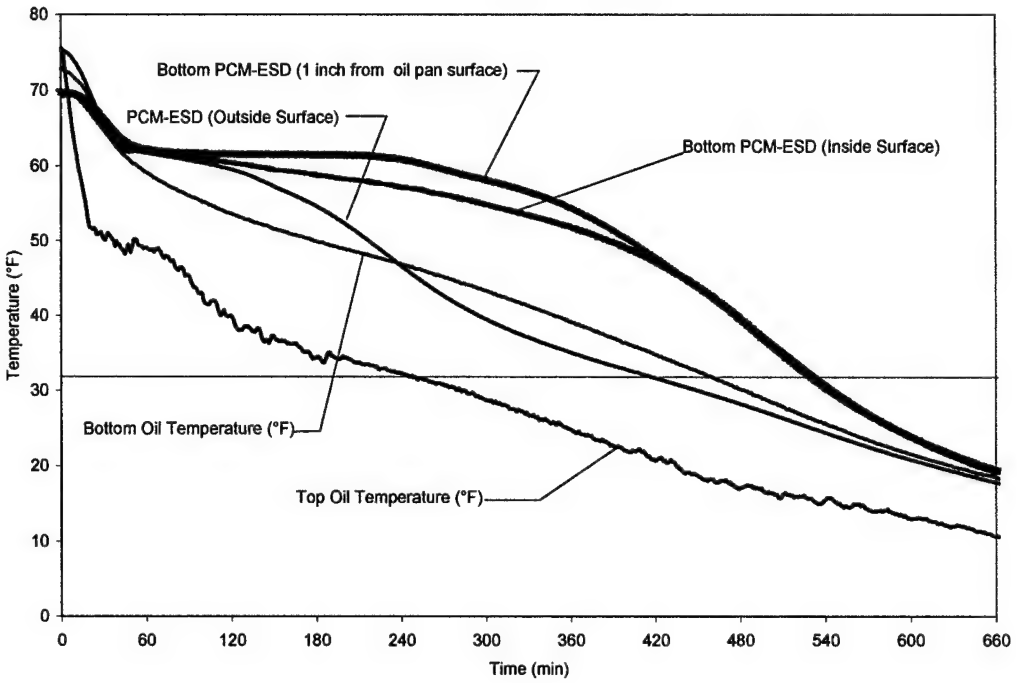


**Figure 4.5**
**Temperatures Inside of ESD# 3 During the Cold Chamber Tests of the Oil Pan**

### 4.1.3 Oil Filter PCM-ESD Cold Chamber Test Results

The results from the baseline oil filter cool down tests conducted in the cold chamber are shown in Figure 4.6. The oil filter outer surface quickly cooled during the test reaching 32°F in less than sixteen minutes after exposure to the cold. The temperature at the center of the oil filter initially showed a plateau because of the time required to conduct heat through to the center of the filter, and then dropped steadily throughout the rest of the test, decreasing to 32°F in just over 2 hours.

The temperatures of the oil measured at the center of the filter for the baseline oil filter is compared to the oil temperature at the center of the PCM-ESD-equipped oil filter in Figure 4.7. It can clearly be seen that the PCM-ESD is an effective means of maintaining the oil temperature at an elevated temperature. The oil filter equipped with the PCM-ESD required over 4 times as much time to drop to 32°F as the baseline oil filter.

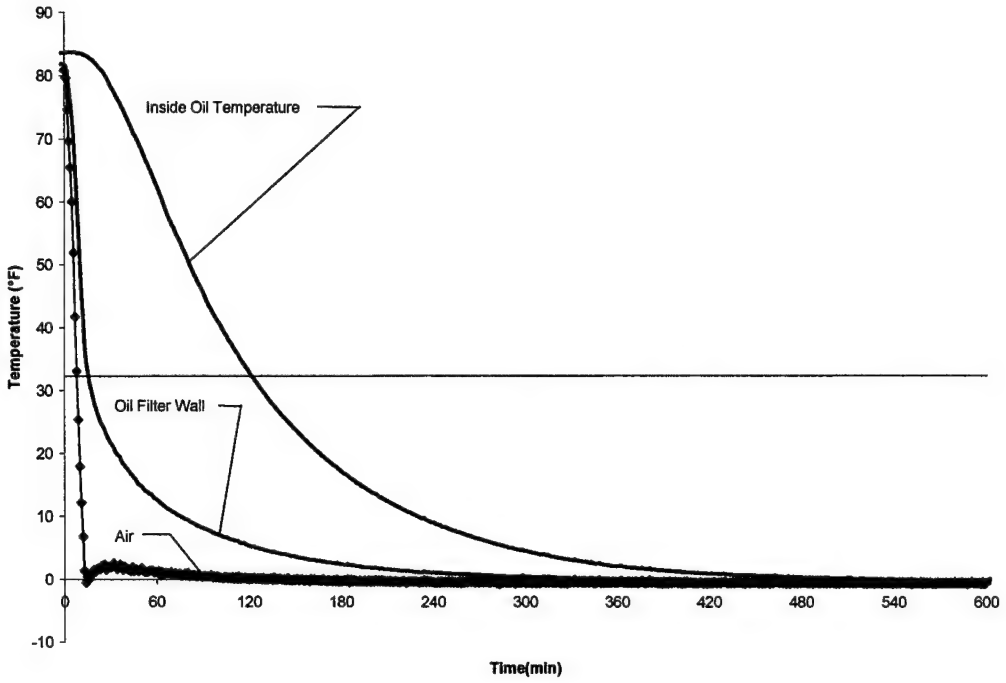


**Figure 4.6**
**Baseline Tests of the Oil Filter in the Cold Chamber**

The temperatures measured on the surface of the oil filter PCM-ESD and at the center of the PCM-ESD during the test are shown in Figure 4.8. After an initial decrease in temperature of the ESD as the sensible energy of the melted PCM decreased, the temperature at the center of the PCM-ESD showed a very slow drop off as the PCM froze. The oil temperature at the center of the oil filter dropped below the temperature of the ESD after the initial portion of the test and was observed to drop at a slower rate while the PCM in the ESD was releasing its latent heat of fusion. The oil filter ESD showed a larger temperature difference between inside wall temperature and the temperature of the PCM measured at the center of the filter than was noted for the oil pan ESD#3. It is thought that there are two reasons for larger temperature difference: (1) The measurement location inside of the ESD was further away from the inside wall for the oil filter ESD (1.5" vs. 1") than it was for ESD#3, and (2) the Flexcore aluminum honeycomb, which is used to enhance conduction, was not packed as tight for the oil filter ESD as it was for the oil pan ESD, resulting in more thermal resistance through the PCM-ESD.

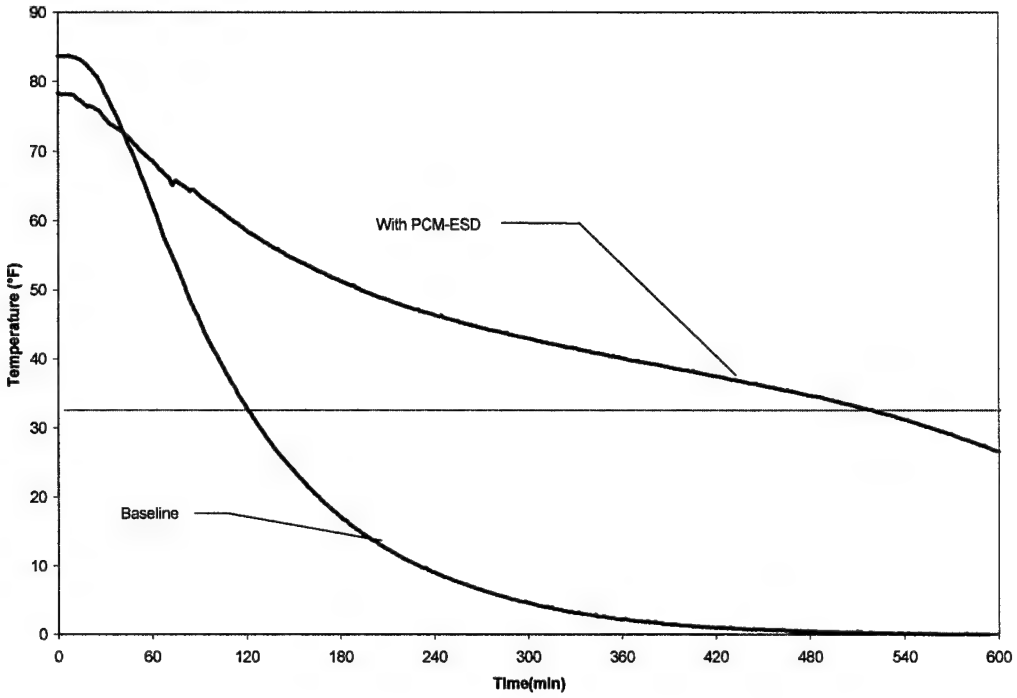


**Figure 4.7**
**Comparison of the Oil Temperatures Measured at the Center of the Oil Filter during Cold Chamber Tests**

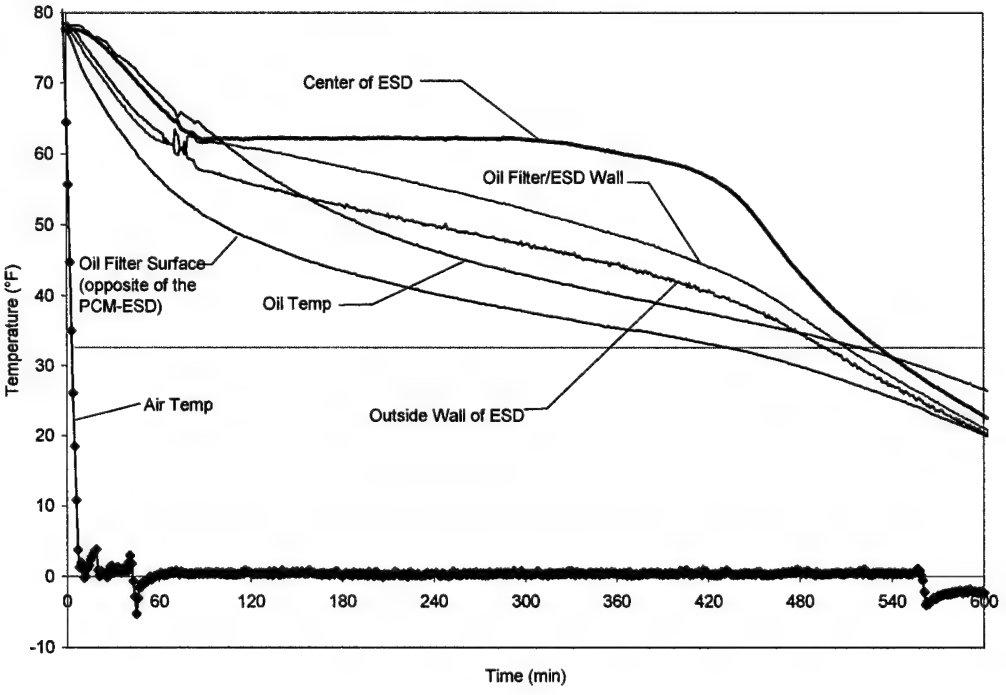


**Figure 4.8**
**Cold Chamber Test of the Oil Filter Equipped with PCM-ESD**

### 4.1.4 Insulated Battery Box Cold Chamber Tests

Because of the delays in obtaining the insulation, all of the tests on the battery box were conducted in cold chambers at the University of Dayton. Figure 4.9 shows the measured temperatures during a baseline cool down test of a single battery. For this test the battery was placed in a carbon steel box which had 1" clearance on all sides of the battery. The top surface of the battery was covered with a 3 inch-thick layer of open cell insulation foam to simulate the seat cushion. At the start of the test the temperature in the chamber was decreased to near (0°F) and maintained near this level for the rest of the test. The average temperature during the test was 1.3°F. The two battery cell temperatures, which were measured approximately two inches below the top surface of the battery acid, were nearly identical throughout the test. The surface temperatures of the sides of the battery were also close to battery cell temperatures throughout the test. The battery cell temperature dropped to 9°F by the end of the test.

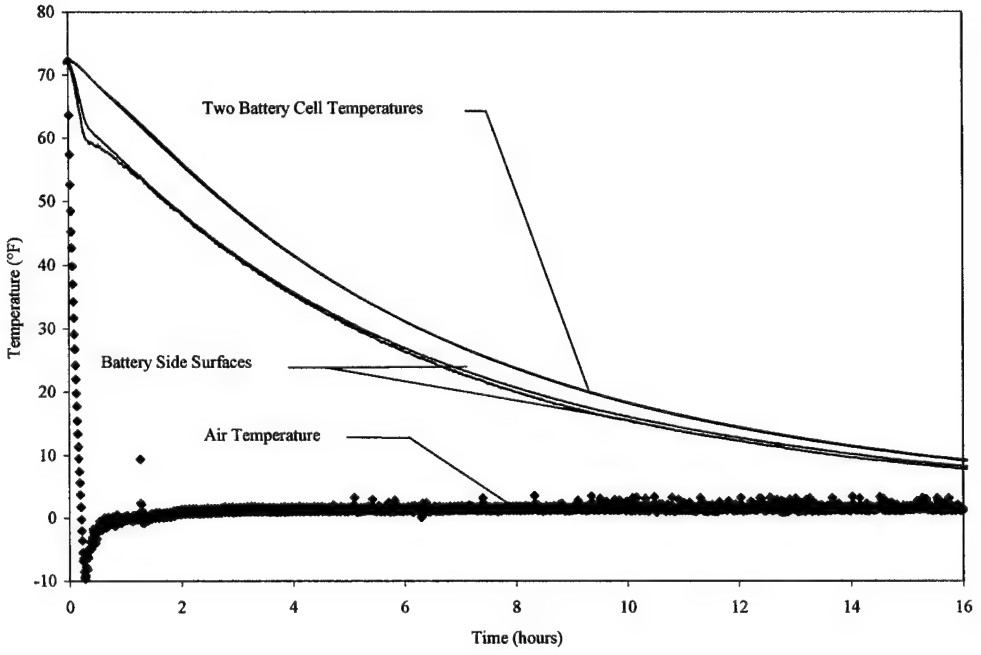


**Figure 4.9**
**Battery Cell and Surface Temperatures Measured during the Baseline Cool-Down Test**

The battery cell temperatures from the single battery experiment were fitted with an exponential curve, which is the thermal response for a first-order (lumped mass) system. The exponential curve fit was expressed as:

$$T(t) = T_\infty + (T_i - T_\infty)e^{-yt} \tag{4.1}$$

where, T is the temperature, t is the time, $T_i$ is the initial temperature, $T_\infty$ is the ambient air temperature, and:

$$y = (hA / mc_p) \tag{4.2}$$

where, h = convection film coefficient, A = surface area of batteries, m = battery mass, $C_p$ = average specific heat of the batteries

The results of the curve fit for the baseline case are shown in Figure 4.10. The fit between the data and the curve fit for the single battery baseline case agreed within 2°F, with the greatest temperature differences occurring early in the test.

Because all of the sides of a single battery are facing out toward the cold exterior, the battery is expected to cool faster than if it was one of four batteries arranged in a rectangular pattern. In a box containing four batteries in a rectangular pattern, only two of the vertical slides of each battery are facing out toward the cold outside surface of the battery box, while the other two surfaces are exposed to the sides of adjacent batteries. A first order model of the baseline performance for four batteries in a battery box was made by dividing the term y used to fit the single battery experiment (equations 4.1 and 4.2) by the appropriate masses and outer surface areas for the four batteries. The resulting predicted temperature history is shown in Figure 4.10 along with the single battery. The predicted temperature for four batteries in the baseline battery box dropped to 32°F in less than 12 hrs and was less than 20°F at the end of 16 hrs.

It should be noted that the only thermal paths for the baseline battery experiments in the cold chamber were through the walls of the battery box or through the top of the foam. There were no additional leak paths because the battery cables were not available for the experiment. In addition, there were no ventilation holes added to the top of the box. For the insulated battery box tests, both the starter and the jumpstart cables were attached to the four

batteries and the other end of the cables was electrically insulated and exposed to the cold chamber. In addition, the insulated battery box was equipped with the same size (1.5"-diameter) hydrogen ventilation hole that was used in the battery box for the test vehicle, which provided another thermal path from the warm batteries to the cold surroundings.

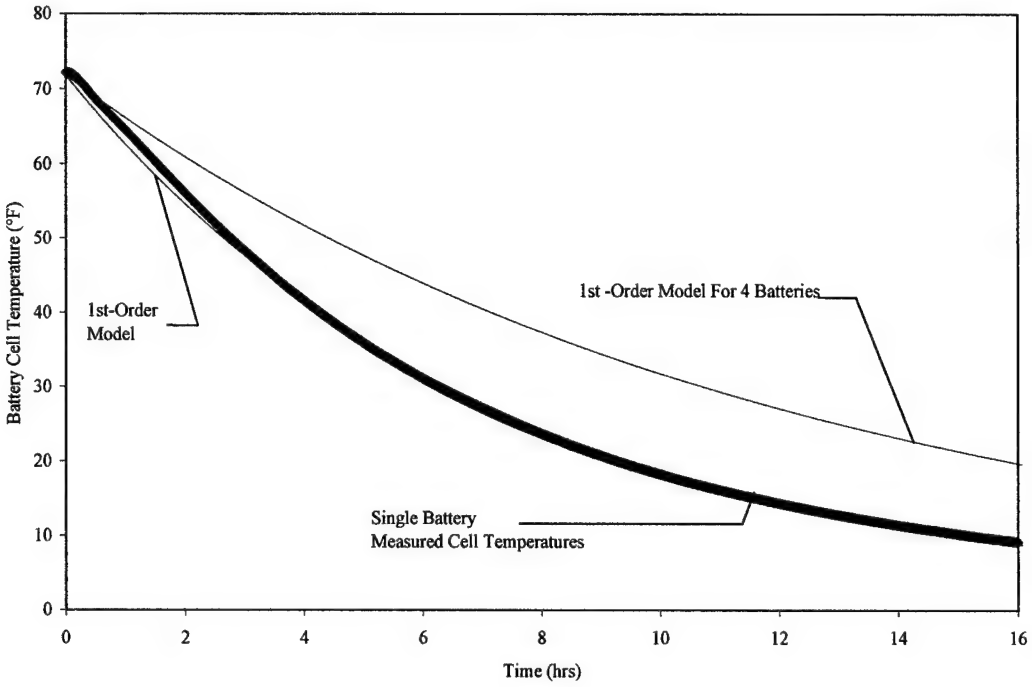


**Figure 4.10**
**Comparison of First-Order Thermal Models for a Single Battery and Four Batteries (Ambient Temperature = 0°F)**

The facility that was used for the test of insulated battery box was a 10ftx12ftx10ft cold chamber that is also used for the storage of temperature sensitive composite materials. The battery cell temperatures measured inside the four batteries for the insulated case are shown in Figure 4.11 along with the air temperature inside of the chamber. The air temperature was cycled throughout the entire test but averaged 2.3°F over the length of the test. The entire data system, which was placed inside of the thermostatically controlled enclosure, was also placed inside the cold chamber for the entire test.

The bumps in the curves of the battery cell temperatures vs. time were caused by temperature difference between the termination point of the thermocouple leads and the location of the cold junction compensation on the board. This temperature difference was caused by the rapid temperature change of the data system after the thermostat turned the data system heater off. The relationship of the data system temperature change to the battery

cell temperature measurements can be seen more clearly in Figure 4.12. This figure also shows the cold junction temperature that was used for the conversion of the thermocouple voltages to temperatures. The regions of the bumps on the temperature curves correspond to high rates of change of the cold junction temperature. Nonetheless, the deviation from the temperature curves for the battery cells caused by the temperature mismatch between the cold junction and the thermocouple termination points was less than 1°F.

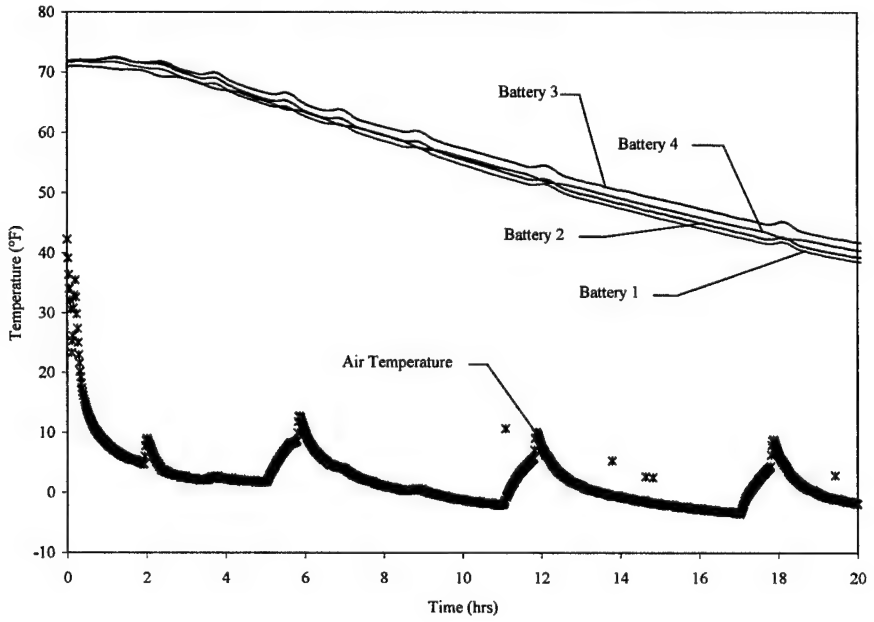


**Figure 4.11**
**The Battery Cell Temperatures Measured During the Cold Chamber Test of the Insulated Battery Box**

The temperature differences between the four batteries were less than 4°F at the end of the test and appear to be related to the differences between the thermal loads for the individual batteries, which include the starter and jump-start battery cables and the ventilation hole for the battery box.

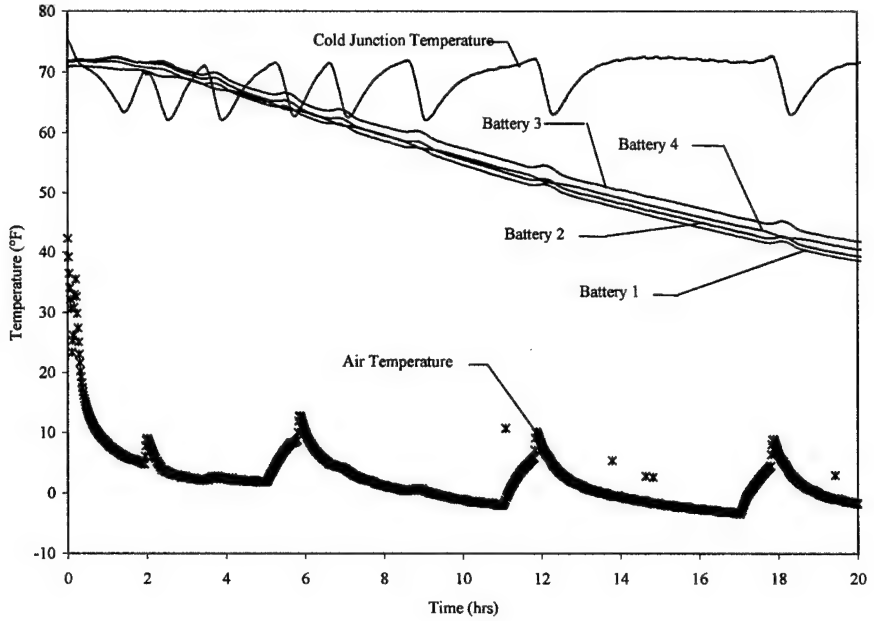


**Figure 4.12**
**The Battery Cell Temperatures and the Cold Junction Temperature of the Data System during the Cold Chamber Test of the Insulated Battery Box**

The average of the four battery temperatures measured for the insulated case is compared to the baseline prediction case in Figure 4.13. It can be seen that the vacuum insulation made a large reduction in the rate of cooling for the batteries. The average battery cell temperature decreased less than 26 °F to 45°F by the end of the 16 hrs. In contrast, the average battery cell temperature for the baseline prediction drops to this level in less than 5.5 hrs and decreases to less than 20°F by the end of the 6 hr test period.

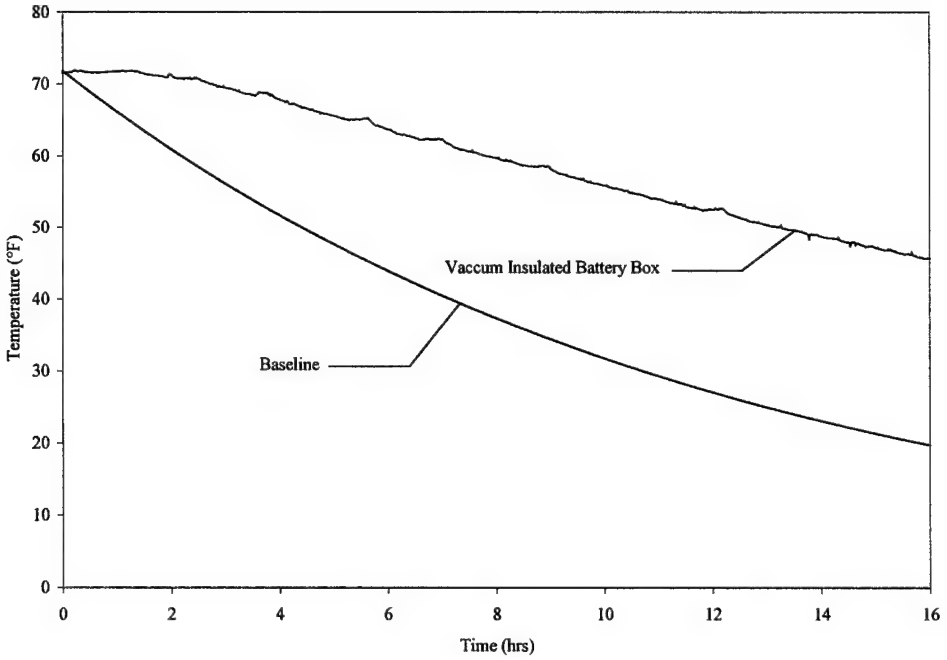


**Figure 4.13**
**Comparison of the insulated Battery Box and the Baseline Thermal Model for Four Batteries**

The measured battery temperatures were compared to the ideal predicted battery cell temperatures obtained from a simplified finite difference thermal model that assumed that the batteries were a single lumped mass. The heat loss for the ideal model was assumed to occur through idealized one dimensional paths, and included loss terms for the battery cables and battery supports. The results from the thermal model represent an ideal performance that could be expected if secondary heat losses could be eliminated. Examples of the secondary heat loss paths not accounted for in the model include the conduction through corners and taped joints of the insulation, and the loss of air through the ventilation hole. It is thought that much of the secondary heat loss could be reduced by small design changes in the battery box and insulation.

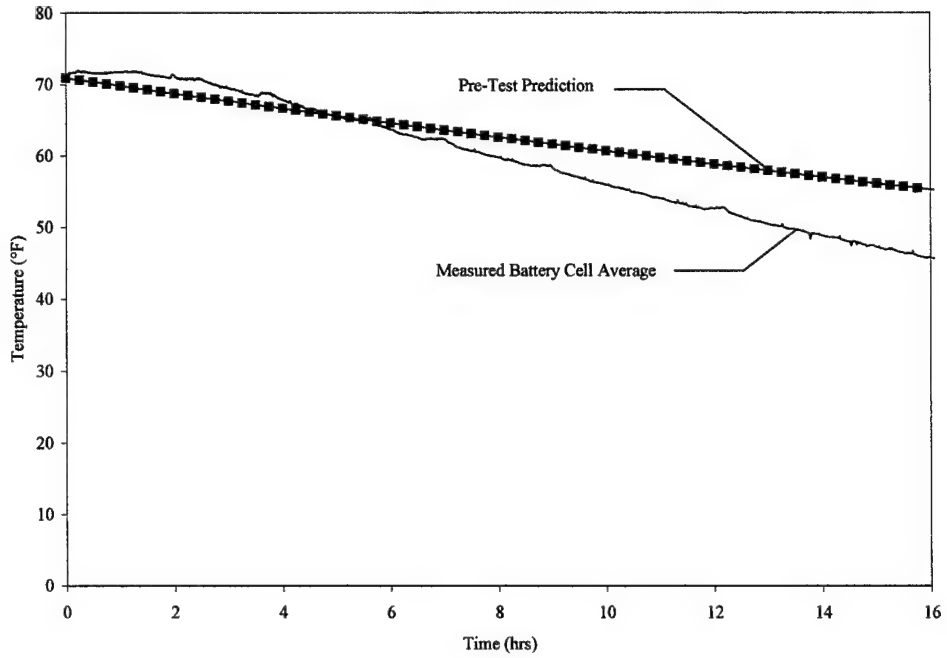


**Figure 4.14**
**Comparison of the Average Battery Cell Temperature for the Insulated Battery Box Case and the Pretest Prediction of the Battery Cell Performance**

The energy required to reheat the batteries back to room temperature at the end of 16 hrs can be calculated by multiplying the temperature change of the batteries by the thermal capacity of the batteries as follows:

Energy to Reheat Batteries = $(mC_p)\Delta T$ = (243 BTU/°F) (26 °F) = 6300 BTU= 6700kJ

Assuming that the batteries are reheated in 8 hrs of vehicle operation the power required to heat the batteries would be less than 240 Watts. The power required to reheat the batteries could come from resistance heating or could be supplied by engine coolant pumped through battery pads such as those shown in Figure 1.5. Note that the required power level corresponds to 10 amps of current drawn from the alternator at a voltage of 24 volts. The alternator for the test vehicle is capable of supplying 60 amps, so the insulated battery box with electric resistance heating is a practical solution to the problem of maintaining the batteries at a temperature level high enough to start the engine in cold weather.

The battery box for the test vehicle was located in the cab of the truck which will usually be at a higher temperature than the environment because of the cab heating system,

and the trapped solar radiation on sunny days. Therefore, a system developed to withstand cold temperatures on all sides of the battery box will have excess capability when installed in the actual vehicle.

## 4.2 Baseline Engine Test Program

The engine test program was divided into two phases, a first (baseline) phase in which no PCM was added to the engine and a second phase to assess performance of the PCM-ESD system relative to the baseline engine.

During the baseline test program, the baseline cool-down rates of engine component, starting performance, and the effect of insulating engine components were determined. The information gathered during these tests was used to:

1. Assess the potential benefit of applying a passive PCM-ESD thermal management system to various engine components and systems that influence engine starting and operation.
2. Measure typical temperatures of the engine components during engine operation, which was used for the design of the PCM-ESD system.
3. Provide a baseline to compare with the performance of the PCM-ESD thermal management system that was tested in Phase 2.

### 4.2.1 Engine Temperatures during Driving of the Baseline Vehicle

In the first baseline engine test, the test vehicle was instrumented with thermocouples and was driven for three hours under typical driving conditions including both interstate and city driving. The maximum speed during operation was limited to less than 45 mph because of vehicle safety restrictions imposed by the brake design of the test vehicle. The engine block and oil temperatures measured during the test are shown in Figure 4.15. During operation, the block and oil temperatures reached approximately steady temperature levels after about 30 minutes of operation. The engine cooling system, which is a traditional thermostatically controlled coolant jacket-radiator system, controlled the temperatures of the block, oil (and other engine components). The coolant system was observed to maintain approximately steady oil and block temperatures over a range of engine loads after the engine had warmed up to operating conditions during the first thirty minutes of operation.

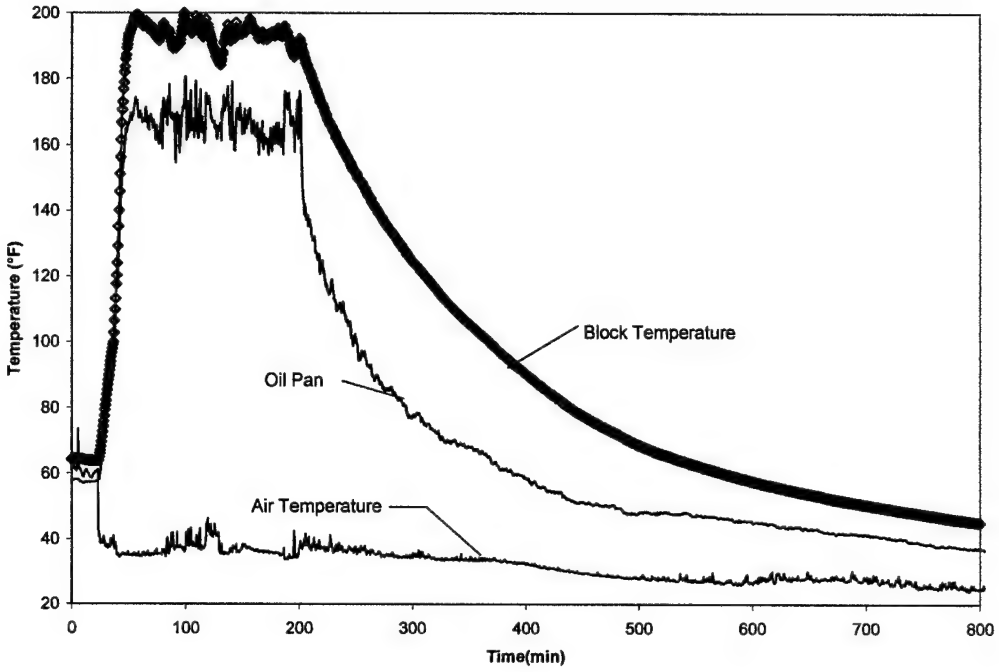


**Figure 4.15**
**Engine Block and Oil Pan Temperature Measured During Driving of the Test Vehicle On January 25,1999 (Engine Shut Off at 201 Minutes)**

### 4.2.2 Baseline Engine Cool Down Tests

The initial series of baseline cooling tests were conducted during February and March of 1999 in the parking lot of Organizational Maintenance Shop (OMS) #20 of the Ohio Army National Guard in Piqua, Ohio (38 miles north of Dayton). Further baseline cool-down tests as well as the engine tests of the PCM-ESD system were conducted in the parking lot of the Shroyer Park Center of the University of Dayton from Dec 1999-March 2000.

Because of concerns about liability and safety, operation of the vehicle by University of Dayton personnel over the open road was not permitted. Furthermore, the availability of National Guard personnel to drive the test vehicle was limited due to their many other obligations. Therefore, all subsequent engine tests were conducted without actually driving the truck. Instead, the engine was operated over a range of speeds with the transmission placed in park. During the baseline tests, the engine was operated until it was hot enough to turn on the engine clutch fan, which was activated at a repeatable temperature under thermostat control. The typical sequence of events during the engine operation portion of the baseline tests is shown in Table 4.1. During operation engine speed was increased in

approximately 500-rpm steps to 2000 rpm, which is 200 rpm less than the governed speed limit of the engine. The engine was then operated at 2000 rpm until the engine was warm enough to turn on the clutch fan to pull air through the radiator. After the clutch fan was activated the throttle was placed back into the idle position and then the engine was shut off after idling for 5 minutes. This procedure provided repeatable engine and engine fluid temperatures at the start of each of the baseline cool-down tests.

**Table 4.1**
**Engine Operation Schedule for the Baseline Tests**

| Event | Time during the test |
|---|---|
| Start engine | 0 minutes |
| engine operated at idle (engine speed 500-550 rpm) | 0-7 minutes |
| Operate engine at 1000 rpm | 7-14 minutes |
| Operate engine at 1500 rpm | 14-21 minutes |
| Operate engine at 2000 rpm until clutch fan is activated | 21 to 45 minutes |
| Operate engine at idle | 45-50 minutes |
| Shut off engine | 50 minutes |

Engine system temperatures from a typical baseline cool-down test are shown in Figures 4.16 through 4.20. Note that for all time-temperature plots which are shown in this report, the time period before zero minutes corresponds to engine operation and the time period after zero minutes corresponds to engine shut off and cool-down.

Figure 4.16 shows the block temperatures, measured at four vertical locations on the outside surface of the engine block that were approximately at the middle of the block length. Note that the block temperatures were close to the block temperature measured during the driving test. The oil system temperatures are shown in Figure 4.17. The oil temperature for all of the cool-down tests was measured by a thermocouple, which was attached to the tip of the dipstick. The dipstick oil temperature was higher than the surface temperatures of the oil pan and oil filter throughout both cool-down and normal operation. However, it was noted that the surface temperatures of the oil pan and oil filter were high enough to allow significant heat transfer to a passive PCM-ESD coupled to the oil pan.

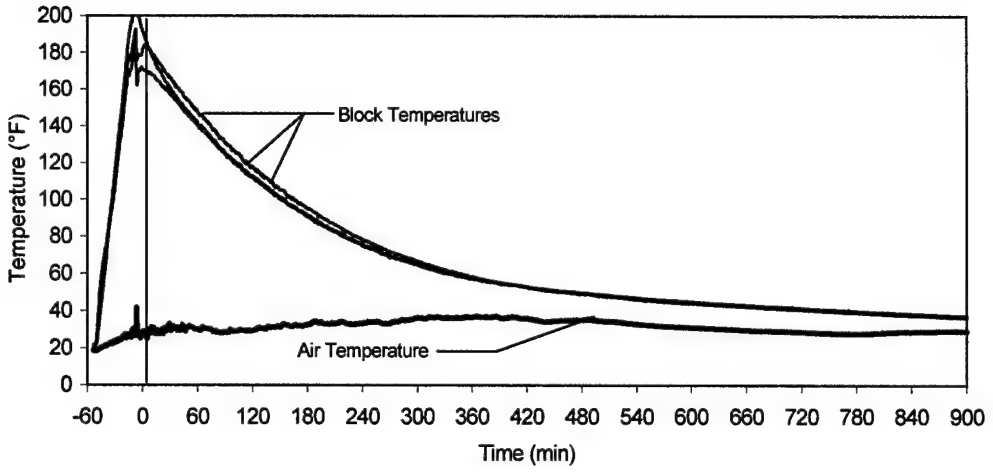


**Figure 4.16**
**Block Temperatures Measured During Cool-Down Test on February 14,1999**

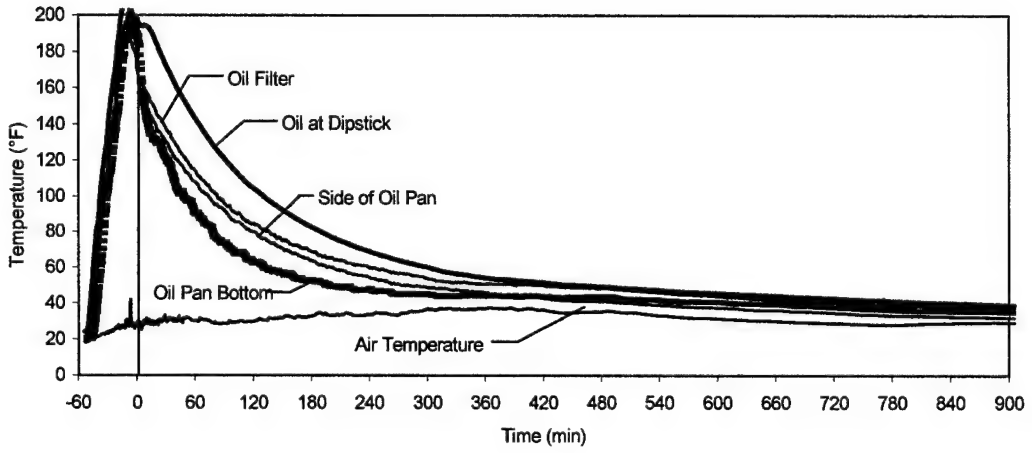


**Figure 4.17**
**Oil System Temperatures Measured During Cool-Down Test on February 14,1999**

The exhaust pipe temperature, measured on the outer surface of the exhaust pipe section that was under the cab is shown in Figure 4.18. The changes in the slope of the temperature-time curve correspond to changes in engine operation speed. A maximum temperature of 300°F was measured during the tests. It is recognized that because of the high temperature of the exhaust and exhaust pipe, the exhaust pipe offers the potential to readily heat a PCM storage device for later use for applications such as warming engine components, warming other equipment, or even cooking food. However the use of this stored energy would require a means of moving the stored energy from the area of the exhaust to the point

of use. This would require either the manual movement of an energy storage device or the use of a thermal transport system, such as a pumped coolant loop. Because it was thought that a passive system with no daily intervention would be more useful than an active system, concepts involving thermal storage of the exhaust stream were not considered further for the present study.

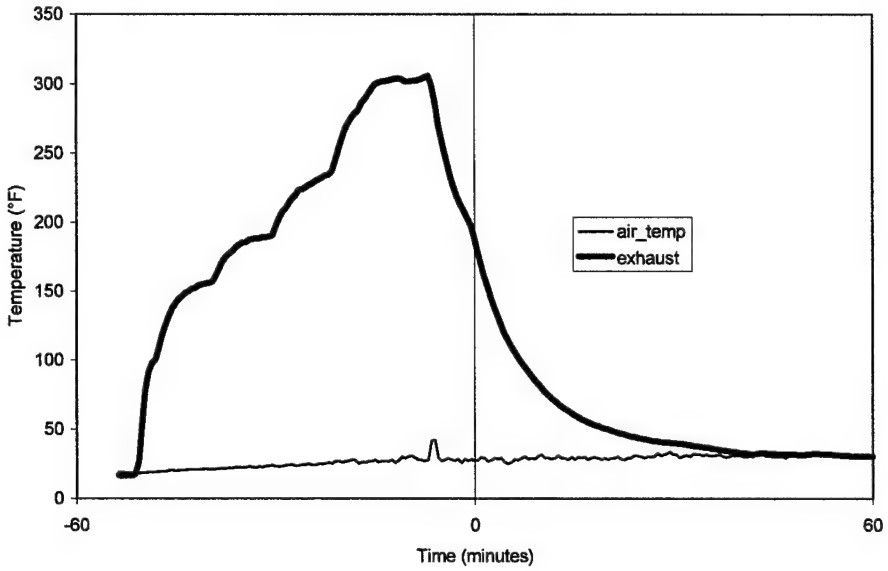


**Figure 4.18**
**Exhaust Pipe Temperatures Measured During Cool-Down Test on February 14,1999**

A common cold starting problem is gelling of the fuel at low temperatures, which leads to blockage in the fuel lines. One of the critical points for blockage in the fuel system is the fuel filter. The fuel filter temperature was measured during some of the later baseline tests and the filter temperature measured in a typical test is shown in Figure 4.19. During operation, the fuel filter temperature was found to increase much less than the block or the oil system temperatures. It is thought that the heat transfer from the engine block to the filter was absorbed by the flow of cold fuel through the filter. Indeed, the fuel filter temperature continued to increase as a result of heat transfer from the engine block after the engine was shut off. As a result of the fuel filter measurements it was concluded that the use of a totally passive PCM-ESD system would not be as effective for the fuel filter as it would be for the oil filter, which was maintained at much higher surface temperatures.

Because of the reduced payoff for the implementation of a totally passive PCM-ESD system to the fuel system, development of a passive thermal protection system for the fuel system was not investigated further during this study. However, in environments where fuel gelling is a problem, the use of a PCM-ESD system, which would incorporate active heating of the PCM (engine coolant, or electrical resistance heating) to maintain an elevated temperature for the fuel filter or other fuel system components.

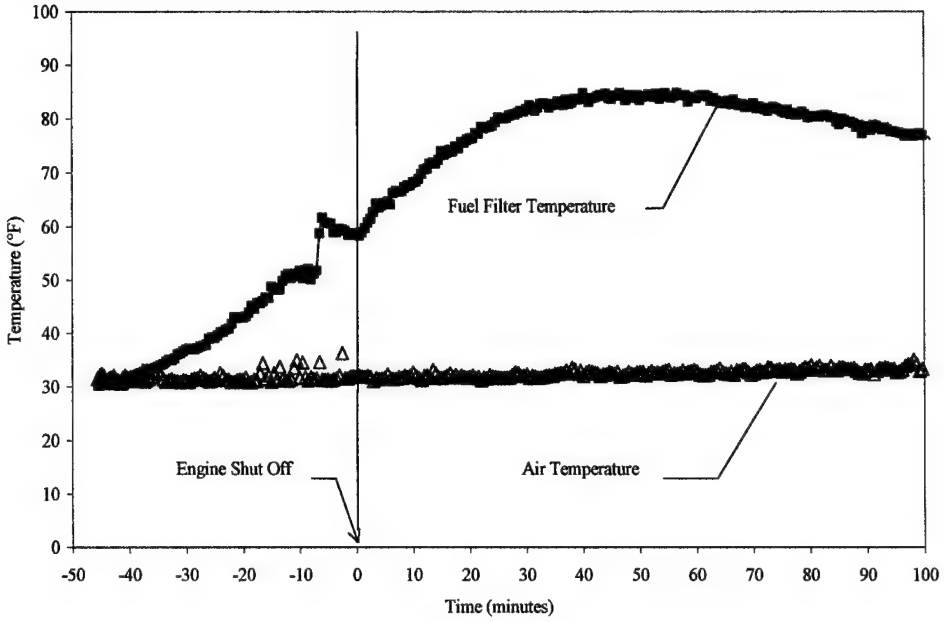


**Figure 4.19**
**Fuel Filter Temperatures during Typical Baseline Test**

At the start of the program it was recognized that battery performance, which is known to be temperature-dependant, would be an issue. A major concern about a battery thermal protection system that relies on the insulation of the batteries, was the possibility of overheating the batteries as a result of the heat generated during battery charging, because of the inefficiencies of the charging process. An experiment was conducted to determine the magnitude of the temperature increase of the batteries during charging. Previous to this test the batteries had been discharged. The engine was jump-started and operated at an engine speed of 1500 rpm for 3.5 hrs (to recharge the battery) and then shut off. Figure 4.20 shows the battery, outside air, inside cab temperatures during the test. The air temperatures inside and outside of the cab are the thermal boundary conditions for the batteries. Throughout the charging period (engine operation – Time < 0) the thermal boundaries of the battery box

were at a higher temperature than the battery. The implication of the thermal boundary conditions for this test was that heat was supplied from the surroundings during charging, so that the test was an even worse case than a totally insulated battery box, which would only be affected by the heat generated during charging. During the 210 minute charging battery period, the temperature of the batteries only increased by 8.5°F. Therefore, it was concluded that an insulated battery box could be built with little concern of overheating because of the heat generated during charging.

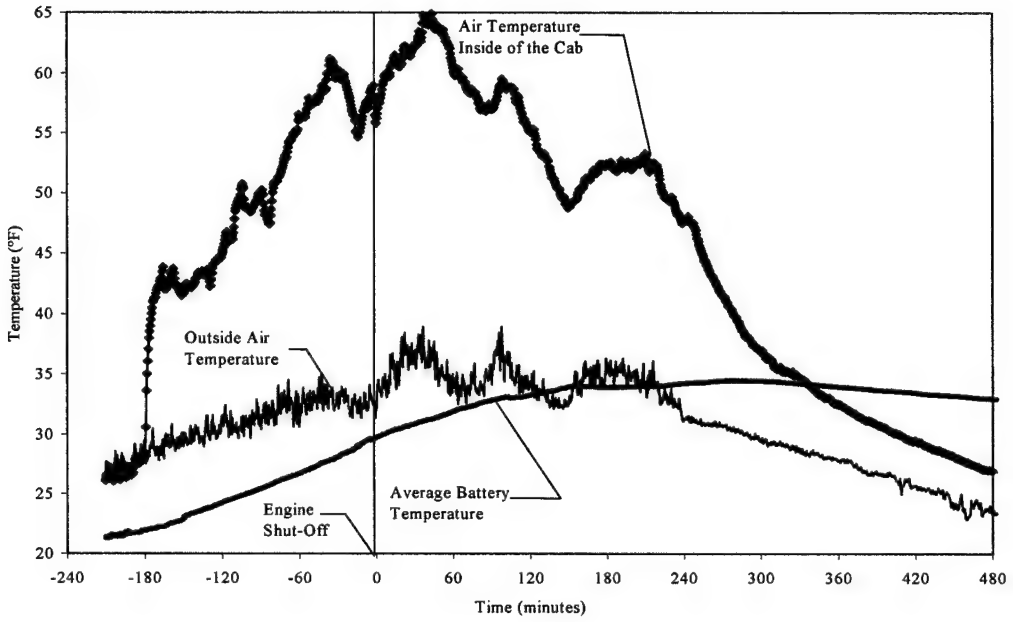


**Figure 4.20**
**Average Battery Cell, Truck Cab and Ambient Air Temperatures during Battery Recharging Experiment**

A summary of the conditions during the baseline cool down tests conducted is shown in Table 4.2. The oil temperature at the dipstick and the block temperature measured during baseline cool-down tests are plotted vs. the average air temperature during cool-down in Figure 4.21 at 10 and 12 hr intervals after engine shutdown. It can be seen that the oil and the block temperatures were approximately equal after 10 hours and that both temperatures were close to the average air temperatures after 12 hrs.

## Table 4.2
## The Conditions during Baseline and Insulated Oil System Engine Cool-Down Tests

| Test started | | Cool Down Environment | | Temperatures at End of Test | | | |
|---|---|---|---|---|---|---|---|
| Date/Time | Configuration | Cool-Down Time (Min) | Average Air Temp (°F) | Dipstick Temp (°F) | Block Temp (°F) | Oil Filter (°F) | Battery Temp (°F) |
| 2/13/99 7:07 AM | Baseline | 312.7 | 19.5 | 49.8 | 51.7 | 39.3 | 29.1 |
| 2/14/99 7:34 AM | Baseline | 1284.7 | 30.9 | 35.4 | 32.1 | 34.0 | 31.5 |
| 2/17/99 11:48 AM | Insulated Pan | 1166.0 | 31.2 | 35.3 | 31.1 | 30.3 | 34.9 |
| 2/19/99 3:40 PM | Insulated Pan | 944.4 | 28.9 | 36.1 | 31.0 | 28.5 | 30.8 |
| 2/24/99 11:20 AM | Insulated Pan &Filter | 1226.4 | 33.6 | 38.7 | 35.1 | 35.6 | 33.7 |
| 3/1/99 8:20 AM | Insulated Pan &Filter | 1419.9 | 33.2 | 35.8 | 33.0 | 34.1 | 34.7 |
| 3/22/99 8:57 AM | Insulated Pan &Filter | 1408.0 | 35.5 | 44.1 | 40.4 | 38.7 | 33.8 |
| 12/17/00 6:14 PM | Baseline | 477.3 | 43.7 | 57.6 | 61.3 | 52.6 | 41.5 |
| 12/20/00 9:20 AM | Baseline | 896.7 | 27.2 | 26.3 | 28.1 | 24.8 | 31.1 |
| 12/21/00 8:58 AM | Baseline | 581.8 | 26.7 | 41.3 | 45.2 | | 33.2 |
| 12/21/00 7:45 PM | Baseline | 720.1 | 18.5 | 25.4 | 26.1 | | 25.2 |
| 12/22/00 8:31 AM | Baseline | 1327.3 | 29.6 | 30.9 | 29.4 | | 30.9 |
| 12/23/00 7:42 AM | Baseline | 1385.8 | 23.0 | 22.9 | 23.4 | | 26.9 |
| 1/13/00 8:30 PM | Baseline | 642.1 | 17.4 | 21.2 | 28.6 | 26.2 | 28.2 |
| 1/20/00 6:30 PM | Baseline | 745.4 | -4.2 | 10.4 | 9.8 | 6.2 | 19.3 |

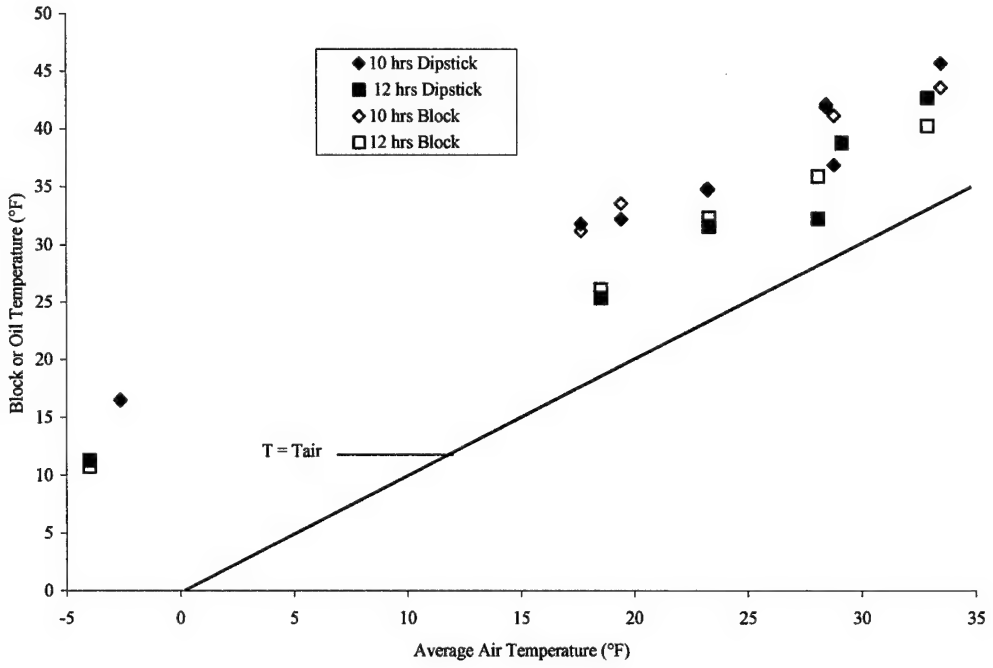


## Figure 4.21
## The Oil and Block Temperatures Measured during Baseline Cool-Down Tests

### 4.2.3 Effect of Insulation on Oil pan and Oil filter

Several tests were conducted to determine the effect of oil pan insulation on the oil temperature during operation and cool-down. The oil pan was insulated using a shell formed from 7/16"-thick polyisocyanurate insulation (R-Value=3.5). The oil temperatures measured during two typical operation and cool-down tests with and without the oil pan insulation are shown in Figure 4.22. The average air temperature during the first fourteen hours of engine shut-off was approximately the same (32°F) for both cases. The case with the insulated pan showed nearly identical oil temperatures during operation but exhibited slower cooling after engine shut-off than the baseline case because of the reduced heat loss through the oil pan. For reference purposes the temperature level for an 86% step change between the temperature at engine shut off and the average ambient air temperature is shown. The 86% step change is significant because it corresponds to the temperature change during two time constants for a first order system. The time required for the oil temperature to decrease down to this level is increased by approximately 60% by the presence of the insulation.

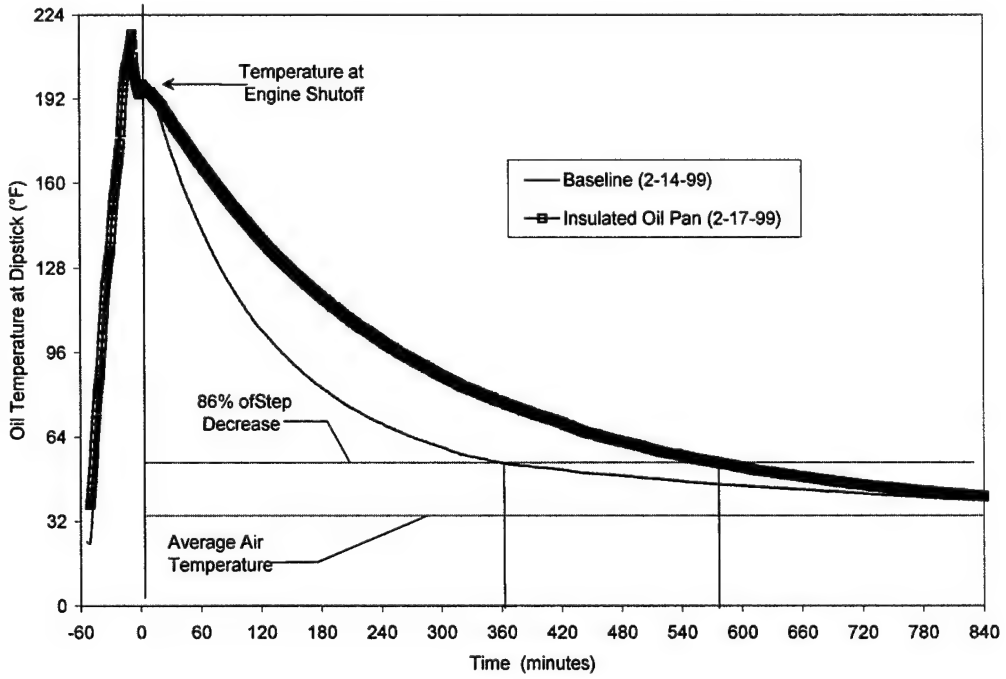


**Figure 4.22**
**The Effect of Insulating the Oil Pan on the Oil Temperature Measured at the Dipstick During Operation (Average Air Temperature During Cool-Down = 32°F for Both Tests)**

As the time after engine shut off increased further, the difference between the oil temperature for the insulated oil pan and the baseline case began to decrease until the oil temperatures was approximately the same as the baseline case. The reason for the eventual merging of the two cases was the heat loss through the engine block into the surroundings. While the heat transfer through the oil pan was decreased by the insulation, the thermal resistance between the oil in the pan and the engine block was not changed, so that the thermal energy was lost through the block.

The effect of adding insulation to the oil filter was also investigated by insulating the oil filter with a ½" thick sheet of foam rubber, which was wrapped around the filter as shown in Figure 4.23 and secured in place by plastic tie wraps. The oil filter temperatures measured for the baseline and insulated configurations measured during typical operation, are expressed as the difference between the filter temperature and the average air temperature during cool-down are shown in Figure 4.24. The filter temperatures were expressed as a temperature difference because the average air temperature during the cool-down was 4°F higher for the test of the insulated configuration than it was for the baseline case. As shown in Figure 4.24 there was little difference between the oil filter temperature during operation for the two configurations. After engine shutoff the insulated oil filter was seen to cool at a slower rate than the baseline case. The insulated oil filter required over 135 minutes more time than the baseline (a 60% increase) to reach a temperature level of 32°F above the ambient air temperature. At extended times the difference between the insulated and baseline cases is less apparent. Similar to the insulated oil pan, while the sides of the oil filter were insulated, the conduction path through the top of the oil filter was unaltered, so that the excess thermal energy eventually escaped through the top of the oil filter.


**Figure 4.23**
**Oil Filter Insulation Installed on the Engine**

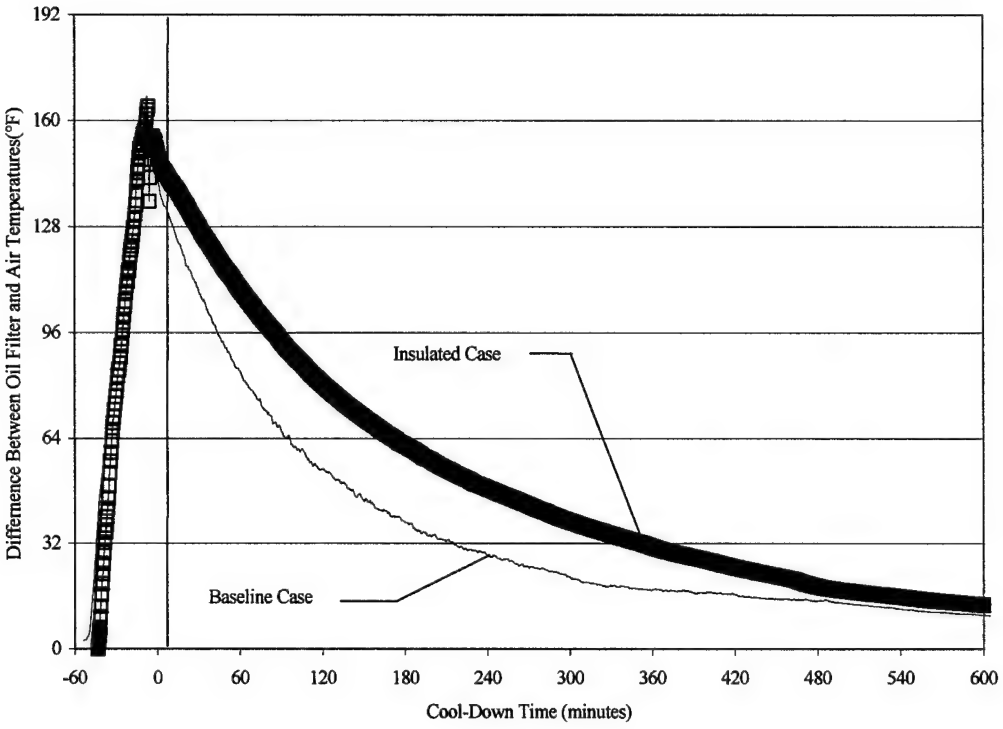


**Figure 4.24**
**Effect of Oil Filter Insulation on the Oil Filter Temperature during Cool Down**

In summary the tests of the insulated oil filter and oil pan showed that:

1. The two components could be insulated without overheating during operation.
2. The application of insulation allows higher oil temperatures to be maintained for a few hours after shutoff.
3. The difference between the oil temperature for the baseline and the insulated cases was small after an extended shutdown period.

The results of the insulated oil system components implied that additional thermal mass added to the filter and oil pan by the use of PCM in combination with the insulation would extend the time that the oil pan and filter could be maintained at a higher level.

### 4.2.4 Baseline Starting and Cranking Performance Tests

The test vehicle was equipped to measure the engine speed, as well as the battery current and voltage during starting for the tests conducted at the University of Dayton. The emphasis of the test was to develop a database of cranking performance of the baseline engine configuration over a range of block, oil system, air, and battery conditions. For the tests the vehicle was exposed to winter environment in Dayton, and the test conditions (ambient air, battery, block and oil system temperatures) for the cranking tests were a function of the ambient environment during the engine shut-off period and the time after the previous engine shutdown. In general, there was no independent control of the battery, block, and oil temperatures during the tests.

During the cranking tests the computer data acquisition system acquired data in "fast mode" (100 Hz for early tests, and 200 Hz for the later tests) for 1 minute before reverting to "slow" mode (data averaged at 1 sample/minute per channel) for the rest of the test. Cranking was initiated by turning the starter switch on and cranking the engine until it was judged by the operator that the engine would continue to run on its own. Sometimes this procedure resulted in the premature end of engine cranking and a non-start. When a non-start occurred, the engine was immediately cranked again until it started. It was observed that usually cranking was easier after a near start.

It is emphasized that the ether system for the truck was not used during any of the cranking tests for either the baseline or the PCM-ESD equipped tests. In fact, the ether canister was empty when the truck was turned over to UDRI for the winter tests.

The cranking performance was characterized by several measures. First, there was the question of whether the engine started or not. The second measure of cranking performance was the total work during cranking which was determined from the integration of the cranking power, which in turn, was calculated from the product of the measured battery voltage and current, over the cranking period. The cranking work is important because it is related to the drain of the battery capacity during starting. A third characteristic of cranking performance, related to the cranking work, is the total cranking time in seconds.

The current, voltage and engine speed, measured during two typical starting transients, are shown in Figures 4.25 and 4.26. During the cranking test on December 10$^{th}$ 1999, shown in Figure 4.25, the ambient air, engine block, oil (at the dipstick) and battery

temperatures for this test were all above 47°F and the engine started in less than 1 second. In contrast, the ambient air and the engine block, oil, and battery temperatures were more than 25°F lower for the starting test on December 24th, 1999, shown in Figure 4.26. The effect of the lower temperatures for the second test is readily apparent, by comparing the cranking time (which was 30 times greater), and the cranking work (which was almost 40 times greater).

A summary of the cranking tests conducted with the baseline engine configuration is shown in Table 4.3. Cranking tests were conducted over a range of ambient air temperatures from –9°F up to 53°F. The data were obtained by starting the engine after it had been shut-off for at least 8 hrs; often the engine was shut off for a longer time between starts. At the lowest air temperature (also the lowest block, battery and oil temperatures) the engine would not start by cranking with the battery and could only be started after covering the hood with a plastic tarp and using a kerosene space heater to pre-warm the engine above 30 °F. The start at the lowest air temperature (-3°F) was accomplished by starting the engine after only 10 hrs, before the engine block and oil system temperatures dropped too far.

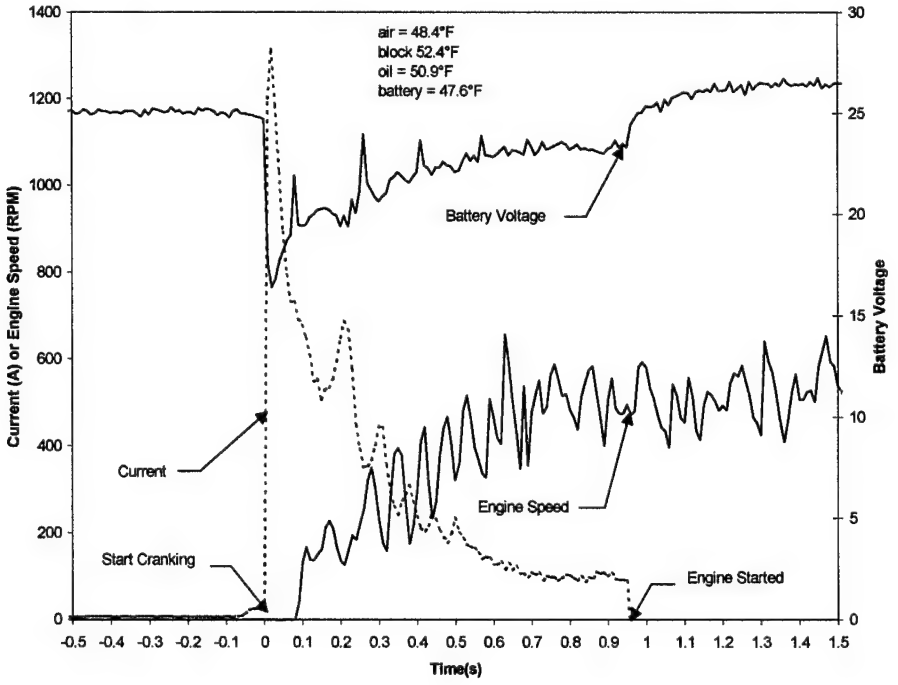


**Figure 4.25**
**Cranking Performance of Engine during Start on December 10, 1999. Total Cranking Time = 0.95 seconds, Total Cranking Work = 6.1 kJ.**

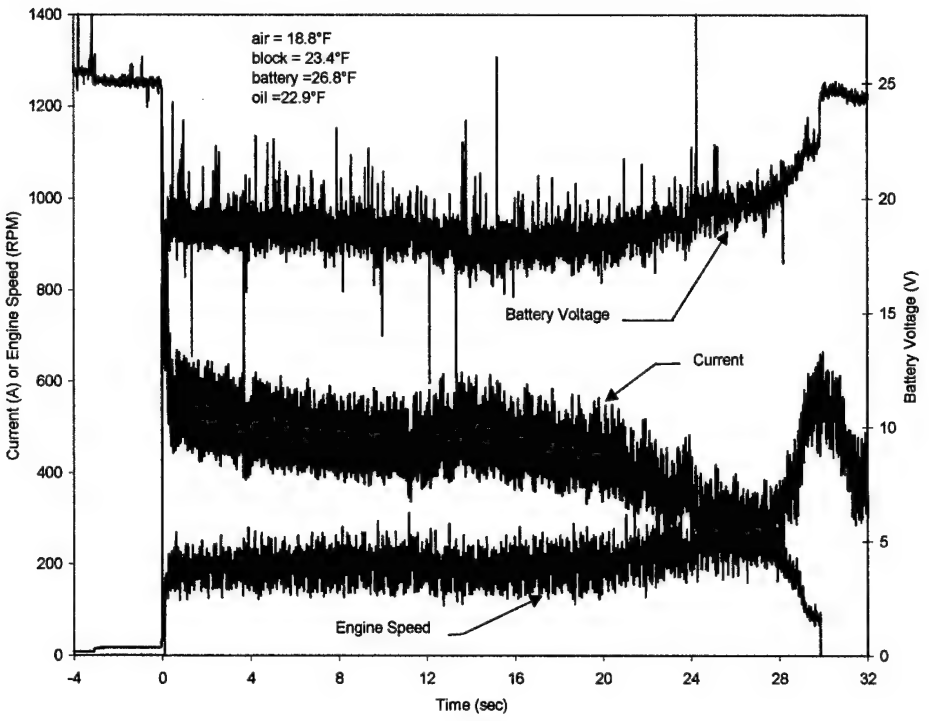


**Figure 4.26**
**Cranking Performance of Engine During Start on December 24, 1999 Total Cranking Time = 30.7 seconds, Total Cranking Work = 240 kJ**

The total cranking work and time-averaged cranking power for the baseline tests is plotted against the cranking time in Figure 4.27. The average power required during the cranking exhibited some scatter, but in general, increased as the total cranking time increased, which explains the increasing slope of the work vs. time curve.

**Table 4.3**
**Summary of Baseline Cranking Test Data**

| Test Conducted | Cranking Performance | | | | Conditions at Startup | | | | | |
|---|---|---|---|---|---|---|---|---|---|---|
| Test Date and Time | start | Start Attempts | Cranking Time (sec) | Cranking Work (kJ) | Dipstick Temp (°F) | Air Temp (°F) | Ave. Block Temp (°F) | Ave. Battery Temp (°F) | Oil Filter Temp (°F) | Bottom Oil Temp (°F) |
| 12/8/99 5:32 PM | yes | 1 | 1.95 | 10.2 | 49.3 | 45.6 | 49.2 | 43.0 | 48.0 | - |
| 12/9/99 9:05 AM | yes | 3 | 10.85 | 54.3 | 38.4 | 39.5 | 37.5 | 39.7 | 38.8 | - |
| 12/9/99 5:15 PM | yes | 1 | 1.51 | 7.3 | 58.4 | 53.5 | 64.4 | 44.9 | 56.5 | - |
| 12/10/99 8:08 AM | yes | 1 | 0.95 | 6.1 | 50.4 | 48.4 | 52.4 | 47.6 | 50.9 | - |
| 12/13/99 9:22 AM | yes | 2 | 11.41 | 49.0 | 37.3 | 35.4 | 36.4 | 37.3 | 36.2 | - |
| 12/16/99 9:13 AM | yes | 3 | 18.57 | 105.7 | 32.2 | 33.0 | 34.6 | 35.2 | 33.2 | - |
| 12/17/99 9:29 AM | yes | 2 | 13.98 | 79.1 | 33.6 | 32.5 | 34.7 | 33.7 | 32.6 | - |
| 12/17/99 6:14 PM | yes | 1 | 2.02 | 8.3 | 57.2 | 44.7 | 60.8 | 41.4 | 52.3 | - |
| 12/19/99 7:58 AM | yes | 1 | 17.33 | 116.0 | 29.1 | 28.5 | 30.1 | 32.1 | 29.5 | - |
| 12/20/99 5:08 PM | yes | 2 | 9.82 | 44.5 | 37.4 | 31.8 | 37.1 | 40.9 | - | - |
| 12/21/99 8:58 AM | yes | 1 | 24.98 | 173.0 | 26.6 | 19.5 | 28.1 | 31.0 | 24.5 | - |
| 12/21/99 8:00 PM | yes | 1 | 4.48 | 19.4 | 41.4 | 23.3 | 44.5 | 33.1 | - | - |
| 12/22/99 8:43 PM | yes | 1 | 22.89 | 159.0 | 25.4 | 14.7 | 26.1 | 25.0 | - | - |
| 12/23/99 7:48 AM | yes | 1 | 21.59 | 139.8 | 28.4 | 22.1 | 27.9 | 30.2 | - | - |
| 12/24/99 7:48 AM | yes | 1 | 30.73 | 240.6 | 23.6 | 18.8 | 23.2 | 26.8 | - | - |
| 1/6/00 6:51 AM | yes | 1 | 16.52 | 100.6 | 31.9 | 27.8 | 31.4 | 31.9 | - | - |
| 1/8/00 8:58 AM | yes | 1 | 18.65 | 122.8 | 36.8 | 30.8 | 29.2 | 33.0 | 29.1 | - |
| 1/9/00 7:59 AM | yes | 1 | 5.6 | 28.3 | 45.6 | 34.8 | 36.8 | 37.6 | 40.5 | - |
| 1/13/00 8:33 PM | yes | 1 | 17.22 | 109.0 | 27.5 | 25.5 | 28.3 | 34.3 | 29.1 | 27.9 |
| 1/14/00 8:00 AM | yes | 1 | 17.52 | 109.5 | 29.4 | 12.9 | 28.6 | 28.2 | 26.2 | 21.2 |
| 1/21/00 7:40 AM | no | 4 | 36.66 | 323.8 | 10.4 | -9.0 | 9.8 | 19.9 | 6.2 | 2.8 |
| 1/28/00 4:47 AM | yes | 1 | 20.33 | 147.7 | 20.8 | -3.4 | 22.1 | 20.7 | 15.4 | 9.65 |

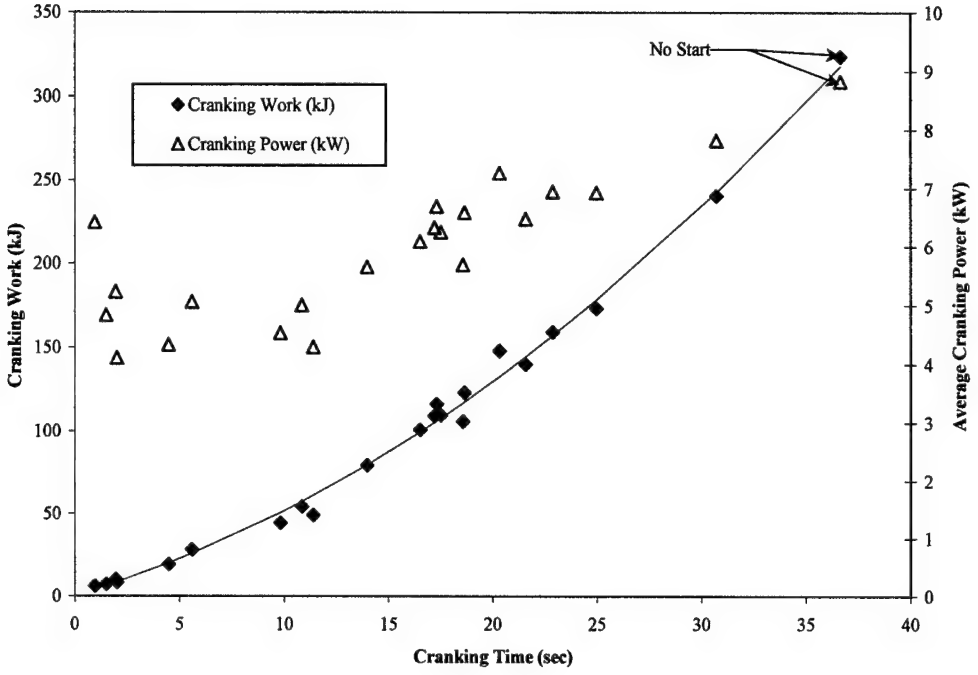


**Figure 4.27**
**Relationship Between the Cranking Work and Cranking Time Measured during the Baseline Tests**

The cranking work measured in the baseline tests is plotted vs. the oil temperature at the dipstick Figure 4.28. As the temperature of the oil decreased the cranking work was observed to increase. The cranking work strongly increased as the oil temperature decreased below 40°F. The plots of cranking work vs. oil filter and engine block temperatures, shown in Figures 4.29 and 4.30 respectively, exhibit a similar shape, which could be expected because block, oil and oil filter will all be at approximately the same temperature after an extended cool-down period.

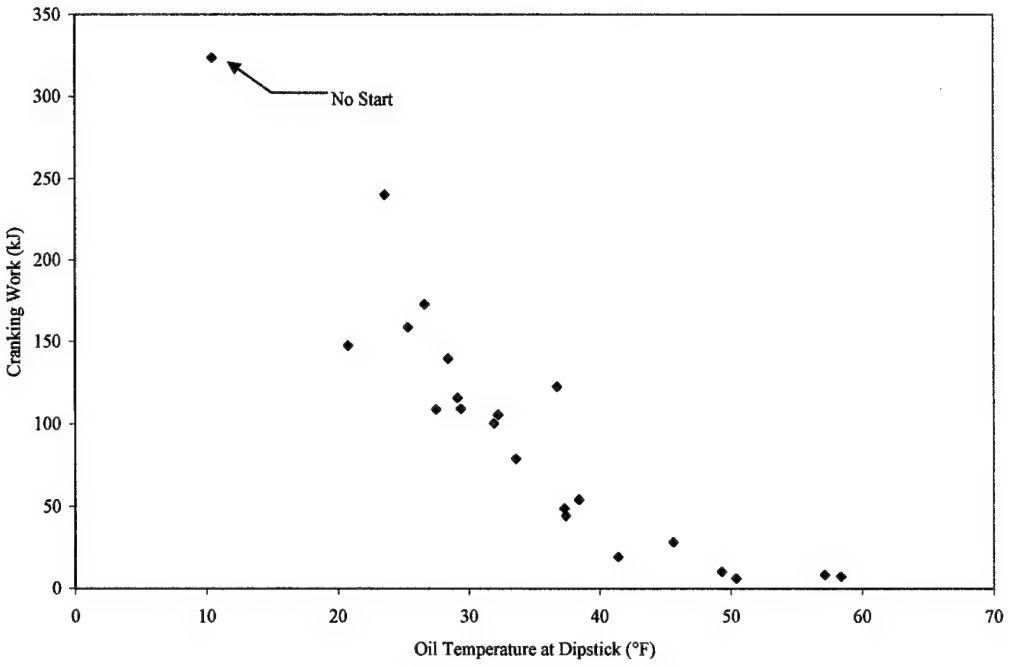


**Figure 4.28**
**Cranking Work vs. Oil Temperature at the Dipstick for the Baseline Cranking Tests**

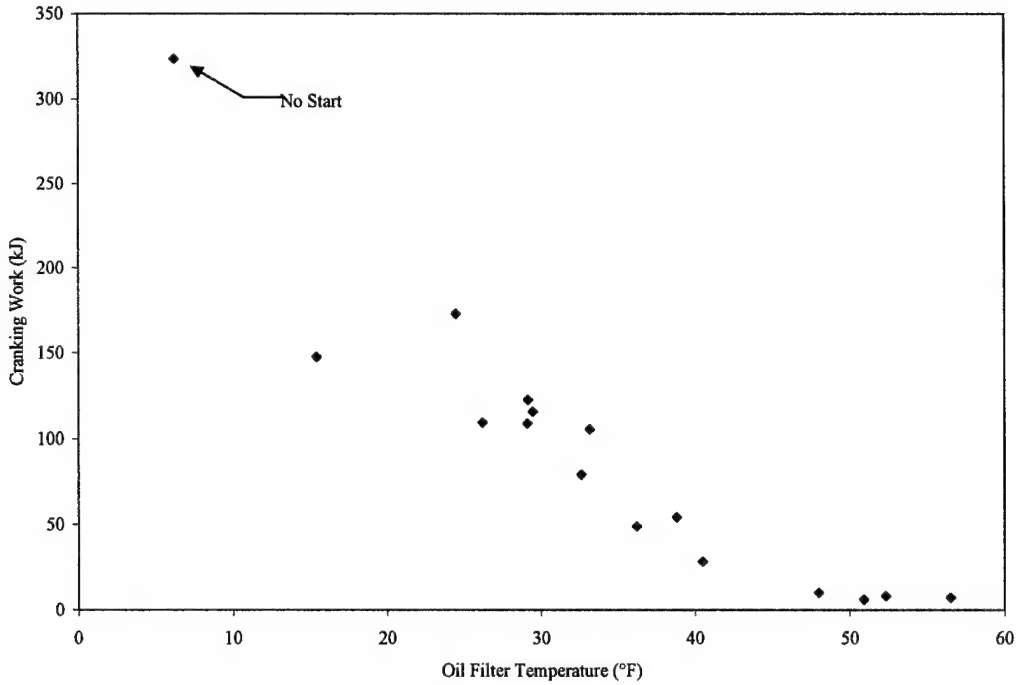


**Figure 4.29**
**Cranking Work vs. Oil Filter Temperature for the Baseline Cranking Tests**

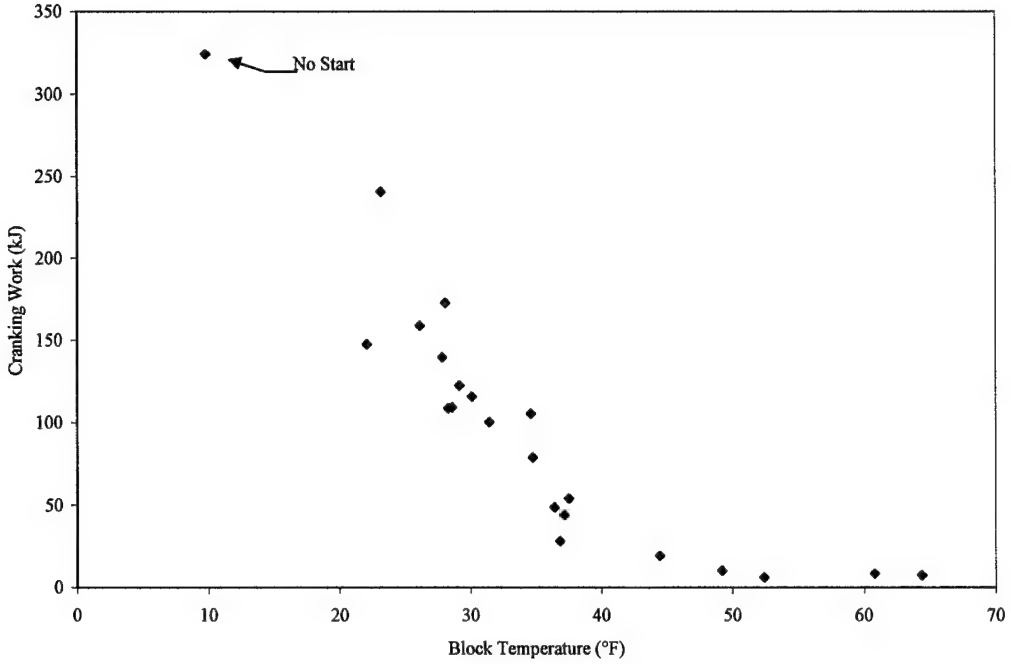


**Figure 4.30**
**Cranking Work vs. the Average Block Temperature for the Baseline Cranking Tests**

The cranking work is plotted vs. the air temperature in Figure 4.31. Although the cranking work increased with decreasing air temperatures, considerably more scatter was observed in the data, because the engine system temperatures are dependent on both the time after engine shut-down and the time history of the ambient air temperature. It should be noted that, in the extreme case a warm engine will readily restart soon after engine shutdown, even if the air temperature is low.

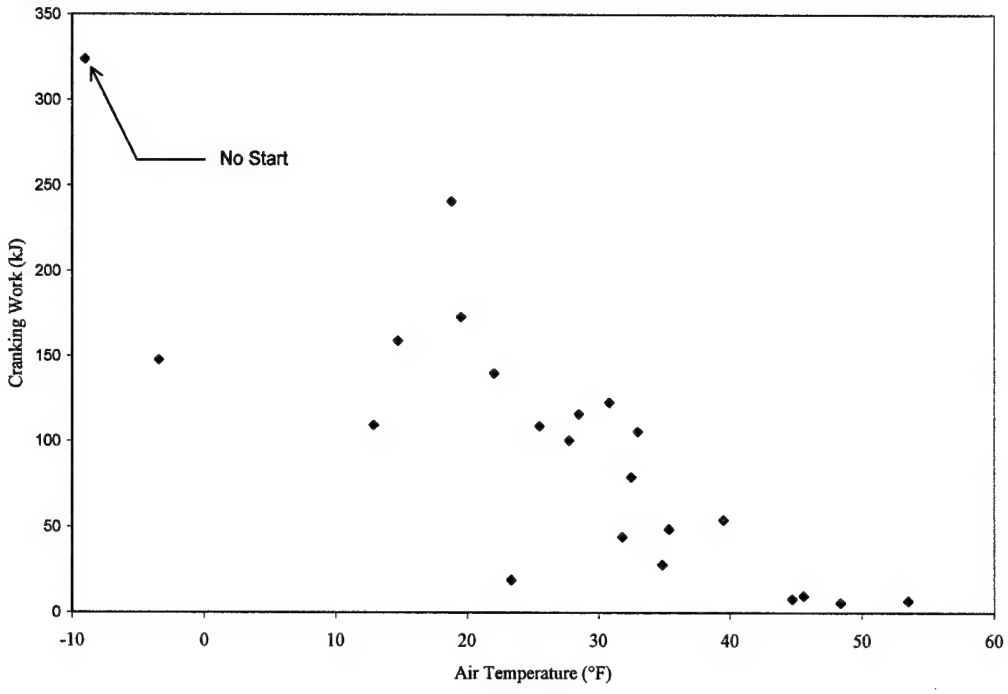


**Figure 4.31**
**Cranking Work vs. the Ambient Air Temperature for the Baseline Cranking Tests**

## 4.3 Experimental Tests with the PCM-ESD System Applied to the Engine

### 4.3.1 Engine Test Program with PCM-ESD Installed on the Engine Oil System

The PCM-ESD system was applied to the engine near the end of January 2000. A total of sixteen cool down and cranking tests were conducted with the PCM-ESD applied to the oil pan. A summary of the test conditions and starting performance during the next morning is shown in Table 4.4. Each cool-down test with the PCM-ESD system was followed by a successful restart on the following morning. The first four tests were conducted with the PCM-ESD system applied to the oil pan only. For the last twelve tests the PCM-ESD was applied to both the oil filter and oil pan. The insulation used for the first fourteen tests with the oil pan ESD, and for all of the oil filter ESD tests was 7/16" polyisocyanurate. For the last two tests, the higher resistance Vacuum insulation was used in place of the Polyisocyanurate insulation on the oil pan ESD.

During the engine operation portion of the test the engine was operated until the thermocouple on the backside of any of the PCM-ESD's reached 180°F. The 180°F limit was selected because it was the highest temperature that the PCM-ESD's were exposed to in the laboratory qualification tests before application to the truck. Also, additional heating of the ESD's would only lead to marginal gains in energy storage. The operating period was largely dependent on the temperatures of the PCM-ESD at the start of the test. As seen in Table 4.4, the engine operating time during tests with the PCM-ESD protection system installed on the engine, ranged from 101 to 165 minutes.

The engine speed during a typical test is shown in Figure 4.32. At the start of engine operation the engine was operated at idle for about 5 minutes. The engine speed was then increased to 1500 rpm in 500-rpm steps and was operated at 1500 rpm for most of the engine operating time. With the throttle set at this level the engine temperatures were maintained at the same levels (by the engine cooling system) that were seen at the end of the baseline tests. The engine was then set at idle for the last five minutes of operation before engine shut-off.

.

## Table 4.4
## Summary of Tests with the PCM-ESD Applied to Oil System

| Engine Operated | | Cool-Down Environment | | Starting Performance | | | Conditions at Startup | | | | | | |
|---|---|---|---|---|---|---|---|---|---|---|---|---|---|
| Date and Time | Engine Run Time (min) | Cool down Time (min) | Average Air Temp (°F) | Start Attempts | Cranking Time (sec) | Cranking Work (kJ) | Dipstick Oil Temp (F) | Bottom Oil Temp (F) | Air Temp (°F) | Block Temp (°F) | Battery Temp (°F) | Oil Filter Backside Temp (°F) | Notes |
| 1/28/00 6:15PM | 117 | 725 | 13.5 | 2 | 8.25 | 53 | 44.2 | 49.7 | 19.8 | 30.3 | 24.2 | 25.5 | First test with Oil Pan ESD |
| 1/29/00 4:28 PM | 150 | 1210 | 29 | 1 | 3.58 | 20.2 | 40.9 | 43.2 | 29.8 | 33.7 | 33 | 30.8 | |
| 1/30/00 3:21 PM | 155 | 1288 | 24.8 | 1 | 5.2 | 29.4 | 31.9 | 31.8 | 30.9 | 30.7 | 31 | 30.4 | |
| 1/31/00 5:39 PM | 149 | 840 | 23.1 | 1 | 3.27 | 17.1 | 42 | 48.8 | 24.9 | 32.2 | 30.8 | 28 | |
| 2/1/00 6:08 PM | 153 | 780 | 21.6 | 1 | 2.92 | 16.1 | 45.1 | 50.94 | 20 | 32.6 | 32.4 | 38.3 | Oil Filter PCM-ESD added |
| 2/3/00 5:42 PM | 165 | 1004 | 29.7 | 1 | 2.05 | 11 | 44.3 | 48.3 | 31.6 | 35 | 36 | 39.2 | |
| 2/4/00 7:04 PM | 101 | 780 | 23.1 | 2 | 3.4 | 17.9 | 46.5 | 51.9 | 21.9 | 33.8 | 34.5 | 45.7 | |
| 2/5/00 5:32 PM | 134 | 840 | 20.8 | 1 | 2.27 | 12.3 | 45.9 | 51 | 24.4 | 34.7 | 33.9 | 39.9 | |
| 2/7/00 5:46 PM | 131 | 800 | 21.8 | 1 | 2.43 | 12.4 | 48.6 | 54.2 | 23 | 36.8 | 39.1 | 42.5 | |
| 2/11/00 5:51 PM | 152 | 840 | 25.9 | 1 | 1.42 | 9.2 | 44.9 | 50.7 | 27.2 | 34.3 | 37.6 | 42.2 | |
| 2/12/00 3:24 PM | 125 | 991 | 29.6 | 1 | 1.68 | 9.1 | 50.6 | 54 | 35.5 | 41.9 | 40.7 | 45.6 | |
| 2/16/00 3:31 PM | 152 | 870 | 25.2 | 1 | 1.85 | 10.3 | 46.8 | 51.9 | 23.7 | 35 | 38 | 42.9 | |
| 2/20/00 4:01PM | 151 | 848 | 24.9 | 1 | 1.78 | 9.2 | 50.5 | 55.3 | 26.6 | 41 | 38.7 | 45.2 | |
| 3/3/00 6:15 PM | 135 | 720 | 27.3 | 1 | 0.83 | 5.8 | 56.6 | 58.7 | 31.7 | 47.6 | 45.5 | 50.8 | |
| 3/12/00 3:52 PM | 123 | 857 | 26.7 | 1 | 0.75 | 6 | 53.2 | 57.3 | 32.4 | 42.9 | 38.6 | 48.8 | Vacuum Insulation Used For Oil Pan PCM-ESD |
| 3/17/00 2:42PM | 157 | 847 | 25.5 | 1 | 1.33 | 8.6 | 46.1 | 52.8 | 22.3 | 34.6 | 35.4 | 41.1 | |

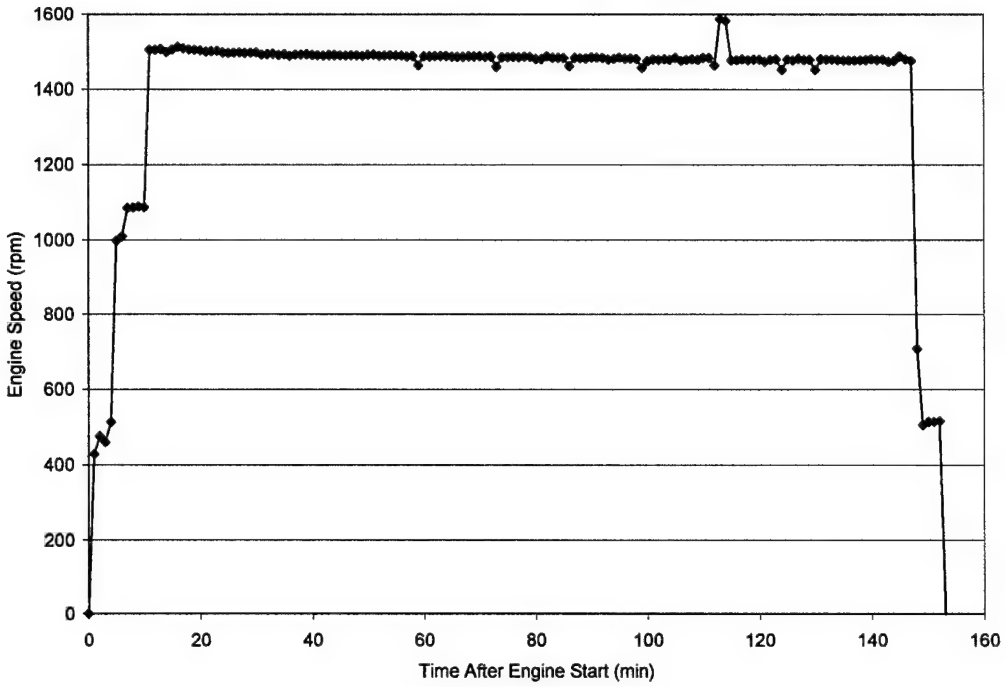


**Figure 4.32**
**Engine Speed during Engine Operation Period of a Typical Test with PCM-ESD Applied to the engine**

The time before restart, or cool-down time, for the engine is shown in Table 4.4. The time before restart for the truck ranged between 12 and 21 hrs, and was determined by a compromise between the minimum air temperature at restart, and maximum exposure time of the engine to the cold weather. Often the decision was made to restart the truck while the oil temperatures were well above the levels required for an easy restart, because of the increasing ambient air temperature

### 4.3.2 Results for Oil Pan PCM-ESD during Operation and Cool-Down Tests

Figure 4.33 shows the oil temperatures measured at the top and bottom of the pan during the first test with the PCM-ESD applied to the oil system. During engine operation, the oil temperature oscillated about a steady level after 53 minutes. The cycling of the engine clutch fan caused the saw-tooth temperature oscillations. When the clutch fan was turned on cold air was drawn through the radiator, which lowered the coolant temperature, which, in turn, lowered the oil temperature in the oil cooler. The ambient air temperature after engine shut-off averaged 13°F, ranged from 7°F to 19°F, and was increasing towards

the end of the engine cool-down period. Because of the increasing ambient air temperature, the cool-down portion of the test was halted and the engine restarted after 725 minutes.

After engine shutoff, the oil temperatures dropped. Initially the oil temperature was higher at the dipstick than it was at the bottom of the pan, because of the warm engine block and the natural convection of the warm oil to the top of the oil pan. After the engine block temperature decreased below the PCM-ESD freezing point, the temperature of the oil at the bottom of the oil pan was maintained at a higher level than the block because of the latent heat release from the PCM. At the end of the engine shut-off period the oil temperatures were 44°F at the top of the pan and 50°F at the bottom of the pan which was significantly higher than the ambient air temperature.

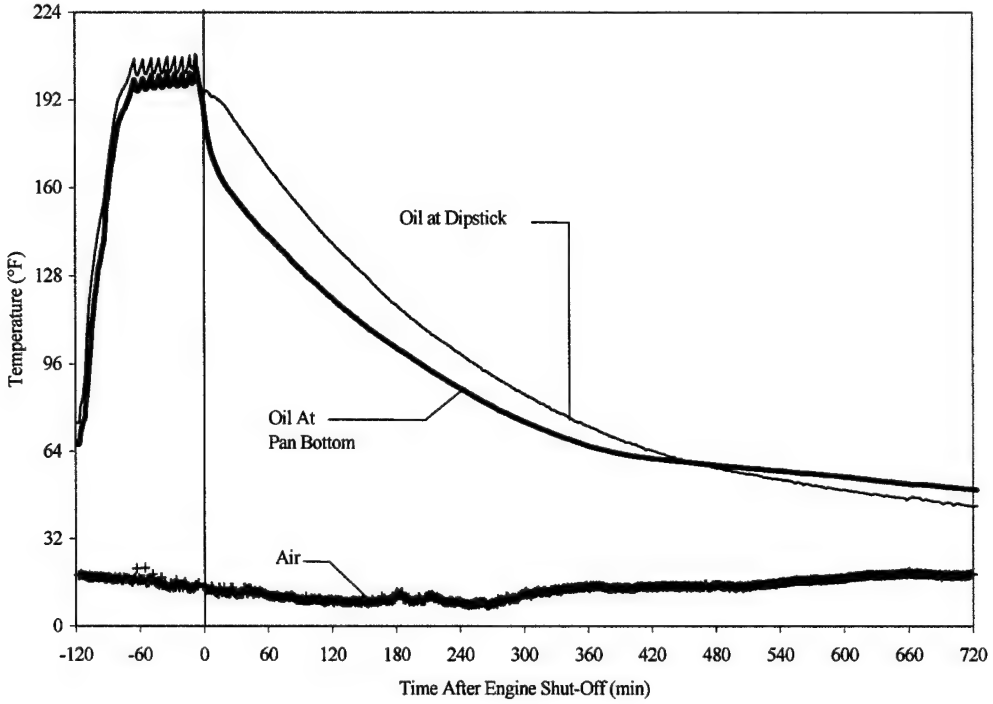


**Figure 4.33**
**Oil Temperatures Measured During the First Test with the PCM-ESD System Applied to the Oil Pan (Jan 28 2000)**

The oil temperatures measured during this same test are compared to those measured during a baseline test during engine cool-down in Figure 4.34. The air average air temperature for the baseline test was over 4 °F warmer than for the PCM-ESD case. As shown in Figure 4.34 the PCM-ESD system had a large positive effect on the oil

temperatures. The oil for PCM-ESD configuration required 725 minutes to reach a temperature of 44°F at the dipstick while the baseline configuration reached this level in only 384 minutes and eventually reached a temperature of 29°F when the engine was restarted (less than 11 hrs.). An even greater benefit was seen for the oil temperature measured near the bottom of the oil pan. At the end of the test with the PCM-ESD the oil temperature at the bottom of the pan was 50°F, while the oil temperature at this location remained above this temperature for only 127 minutes for the baseline case, and eventually decreased to 21°F before engine restart

The temperatures measured on the center of the outside surface of the oil pan PCM-ESD's during the same test are shown in Figure 4.35 along with the oil temperatures. The positions of the four ESD's were shown previously in Figure 2.26. The ESD's were removed from a room temperature environment and applied to the truck roughly 3 hrs before starting, and were still almost completely thawed before the truck was started. The temperature of the PCM-ESD's continuously increased during the operation of the engine, and the maximum temperature observed on the back face of the ESD's occurred within 15 minutes of engine shutoff. The maximum temperature on the backside occurred after engine shutdown because of the time required for heat conduction through the thickness of the ESD from the hot (inner) surface to the cooler (outside) surface.

During the cool-down phase of the experiment the temperature of the PCM-ESD's dropped along with the oil temperatures. An extended temperatures plateau can be seen for each of the ESD's as the PCM changes phase. The temperature of ESD#2, which was the thinnest of the ESD's dropped the fastest and was lower than the oil temperatures at the end of the test. The backside temperature of the other three ESD's remained above the oil temperatures through the end of the test. It should be noted that the backside of the ESD is expected to be the lowest temperature in the ESD, and that the temperature of the PCM inside of the ESD is expected to be higher than that on the outside surface.

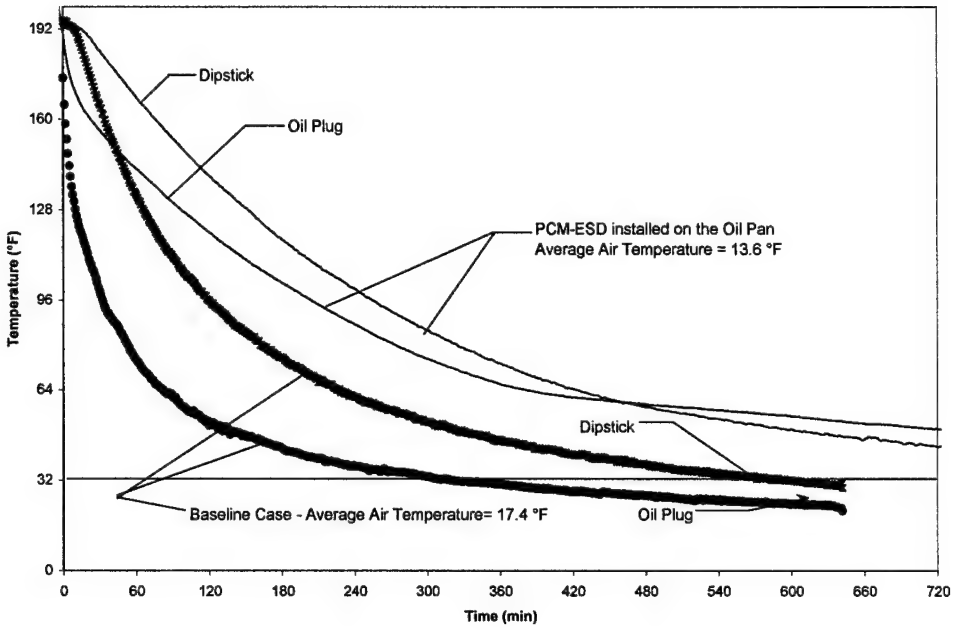


**Figure 4.34**
**Oil Temperatures at the Top (Dipstick) and Bottom (oil plug) of the Oil Pan during Engine Cool-down Tests With and Without the PCM-ESD**

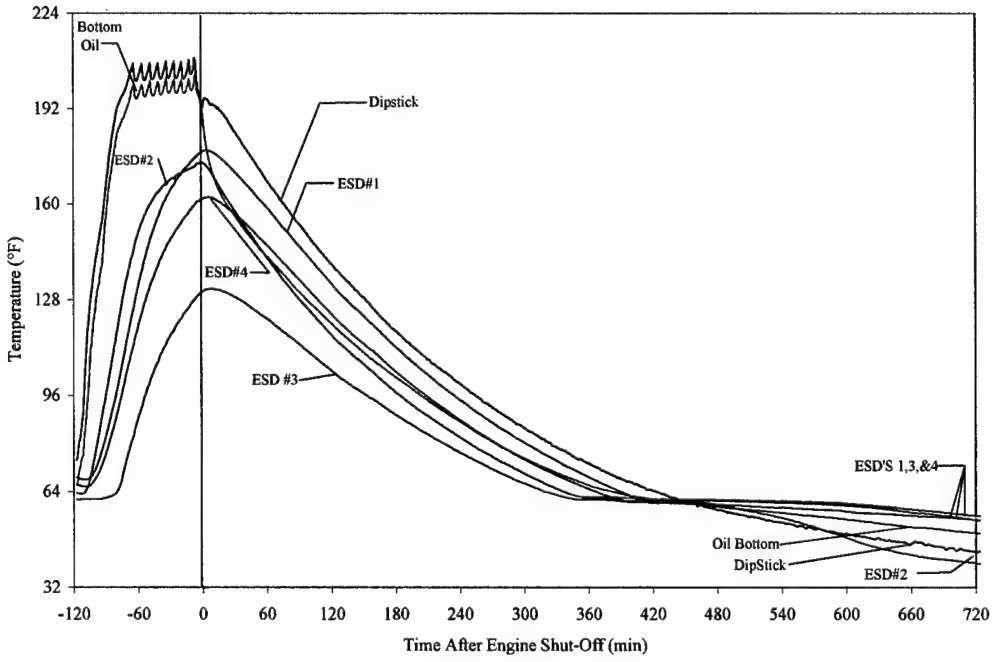


**Figure 4.35**
**The Oil Temperatures and the Temperatures Measured at the Center of the Backside of the Four Oil Pan ESD's During the First Cool-Down Test (January 28 2000)**

Figure 4.36 shows the measured surface temperatures at the backside of the oil pan PCM-ESD's as they were charged from a completely frozen state during restart and operation of the cold-soaked engine. The thinnest ESD (#2) which is mounted on the side of the deep end of the oil pan passed through phase change (T>71°F) in less than 30 minutes of engine operation. The two 2 inch-thick ESD's (#1, and #4) required more time to change phase because of the time required to conduct heat through an additional inch of PCM, while the thickest ESD (#3) required almost 90 minutes to completely change phase. The long time required to pass through phase change during charging of the ESD's is indicative of the large storage capacity of the ESD. It can be seen that after the PCM changes phase, the rate of temperature increase of the ESD increases because energy is only stored as sensible heat. As the temperatures of the ESD's increase the temperature difference between the oil in the pan and the ESD's decreases, and the rate of temperature increase for the ESD's decreases.

A summary of the temperatures measured on the backside of the PCM-ESD's after engine shutoff are shown plotted vs. the average air temperature after engine shut-off at selected times for all of the tests with the PCM-ESD in Figures 4.37-4.40. The temperatures are plotted at time intervals of 4, 8, 12, 14 and 16 hrs. Note that there are fewer data points at the longer time periods because the engine was usually restarted because of the rising air temperature. Note that the average air temperature during the cool-down period is an average from the time of engine shutdown to the time at which the temperatures are plotted and thus will change with time as a result of weather variations. For all of the tests the variation of the temperatures measured on the back of the ESD's at engine shut-off was usually less than 10°F. At four hours after engine shut-off all of the ESD temperatures were well above the melting point of the PCM. From a time of 8 hours onward, the temperatures of most of the ESD's were grouped within the range of phase change (from 71-55°F). After 12 hrs the back side temperature of ESD#2 was below freezing temperature of the PCM (55°F), while the other three ESD's which contained more PCM, remained above 55°F for up to 14 hours.

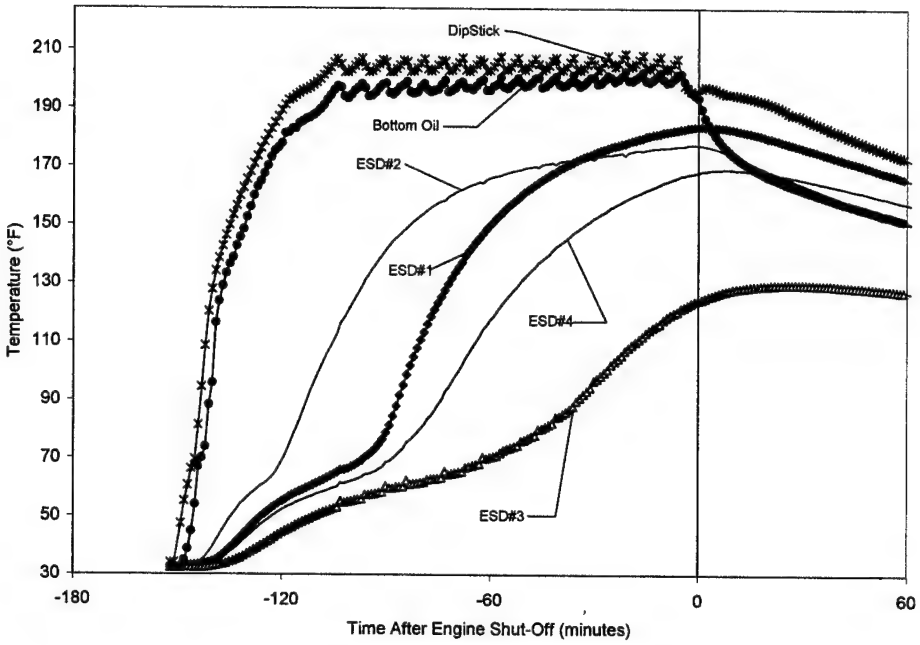


**Figure 4.36**
**Oil Temperatures and Backside ESD Temperatures during Charging of Cold ESD's During Test on February 20 2000**

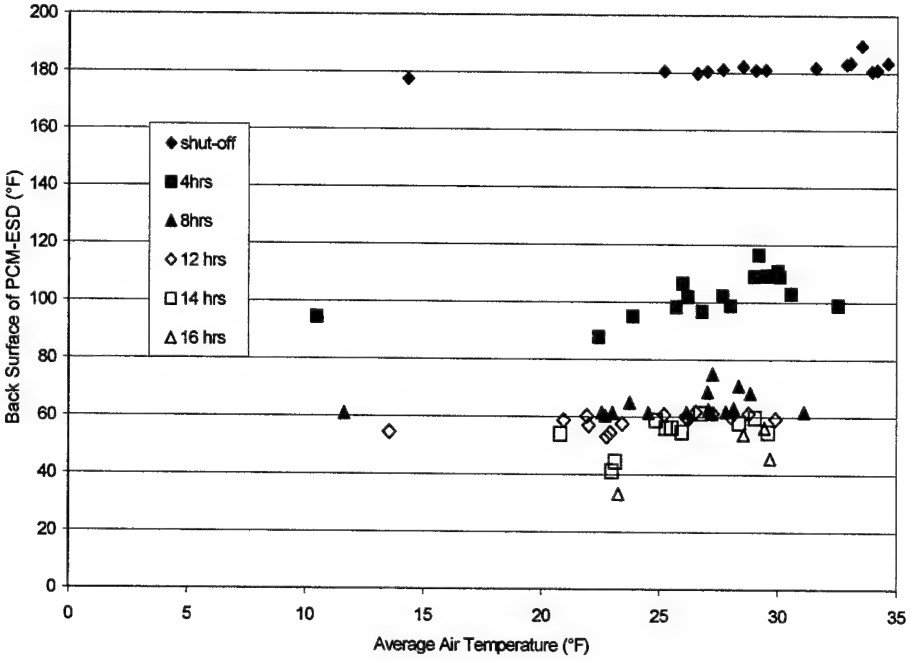


**Figure 4.37**
**Temperature Measured on the Backside of ESD#1 vs. the Average Air Temperature after Engine Shut-off**

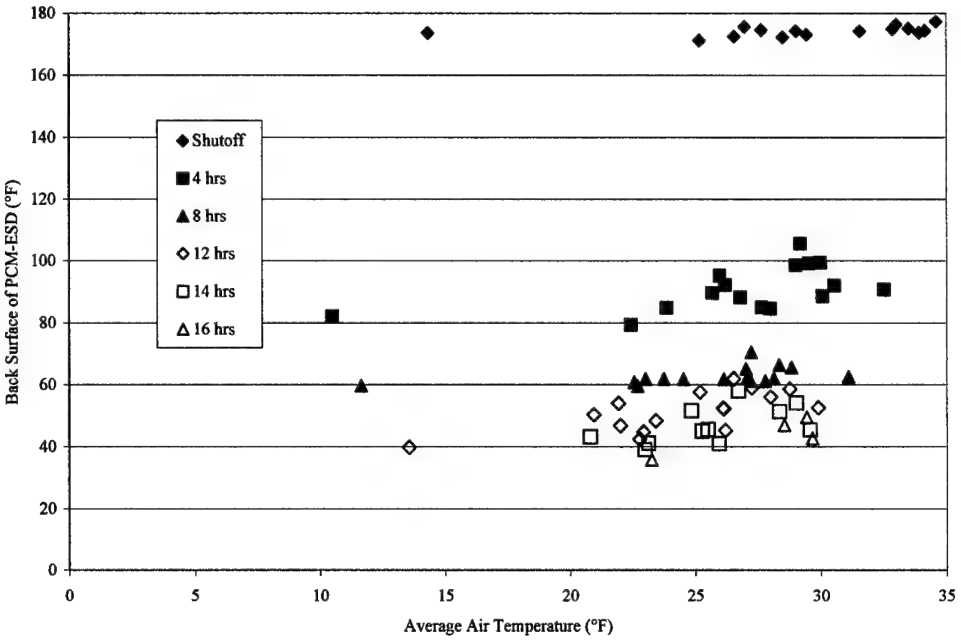


**Figure 4.38**
**Temperature Measured on the Backside of ESD#2 vs. the Average Air Temperature after Engine Shut-off**

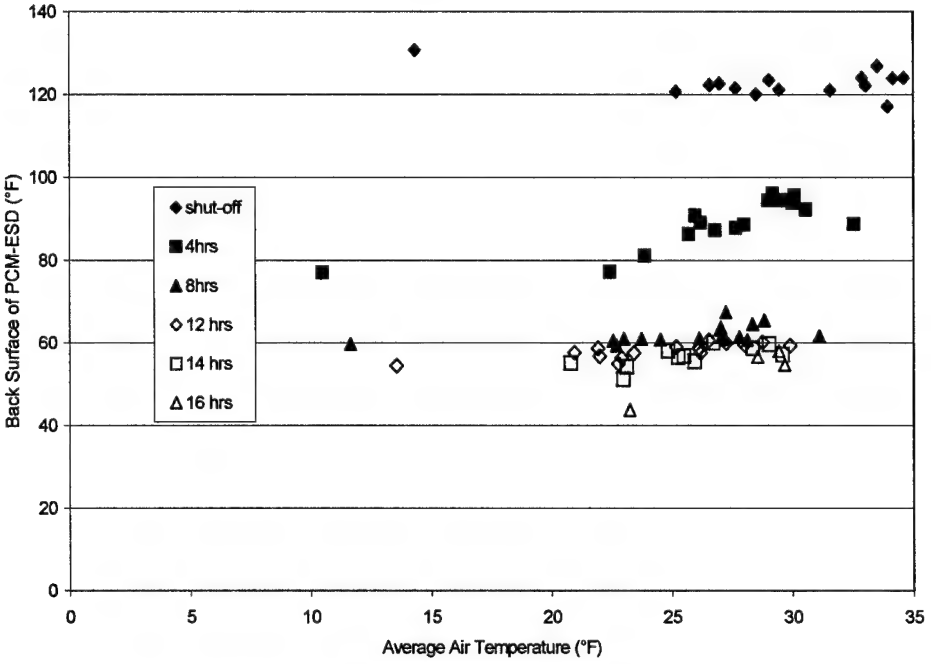


**Figure 4.39**
**Temperature Measured on the Backside of ESD#3 vs. the Average Air Temperature after Engine Shut-off**

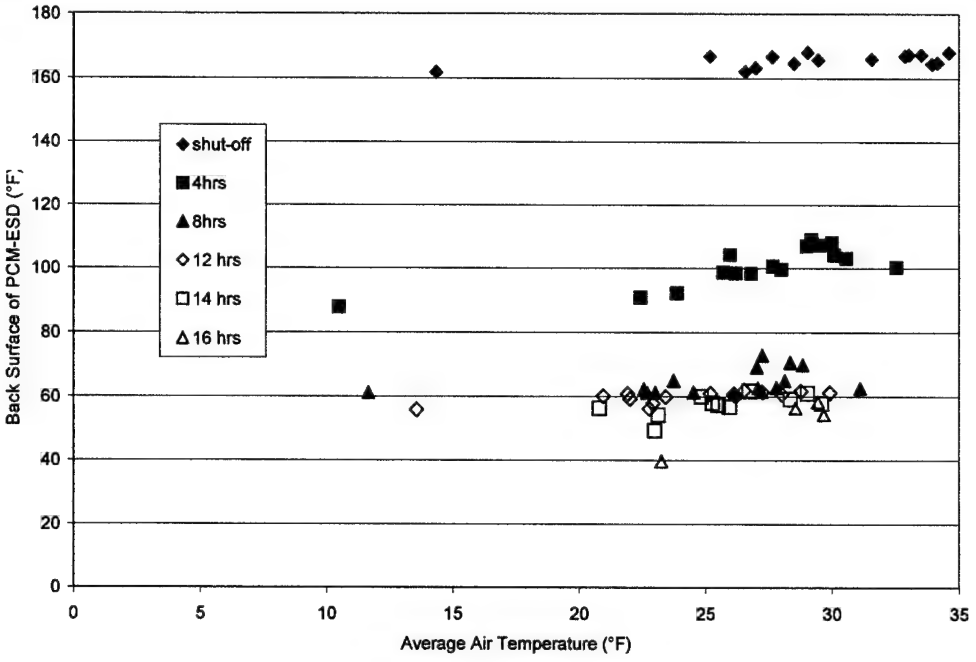


**Figure 4.40**
**Temperature Measured on the Backside of ESD#4 vs. the Average Air Temperature after Engine Shut-off**

A summary of the oil temperatures measured at the top of the oil pan at 12, 14, and 16 hrs after engine shutoff is shown plotted against the average air temperature during cool-down in Figure 4.41. Also, shown for comparison is the oil temperature from the baseline cases and a line corresponding to the average air temperature. The cases with the PCM-ESD applied to the oil system clearly had much higher oil temperatures at the top of the oil. Twelve hours after engine shutdown the oil temperature for most of the baseline tests dropped within 10°F of the average air temperature, while the cases with the PCM-ESD were between 22 and 31°F higher than the average air temperature. Fourteen hours after shutoff the oil temperature for the cases with the PCM-ESD is still 18-27 °F higher than the average air temperature, while the oil temperature for the baseline cases were close to the average air temperature.

A similar graph is shown in Figure 4.42 for the oil temperatures measured at the bottom of the oil pan. Note that because the thermocouple at the bottom of the oil pan was added late in the baseline test program there was only one baseline temperature measurement of the oil at this location. For all of the tests with the PCM-ESD the oil temperatures were even higher than those measured at the dipstick location during the same tests.

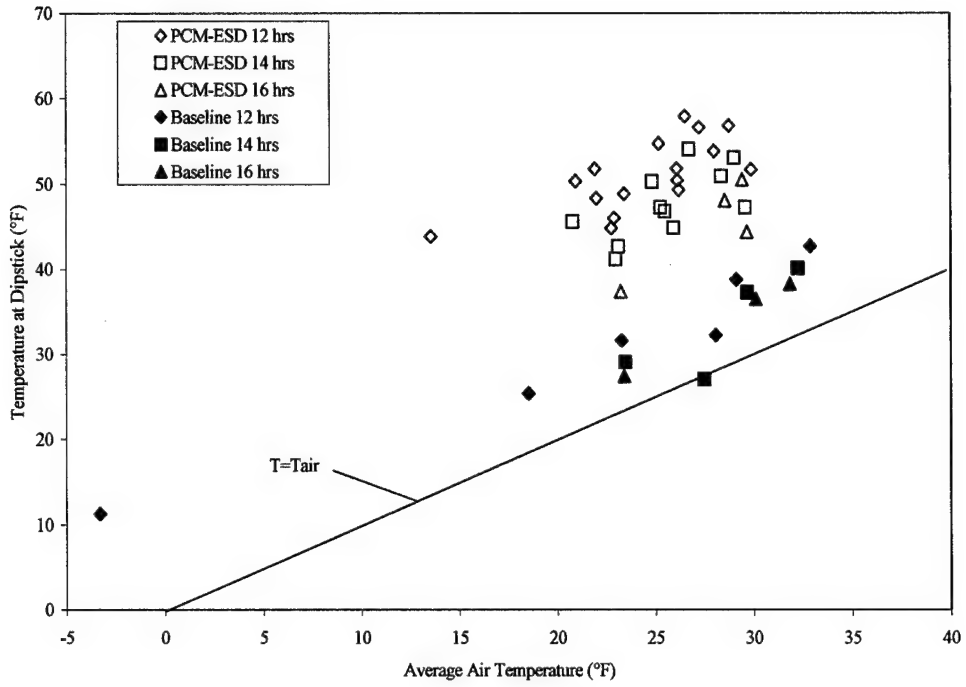


**Figure 4.41**
**The Oil Temperature Measured at the Dipstick at Various Times after Engine Shut-Off vs. the Average Air Temperature**

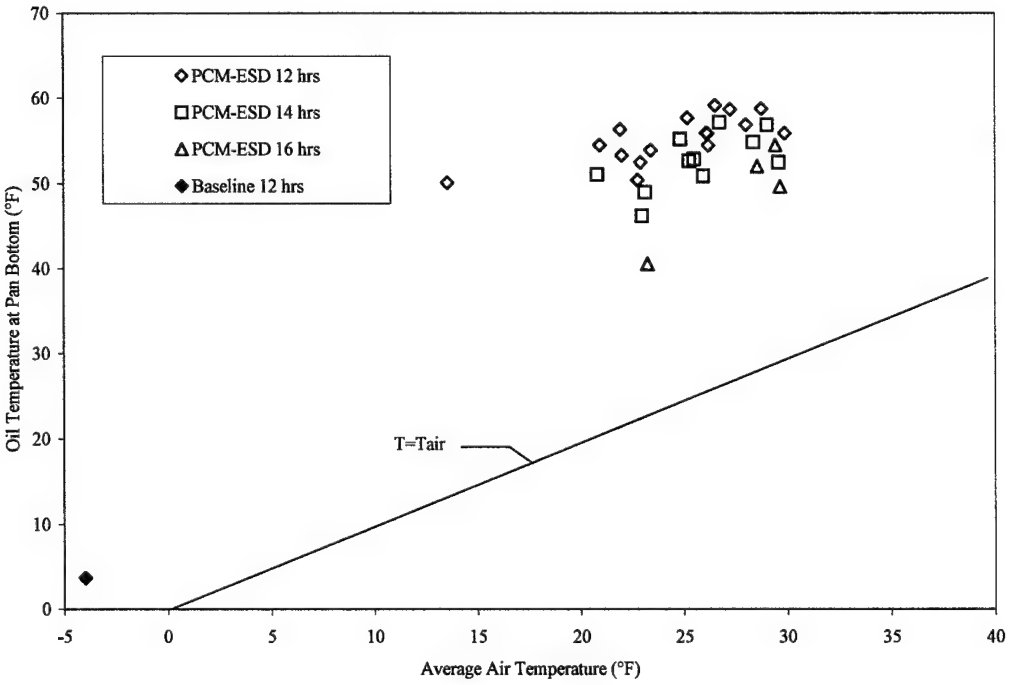


**Figure 4.42**
**Oil Temperature Measured at the Bottom of the Oil Pan at Various Times After Engine Shut-Off vs. the Average Air Temperature**

Figure 4.43 shows the difference between the oil temperature at the bottom of the pan and the air temperature before engine restart along with the average air temperature after engine shut-off plotted vs. the cool down period (time between engine shut-off and restart). For times less than 14 hrs the oil temperature at the bottom of the pan is over 25°F higher than the air temperature. After 16 hours the effect of the PCM-ESD on the oil temperature was seen to decrease significantly.

The difference between the oil temperatures measured at the top and the bottom of the oil pan at the time of engine restart is shown in Figure 4.44. For most of the tests the oil temperature at the bottom of the oil pan was observed to be over 5°F higher than that at the dipstick location for times up to 14 hours. At longer shut-off times the difference between the oil temperatures at the two locations decreased.

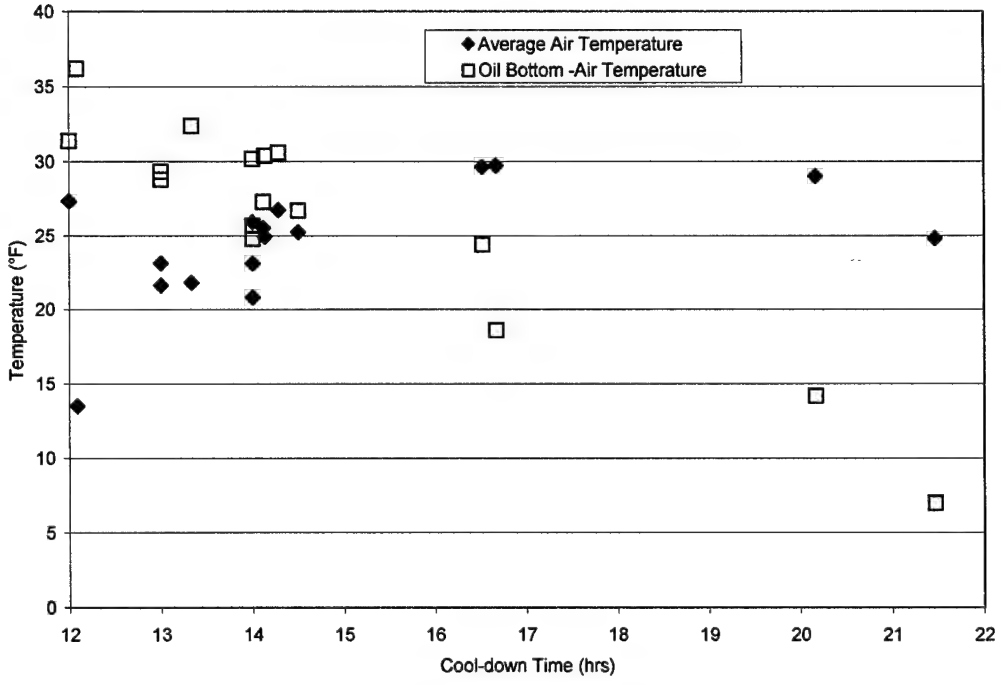


**Figure 4.43**
**The Difference Between the Oil Temperature at the Bottom of the Oil Pan and the Air Temperature (Cases With PCM-ESD)**

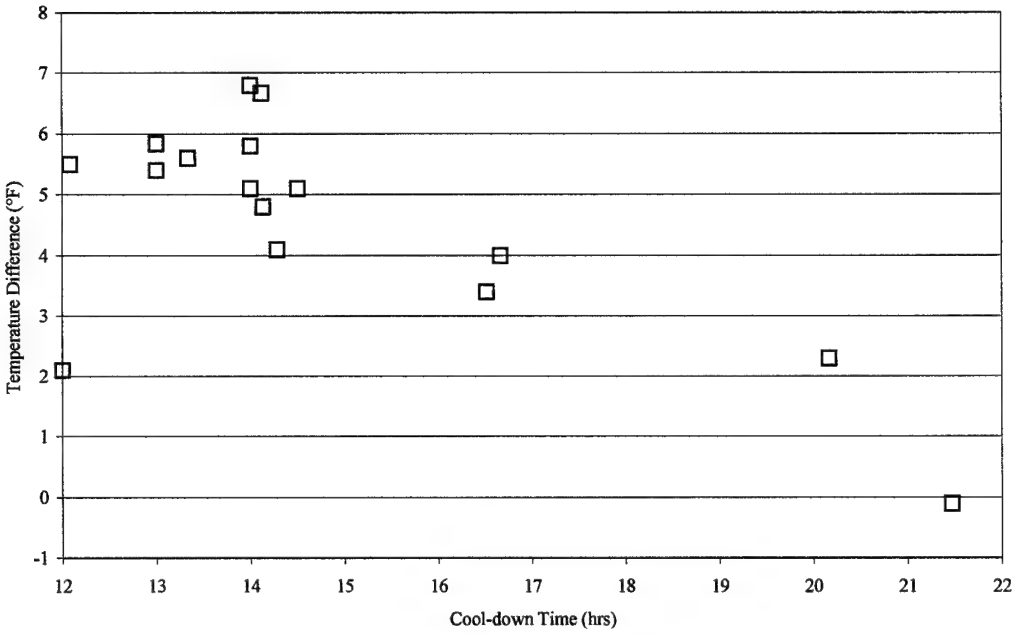


**Figure 4.44**
**Difference Between the Oil Temperature at the Bottom and Top of the Oil Pan for PCM-ESD Cases**

The difference between the oil temperature at the dipstick and the block temperature measured before engine restart is shown plotted vs. the cool down time for both the baseline and PCM-ESD cases in Figure 4.45. The oil temperatures for the baseline cases were all near the block temperatures, while the oil in the pan equipped with the PCM-ESD was maintained above the block temperature. As the time after shutoff increased over 14 hours the oil temperatures for the PCM-ESD cases were seen to approach the block temperatures.

The differences between the block and air temperatures for the baseline and PCM-ESD cases are plotted in Figure 4.46. It can be seen that the presence of the PCM-ESD increased the average temperature of the engine block above that seen in the baseline tests. While the increased block temperature was not the primary reason for the use of PCM in the oil pan, the secondary benefit of increased block temperatures at startup is thought to be a reduction of the cranking work.

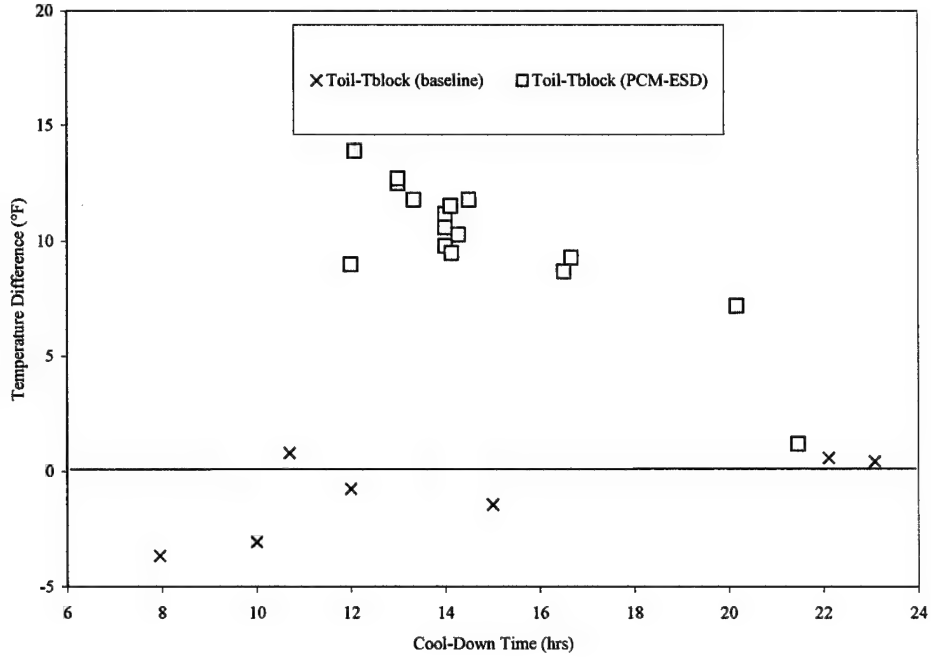


**Figure 4.45**
**The difference Between the Oil Temperature Measured at the Dipstick and the Block Temperature at Engine Restart**

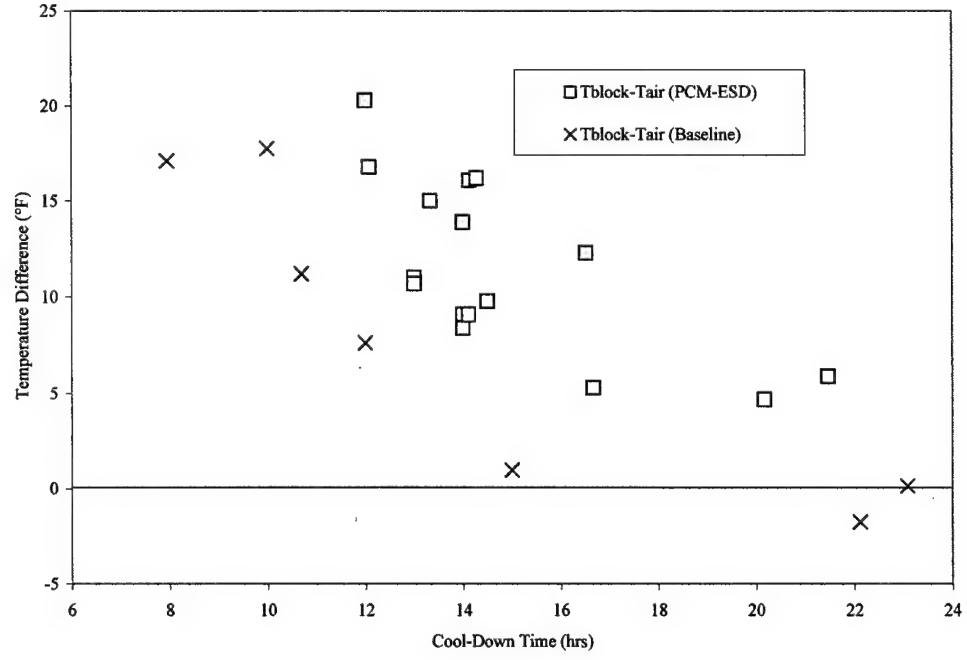


**Figure 4.46**
**Difference Between the Block and Air Temperature**

### 4.3.2.1 The Effect of Insulation Type on the Performance of the Oil Pan-PCM System

For the last two engine tests of the PCM-ESD system the polyisocyanurate insulation on the oil pan PCM- ESD system was replaced with a higher thermal resistance vacuum insulation, to assess the impact of using a higher R-Value insulation. The results from two similar operation and cool down tests conducted under nearly the same environmental conditions are shown in Figures 4.47 and 4.48. The oil pan ESD system was equipped with vacuum insulation for the test conducted on March 17, and with the ordinary polyisocyanurate insulation for the test on February 16. The air temperatures for the two tests were nearly the same for the two tests, varying less than a degree over most of the engine shutoff period and the average wind speeds were within 2 mph for both tests. The higher effectiveness of the Vacuum insulation is clearly shown by the plot of the heat transfer measured on the outside surface of the insulation shell covering ESD# 4 (see Figure 4.47). Over most of the cool-down period the oil pan equipped with the vacuum insulation lost 1/2 to 1/3 of the heat that was lost through the polyisocyanurate insulation panel. The heat transfer measured on the insulation applied to the outside surfaces of the other ESD's showed similar reductions in heat transfer.

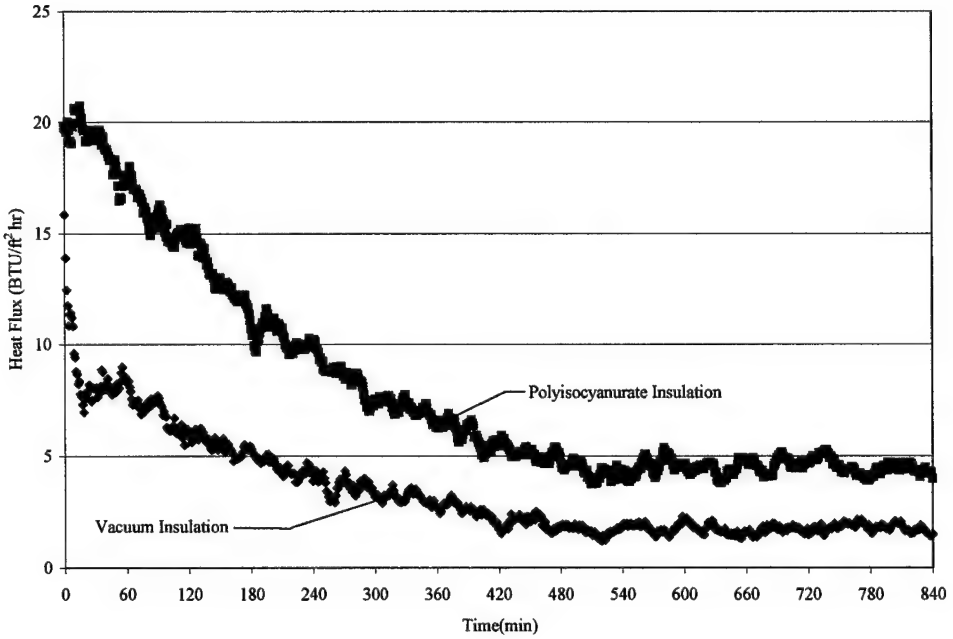


**Figure 4.47**
**Heat Transfer Measured on the Outside Surface of the Oil Pan-ESD Insulation Covering ESD #4 During Tests on February 16, 2000 (Polyisocyanurate Insulation) and March 17, 2000 (Vacuum Insulation)**

The measurements showed that the vacuum insulation looses less energy through the insulation panels. The overall effect of the vacuum insulation on the oil temperature is shown in Figure 4.48, which shows that the oil temperatures measured at the bottom of the oil pan for the two tests differed by less than 1 °F between the two tests throughout the cool-down. There are thought to be two reasons for the small difference between the two cases. First, the geometry of the oil pan and surrounding structure required the use of many (19 different) vacuum panels which were taped together to form an insulation shell instead of a single contiguous shell. It is thought that the majority of the heat lost through the insulated panels was lost through the joints between the insulating panels. Secondly, as was shown previously by the finite element simulations (see Figure 2.25), there is a diminishing return on the investment for higher quality insulation for an application where there is a significant leak path. An analogy can be made that thermal leak path through the engine block is similar to an open window in an otherwise well-insulated house.

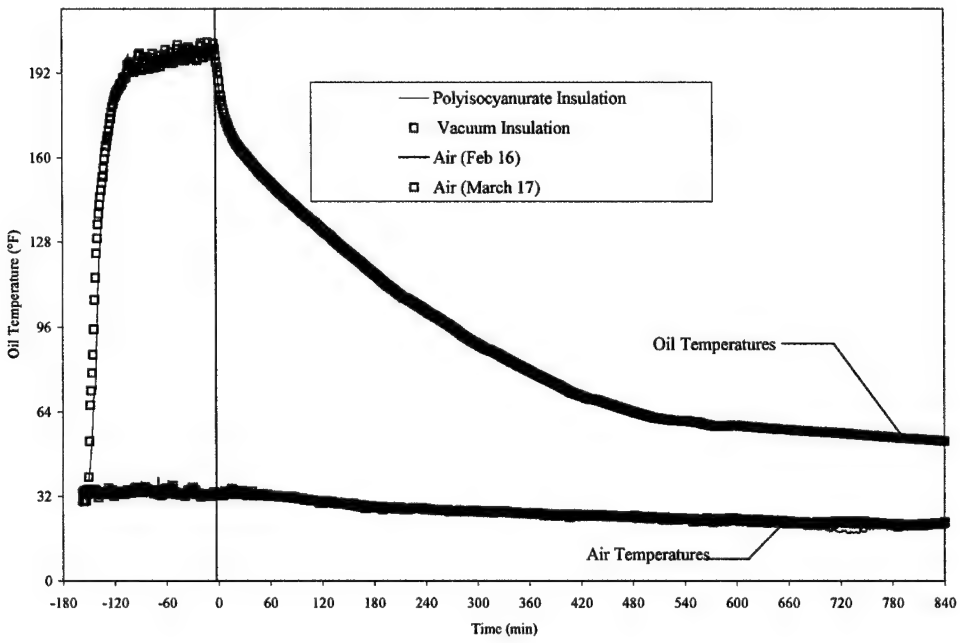


**Figure 4.48**
**The Effect of the Type of Insulation on the Temperature Measured at the Bottom of the Oil Pan Test on March 17 With Vacuum Insulation, Test on February 16 With Polyisocyanurate Insulation.**

### 4.3.3 Oil Filter PCM-ESD Tests

During all of the tests of the PCM-ESD applied to the oil filter, the PCM-ESD system was also applied to the oil pan. As shown in Table 4.4, the PCM-ESD system was applied to the oil filter for the last twelve tests with the oil pan PCM-ESD system. Figure 4.49 shows the oil filter temperatures, along with the temperatures measured on two surfaces of the PCM-ESD. The filter temperatures were measured at the front (adjacent to the attached PCM-ESD) and back surface (opposite from the PCM-ESD). The temperatures, measured on the center height of the side and front outer surfaces of the ESD are also shown. During engine operation the front surface of the oil filter which is in contact with the ESD is at a lower temperature than the back of the oil filter because the ESD is cooler than the oil filter. The surfaces of the ESD were seen to steadily increase toward the oil filter temperature during engine operation.

After engine shutoff, the temperature of the back side of the oil filter decreased below the temperature of the ESD, while the temperature of the front face of the oil filter was maintained at a higher temperature because of contact of the oil filter with the warm PCM-ESD. At the end of the engine cool-down period shown in Figure 4.49 the front surface of the oil filter was less than 5°F lower than the two measured oil filter PCM-ESD surface temperatures.

The effect of the addition of the PCM-ESD to the oil filter can be seen in Figure 4.50 where the temperatures measured on the front and back surfaces of the oil filter are compared for tests conducted with and without the PCM-ESD applied to the oil filter. The average ambient air temperature during the engine cool-down period was approximately the same (23°F) for both of the two tests. After 8 hours the average surface temperature of the baseline oil filter was only 10°F greater than the average air temperature during cool-down, while the average surface temperature for the filter equipped with the PCM-ESD was maintained at a level over 32°F higher than the average air temperature. At the end of the cool-down period the surface of the PCM-ESD case was 45°F, which was still over 23°F higher than the average air temperature. By comparison, the baseline case decreased to this temperature level in only 4.5 hrs.

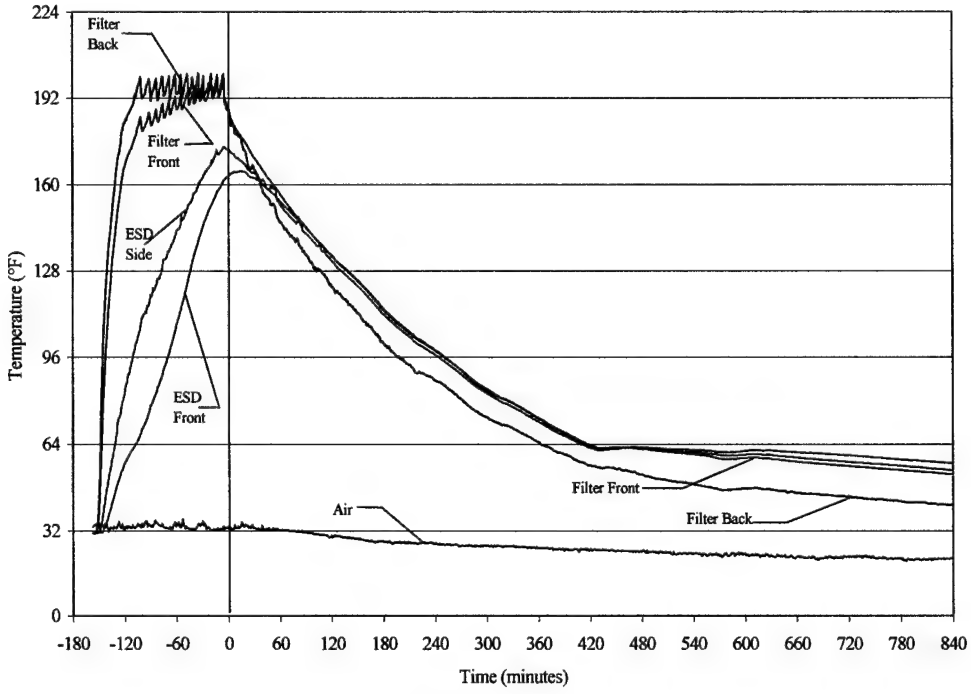


**Figure 4.49**
**Oil Filter and Oil Filter ESD Temperatures during a Typical Operation and Cool-Down Period**

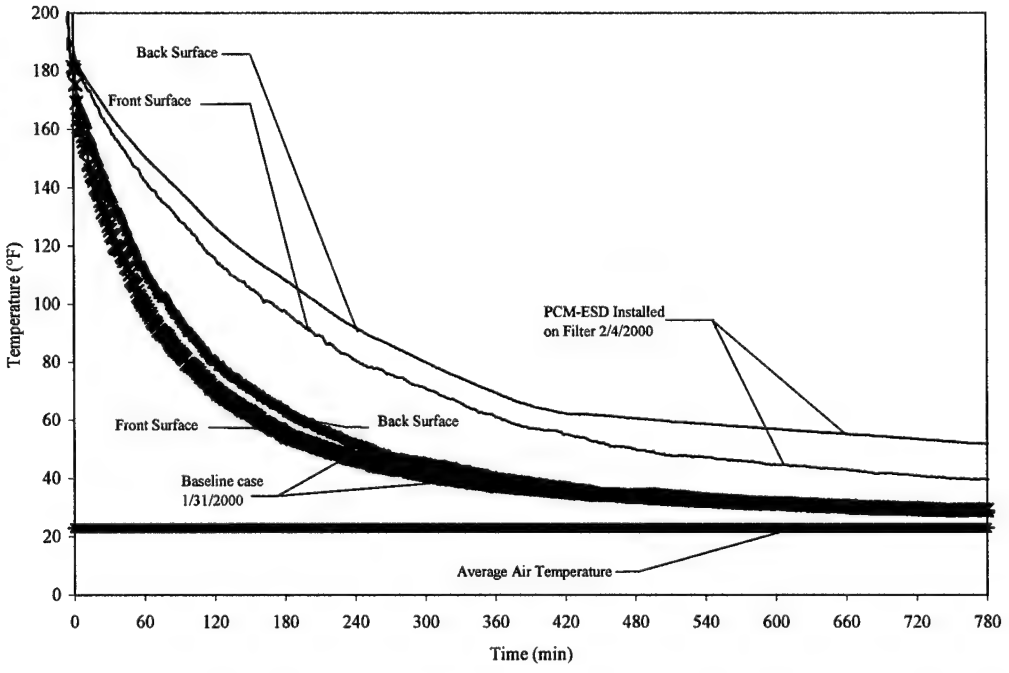


**Figure 4.50**
**Comparison of Oil Filter Surface Temperatures During Engine Cool-Down Tests Showing the Effect of the PCM-ESD (Average Air Temperature for Both Cases = 23°F)**

A summary of the oil filter surface temperatures measured before engine restart for the tests with the oil filter ESD is shown plotted vs. the cool-down time in Figure 4.51. For reference purposes, the average air temperature during cool-down, which was between 20 and 30°F for all of the tests with PCM-ESD applied to the oil filter is also shown. The oil filter PCM maintained the average (of the front and back surfaces) temperature of the oil filter above 45°F for times up to 16 hours after shut off. In contrast, the surface temperature of the baseline oil filter approximately was seen to be approximately equal to the air temperature.

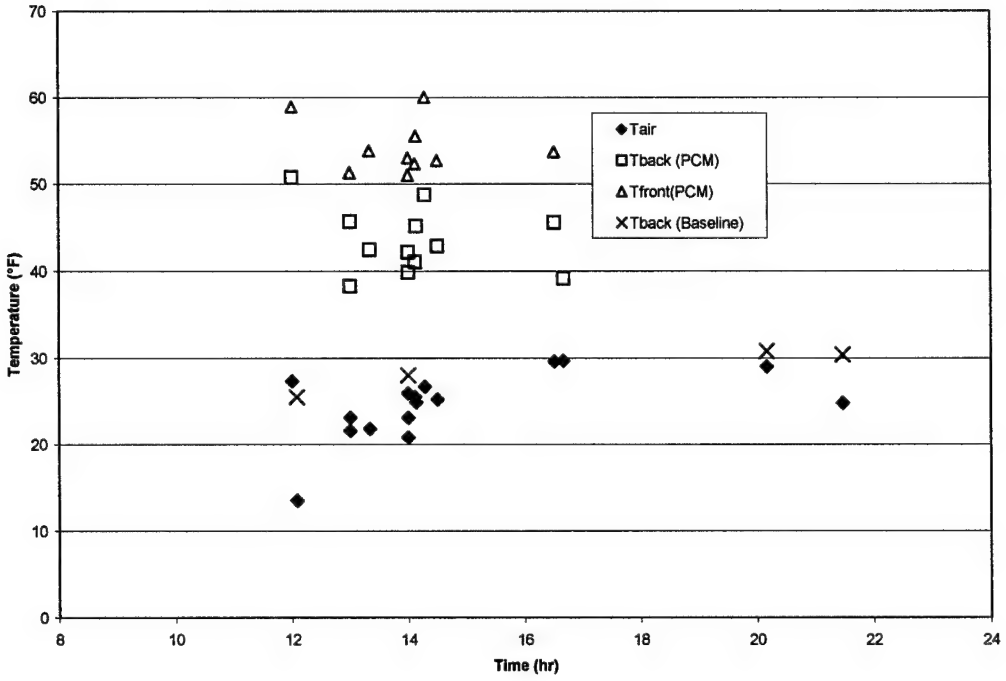


**Figure 4.51**
**Oil Filter Temperature Before Engine Restart as a Function of the Time after Engine Shutdown and Air Temperature**

### 4.3.4 Engine Cranking and Starting Results

It has previously been shown that the oil temperatures in the pan and the filter could be maintained at a higher level by the application of the PCM-ESD system. In addition, the block temperature was maintained at slightly higher temperature levels because of the conduction of heat from the warmer oil pan to the block. The effect of the higher temperature oil in the pan and the filter on the engine starting characteristics is explored in this section.

Previously (see Figure 4.34) the oil temperatures were compared during the engine cool-down period with and without the PCM-ESD applied to the oil pan. The cranking variables during the starting transients are shown in Figure 4.52 for the baseline case and Figure 4.53 for the PCM-ESD case. During the test with the PCM-ESD the truck was exposed for a longer cool-down period at a lower average air temperature than it was for the baseline case. However, the PCM-ESD system maintained the oil in the pan at a higher temperature. For the starting test of the baseline configuration the engine started in 17.5 seconds, and the starter used over 109 kJ (146 hp-s) of energy from the battery. During the start of the PCM-ESD equipped engine the starter was prematurely released after 7 seconds and the engine stopped running one second later. The starter was turned on again and the engine quickly restarted (with the starter on less than 1.3 seconds) and continued to run after the starter switch was turned off. The total cranking time (defined as the total time that the starter switch was turned on) for the PCM-ESD case was only 8.3 seconds, which was less than half of the time required to start the baseline configuration. The total cranking work for the PCM-ESD equipped case was only 53 kJ (71 hp-s) which was less than half of that required for the baseline case.

Table 4.4 lists the starting performance parameters for the tests with the PCM-ESD applied to the oil system. For all of the tests with the PCM-ESD system the engine was restarted after sitting in the cold for more than 12 hours. The cranking times and the average air temperature during cool-down for the PCM-ESD-equipped engine are plotted against the cool-down time in Figure 4.54. The cranking times for baseline cases where the temperature history was monitored before restart are also shown for comparison. The sixteen data points shown for the PCM-ESD all have the PCM-ESD system applied to the oil pan, all but four of the data points are for tests where the PCM-ESD system was also applied to the oil filter. It is apparent that the warmer oil temperatures cause a drastic reduction in the amount of time

required to start the engine. The time required to start the engine after more than 12 hrs (12-21 hrs) of exposure to air temperatures from 29-13°F ranged from 8.3 seconds to only 0.75 seconds.

The cranking work for both the PCM-ESD cases and the baseline cases is plotted vs. the cool-down time in Figure 4.55. The results show that the PCM-ESD cases required much less cranking energy from the battery to restart the engine than the baseline configuration under comparable exposure to the cold weather during engine cool-down. The cranking work for the PCM-ESD equipped cases ranged from 6 to 53 kJ.

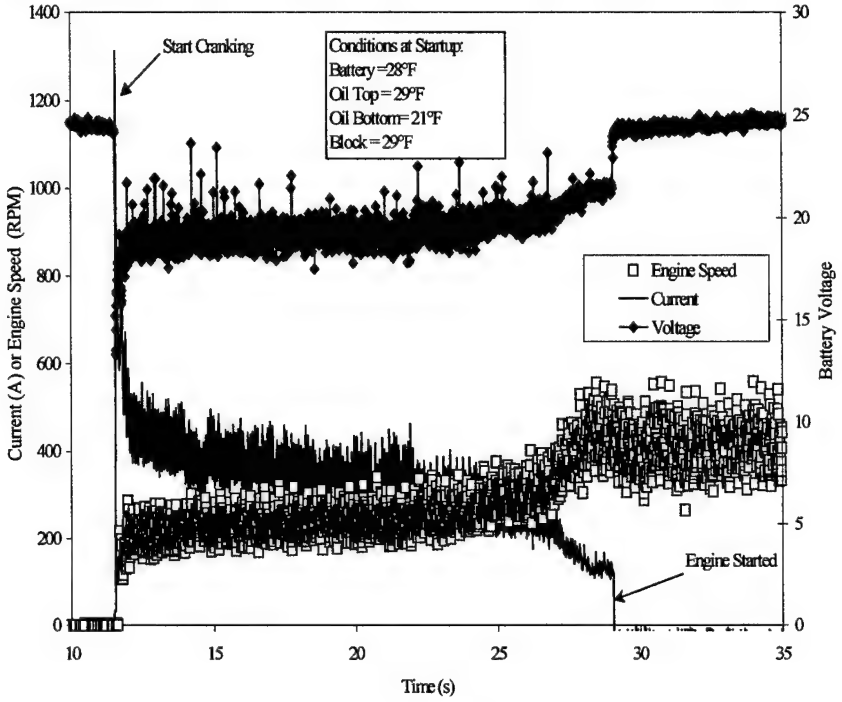


**Figure 4.52**
**Starting Performance of the Baseline Engine Configuration on January 14, 2000. (Cool-Down Time =642 min at an Average Air Temperature of 17.4°F)**

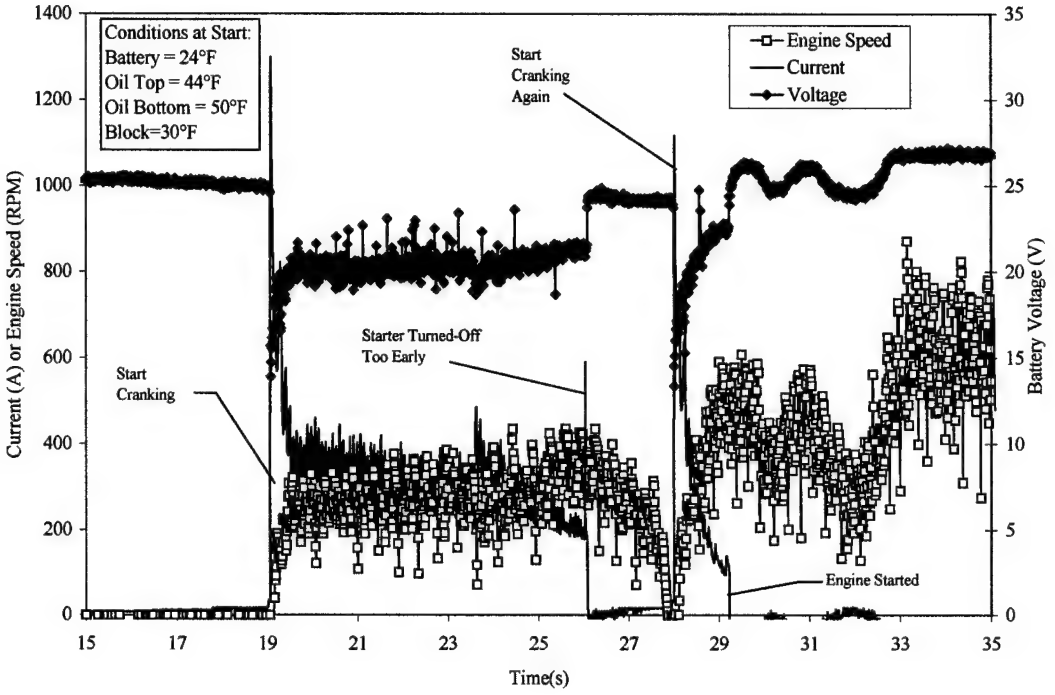


**Figure 4.53**
**Starting Performance of the Engine Configuration With PCM-ESD on January 29, 2000 (Cool-Down Time =725 min at an Average Air Temperature of 13.5°F)**

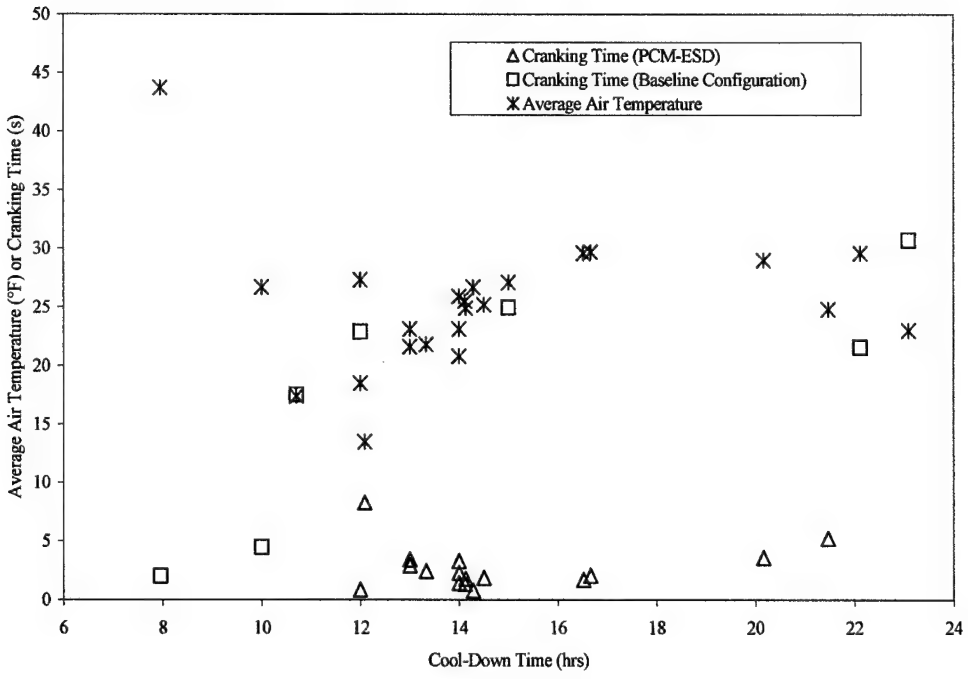


**Figure 4.54**
**Cranking Time and Average Air Temperature vs. Cool-Down Time**

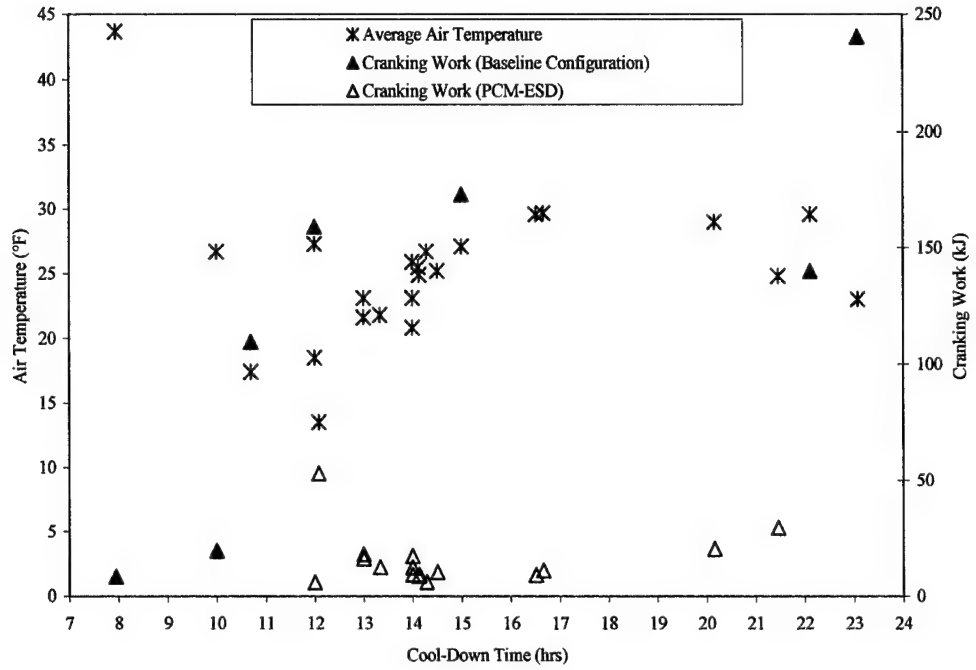


**Figure 4.55**
**Cranking Work vs. Cool-Down Time**

The relationship between the oil temperature and cranking work is shown in Figure 4.56, which shows the cranking work plotted against the dipstick temperature for all of the cranking tests. It can be seen that the cranking work for both the PCM-ESD and baseline cases are comparable for oil temperatures above 40°F.

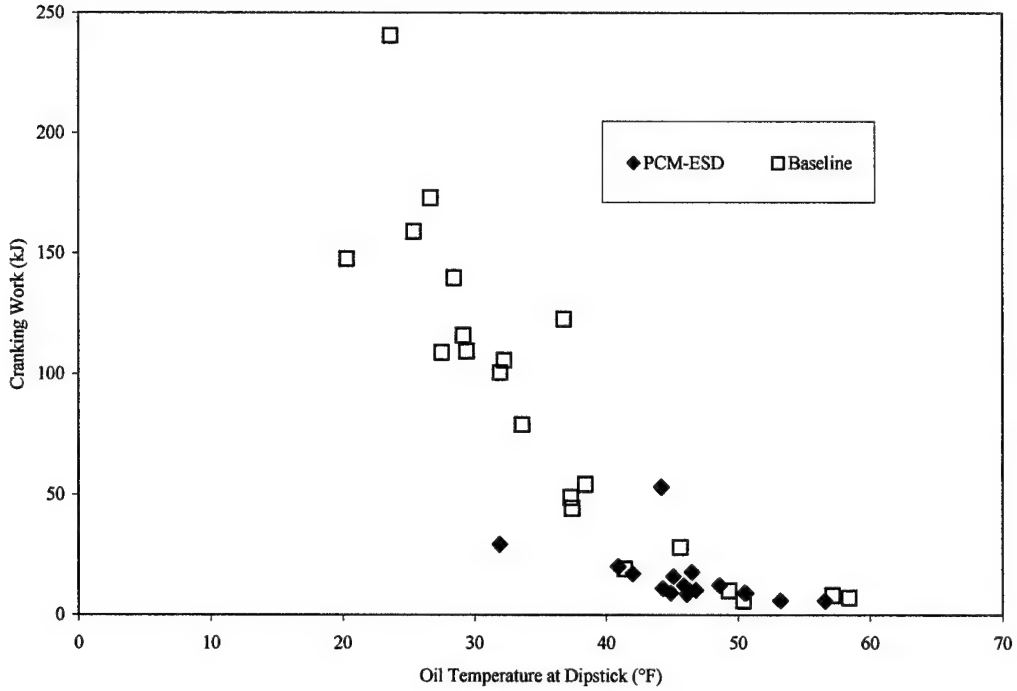


**Figure 4.56**
**The Cranking Work vs. the Oil Temperature at the Dipstick**

For the first four tests with the PCM-ESD applied to the oil pan, the oil filter was in the baseline configuration. The oil filter ESD was used in addition to the oil pan ESD for the last twelve tests. Once it was placed on the oil pan, the PCM-ESD system was kept on the oil pan for the rest of the test program with the hope of exposing the oil pan PCM-ESD system to lower temperatures. Therefore, there were no tests with the PCM-ESD applied to the oil filter alone. Figure 4.57 shows the cranking work for the PCM-ESD cases plotted against the oil filter temperature. The results imply that the addition of PCM-ESD to the oil filter in addition to the oil pan further decreases the cranking work. However, it should be noted that the battery temperatures were lower for the tests which did not use the PCM-ESD system on the oil filter, so that it is difficult to determine conclusively if the higher temperatures in the oil filter helped to improve the starting characteristics of the engine.

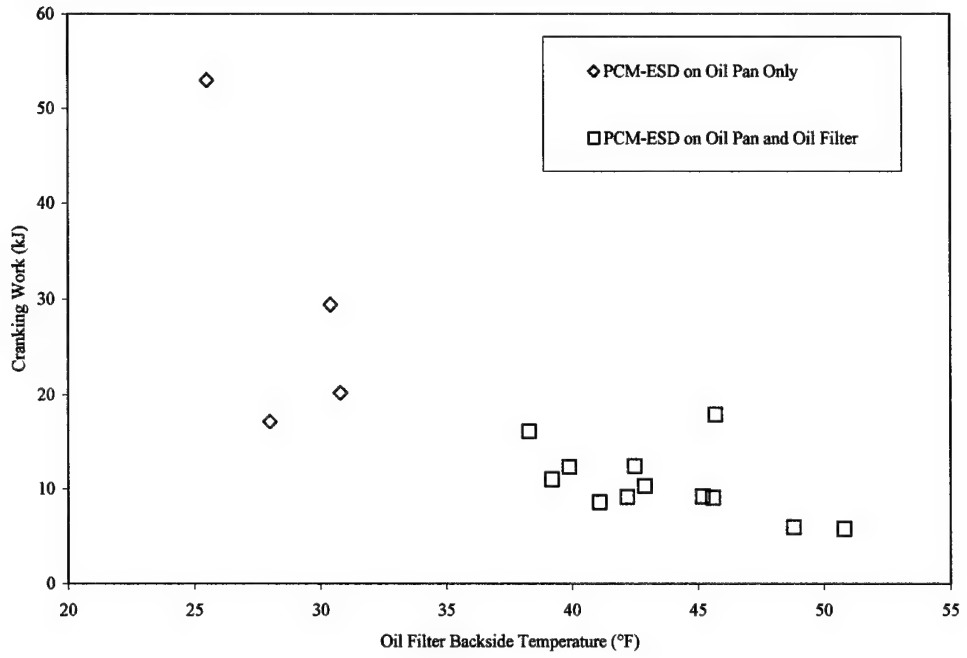


**Figure 4.57**
**Cranking Work vs. Oil Filter Temperature (on Backside of Filter) For Cases with PCM-ESD Applied to the Oil Pan**

# *Section 5*
# *Summary and Conclusions*

## 5. 1 Summary

The purpose of this study was to examine means of storing the waste heat generated during Diesel engine operation to improve the starting performance of Diesel engines after overnight exposure to cold weather. The goal of the program was to develop a system to improve the starting characteristics of the Diesel engine so that it would reliably re-start after exposure to cold weather for a period of at least 12 hours. Thermal management of two critical temperature-sensitive systems, the battery and the oil system, was pursued to accomplish this goal. The battery and oil temperatures are important because of their relation to the cranking speed, which is a critical consideration in the starting of a Diesel Engine. Cold batteries provide less power and cold oil leads to higher resistance during cranking. Therefore, if the oil and batteries are maintained at a higher temperature level the engine will start much easier.

Concept-demonstration thermal management systems were designed for the oil pan, oil filter, and battery box of a US Army five-ton tactical truck. Phase change materials (PCM) and advanced insulation were used in the design of the thermal management systems. The PCM was used in passive energy storage devices (PCM-ESD), which were attached to the oil pan and oil filter. The PCM-ESD stored thermal energy during engine operation and released the energy back to the oil system as the vehicle cooled-down to prevent the temperature of the oil from dropping too low overnight. The insulation prevents the loss of the energy stored in the PCM-ESD to the environment. It was found that the battery produced little waste heat during its charging cycle, therefore the thermal management system for the battery was based on active heating of the batteries by electric resistance heaters and the prevention of heat loss by state of the art vacuum insulation.

All three of the thermal management systems were studied in cooling tests conducted in a 0°F cold chamber. The performance of the thermal management systems was compared to the baseline component cool-down rate. It was found that the thermal management systems reduced the cooling rate for all three of the systems.

The time required to cool at the top of the oil pan from room temperature to 32°F was increased by almost a factor of two with the PCM-ESD system. An even greater effect was seen on the oil at the bottom of the pan; the time required to reach 32°F was extended by a factor of 12. The oil filter PCM-ESD system was also shown to be effective. The presence of the PCM-ESD system on the oil filter increased the time to drop from room temperature to 32°F by a factor of 4. The tests of the insulated battery box showed that the temperature decreased by less than 25°F over a 16 hr period, which was a factor of over 2.9 times the required time for the baseline configuration.

The PCM-ESD thermal management systems for the oil pan and oil filter were tested on the engine during operation, cool-down and restart tests conducted while the truck was exposed to the winter environment in Dayton, OH. The temperatures of the oil system, block, and other components were measured during engine operation and cool-down tests with and without the PCM-ESD system applied to the engine. Cranking performance was determined by measuring the cranking voltage, current and engine speed at startup, for both the baseline engine and the PCM-ESD equipped engine.

The tests showed that that the thermal management system maintained the oil temperature at the bottom of the pan above 50°F for longer than 12 hrs when exposed to average ambient temperatures as low as 13°F. The PCM-ESD system was able to maintain the oil temperature at the bottom of the pan more than 25°F above the ambient air temperature for up to 14-hrs exposure to the cold. The application of PCM-ESD to the oil filter was also shown to be effective in maintaining the oil temperature over 20°F above ambient conditions overnight. The result of the higher oil temperatures in the oil pan and oil filter was that the engine started faster, requiring a factor of 2-6 times less cranking energy from the batteries.

## 5.2 Conclusions

This study resulted in a successful concept demonstration of thermal management systems for the battery and oil system of a US Army 5-ton tactical truck, which are capable of maintaining the temperatures of the oil and battery at elevated temperature during exposure to cold weather overnight. The successful concept demonstration shows that a Diesel engine equipped with passive energy storage devices applied to the oil system can be shut off for longer periods in cold weather and reliably start. The application of a PCM-ESD

system to Diesel engines could reduce or eliminate fuel use and engine wear due to overnight idling in cold weather.

The tests of the concept-demonstration thermal management system for the oil conclusively showed that it is possible to use a totally passive thermal protection based on PCM and insulation to maintain the oil in both the oil pan and oil filter at elevated levels for extended time periods after shutdown. Another benefit of the higher oil temperatures in the pan was that the block temperature was also maintained at higher temperature levels. As a result of the higher oil temperatures, the engine was shown to re-start in much less time, using less cranking energy from the battery. The reduction in the cranking work reduces the charge that must be delivered back to the battery during inefficient battery charging at low temperatures. Another benefit of the higher oil temperatures at startup provided by the PCM-ESD system is the improved flow of the lubricant and the lubrication of engine components. The use of a passive PCM-ESD on the oil filter ensures that the oil filter is not bypassed because of excessive pressure drop.

The cold chamber tests of the battery box showed that it is possible to build a practical actively heated insulated battery box that could maintain batteries at elevated temperatures overnight.

# *Section 6*

# *Suggested Areas for Further Investigation*

## 6.1 Further Studies of the Existing PCM/ESD System

### 6.1.1 Test at Lower Ambient Air Temperatures

The results showed that the PCM-ESD system could reliably maintain the oil temperatures at elevated levels overnight when exposed to temperatures as low as 13°F. It would be interesting to conduct tests of the system in a controlled environment engine test cell at lower temperatures. The authors know of at least one facility that could be rented for this purpose. In addition to providing lower test temperatures and a faster turnaround on tests, an engine cold chamber would allow the battery to be maintained at a constant temperature.

### 6.1.2 Determination of the Effect of the Oil-Filter ESD on Engine Cranking

It has been determined that the oil filter PCM-ESD was able to maintain the oil within the filter at elevated levels. It has not yet been established what effect the warmer oil in the filter has on the cranking work. It would be interesting to evaluate the effect the oil filter PCM-ESD alone has on the starting characteristics.

## 6. 2 Improvements to the Present System

The thermal management systems built during this study were meant to be proof of concept systems, not a final prototype ready for production. Many performance improvements can be made to the design of the thermal management systems using the experience that was gained during the present study. Some key areas for further improvement of the system include, but are not limited to:

1. Reduction of contact resistance between the PCM-ESD and the protected components,
2. Reduction of edge effects and secondary losses in the insulated battery box, and
3. Improved surface coverage of the oil pan surface with PCM-ESD.

As a side point, it should be noted that the oil pan that was protected in the present study was a difficult shape to fit with the PCM-ESD system because of the complex curvature of the pan surface. It is thought that less complex surfaces of other oil pans for other vehicles can be fitted more easily, resulting in more optimal placement of the PCM.

### 6.3 Extension of the System to Operate at Much Lower Operating Temperatures

The system developed for the present study was designed to maintain the temperature of components above 32°F, while exposed to ambient air temperatures around 0°F. In northern Canada and Alaska, vehicles are routinely exposed to much lower temperatures than 0°F and special Arctic oil is used, which has lower viscosity than 15W-40 at low temperatures. Note that other PCM's which freeze at temperatures below 32°F may be used to provide thermal protection in severe Arctic environments by maintaining the components at temperatures well above ambient but below 32°F. The alternative PCM used for this purpose may be a hydrocarbon, an inorganic salt or a water-based compound.

Note that water-based gel compounds would offer about 70% more energy storage per volume than the gel that was used for the present experiment, but are only useful (release the heat of fusion) at temperatures below 32°F.

### 6.4 Application of PCM-ESD to Other Temperature Sensitive Engine Systems

The PCM-ESD approach could be applied to other engine and vehicle systems such as the Engine Block, automatic transmission, and fuel filter, and fuel injection pump. The application of the PCM-ESD to components that have high surface temperatures during operation, such as the transmission would be totally passive, while other applications such as the fuel filter may require active heating of the PCM during engine operation.

# *SECTION 7*

## *References*


1. Diemand, D. "Automotive and Construction Equipment for Arctic Use Heating and Cold Starting,"
   Cold Regions Technical Digest, No. 91-3, April 1991.
2. Diemand, D. "Winterization and Winter Operation of Automotive and Construction Equipment,"
   Cold Regions Technical Digest, No. 92-1, September 1992.
3. Diemand, D."Automotive Fuels at Low Temperatures," Cold Regions Technical Digest, No. 91-2, March 1991.
4. Diemand, D."Automotive Batteries at Low Temperatures," Cold Regions Technical Digest, No. 91-4, May 1991.
5. Personal Communication – Dr. Peter Schihl, US Army TARDEC, July 1998.
6. US ARMY, "Technical Manual Unit, Direct Support, and General Support Maintenance, Truck, 5-Ton 6x6, M939-A2, " ARMY TM 9-2320-358-24&P, 1992.
7. Sanders, N. A., "Engine Heating Device", Final Report, Department of Energy Project Grant Number DE-FG01-82CE15141, 1982.
8. Schatz, Oskar, "Cold Start Improvement by Use of Latent Heat Stores", SAE paper 921605, 1992.
9. American Society of Heating, Refrigeration, and Air Conditioning Engineers, ASHRAE Fundamentals Handbook, 1989.
10. Shapiro, A. B., and Edwards, A.L., "TOPAZ2D Heat Transfer Code and Users Manual", USRL-ID-104558, May 1990.
11. Personal Communication-Mr. James Storey, US Army Test Command, Fort Greeley Alaska, January 1999.